Rapid Colorimetric Detection of Cyanide

Dissertation

zur
Erlangung der naturwissenschaftlichen Doktorwürde

(Dr. sc. nat.)

vorgelegt der

Mathematisch-naturwissenschaftlichen Fakultät

der

Universität Zürich

von

Christine Männel-Croisé
aus Deutschland

Promotionskomitee

Prof. Dr. Roger Alberto (Vorsitz)

Dr. Felix Zelder (Leitung)

Prof. Dr. Roland K. O. Sigel

Zürich 2012

New strategies for the rapid, straightforward colorimetric detection of cyanide in complex samples with corrin-based chemosensors have been developed. In principle, laboratory equipment is not required. The methods are, therefore, promising for applications by non-expert users for the detection of blood cyanide in emergency situations and for water and food analysis, particularly in tropical countries. Challenges in these situations are posed by the complex sample medium, the low levels of detection and the selectivity of the methods.

This thesis presents the first method for the rapid visual detection of blood cyanide using immobilised corrinoids and solid-phase extraction. The result in form of a colour change is obtained within a few minutes using only 1 mL of blood. The semi-quantitative determination of blood cyanide content is achieved by means of a colour chart whereas quantitative determinations are possible by diffuse reflectance spectroscopy or a hand-held spectrophotometer. The new method was evaluated by comparison to the conventional cyanide content determination via microdistillation and voltammetry. Research has been encouraged by the Swiss Toxicological Information Centre which expressed the explicit need for such a rapid diagnostic test. After these proof-of-principle studies under lab conditions, the methodology has to be elucidated in emergency situations.

Colorimetric solid phase extraction with immobilised corrinoids has also been successfully applied for the qualitative and quantitative sensing of cyanide below the allowed upper limit in drinking water as defined by the guideline of the World Health Organisation of 0.05 mg/L.

A detection kit with spatially separated extraction and detection zones has been developed and successfully applied as a rapid, effective and economic method for the optical detection of cyanide in coloured plant materials and of hydrogen cyanide in tobacco smoke. An advantage of this test kit is the possibility to distinguish between cyanide and thiocyanate, which often occur together in biological samples.

A highlight in analytical chemistry for the application of corrinoids as chemosensors for cyanide detection was the real-time monitoring of the enzymatic liberation of endogenous biological cyanide directly on the surface of a freshly cut slice of cassava.

Stopped-flow kinetic measurements were performed successfully with isolated isomers and mixtures of α,β-aquacyano corrinoids and provided first insights into the mechanism of cyanide coordination to the cobalt(III) centre. All the developments and applications of corrinoids as chemosensors are based on these studies.

An immobilisation strategy using hydrophobic silica extended the coordination chemistry at the α-(“lower”) face of natural cobalamins. These studies resulted in a biomimetic model for base-off/histidine-on coordination, resembling structural features of cobalamin-dependent enzyme active sites.

As an alternative to corrin-based chemosensors, metal-indicator complexes were successfully applied for the visual detection of biologically important anions such as phosphate and oxalate. These sensor systems were selected by systematic screening procedures. Advantages are the excellent colour changes and the high sensitivity.

Proof-of-principle studies of the chemosensor systems demonstrated the applicability in water and in complex samples such as food, crude biological plant material, cigarette smoke, wastewater and blood.

Im Rahmen dieser Arbeit wurden neue Strategien zum schnellen Zyanidnachweis mit Hilfe von corrin-basierten Chemosensoren entwickelt. Die neuen Methoden sind in komplexen Medien wie Blut, pflanzlichen Materialien oder Industrieabwässern anwendbar. Die Selektivität und Sensitivität dieser Verfahren, sowie eine einfache Anwendung ohne Laborausrüstung und ausgebildete Spezialisten, erlauben einen Einsatz in Notfallsituationen, aber auch in der Trinkwasser- und Nahrungsmittelkontrolle z.B. in tropischen Ländern.

In dieser Arbeit wird die erste Methode für einen schnellen visuellen Nachweis von Zyanid in Blut mittels immobilisierten Corrinoiden und Festphasenextraktion beschrieben. Für den Test ist nur 1 mL Blut erforderlich und das Ergebnis ist in wenigen Minuten als Farbwechsel auf einer Feststoffoberfläche sichtbar. Die semiquantitative Bestimmung zur Entscheidung über eine Antidotverabreichung ist durch den Vergleich mit einer Farbkarte möglich. Quantitative Resultate können mit diffuser Reflektions-Spektroskopie oder einem Handphotospektrometer erhalten werden. Die Evaluierung erfolgte durch Vergleich mit einer etablierten Methode zur Zyanidbestimmung via Mikrodestillation und Voltametrie. Dieses Projekt wird vom Toxizentrum Schweiz unterstützt, da bisher kein Schnelltest für die Bestimmung von Zyanid im Blut in Notfallsituationen existiert und Erste Hilfe Massnahmen nur aufgrund von Symptomen der Patienten behandelt werden. Nach den grundlegenden Untersuchungen unter Laborbedingungen sind Tests in realen Situationen geplant.

Die Methode der Festphasenextraktion mit immobilisierten farbigen Corrinoiden wurde ausserdem für die qualitative und quantitative Bestimmung von Zyanid in Wasser eingeführt. Damit ist es möglich, Zyanid im Trinkwasser unterhalb der Richtlinie der Weltgesundheitsorganisation (WHO) von 0.05 mg/L visuell nachzuweisen.

Ein Testkit mit räumlich getrennten Extraktions- und Nachweiszonen wurde für den schnellen, effektiven und ökonomischen optischen Nachweis von Zyanid aus Mehrkomponenten-Medien entwickelt. Anwendungen für den Zyanidnachweis in farbigem Pflanzenmaterial und Zigarettenrauch wurden gezeigt. Ein weiterer wesentlicher Vorteil dieses Testkits ist die Möglichkeit zur Unterscheidung zwischen Zyanid und Thiozyanat in der Probe. Beide Anionen kommen oft zusammen in

biologischen Proben vor und sind mit herkömmlichen Schnelltests nicht zu unterscheiden.

Ein besonderer Erfolg für den spezifischen und erfolgreichen Einsatz von corrinoidhaltigen Chemosensoren für den Zyanidnachweis im Bereich der analytischen Chemie ist die zeitliche Verfolgung der enzymatischen Freisetzung von endogenem Zyanid direkt auf der Oberfläche einer frisch geschnittenen Maniokwurzel.

Grundlegende kinetische Untersuchungen zum Reaktionsmechanismus der Koordination von Zyanid an das Co(III)-Zentrum in Corrinoiden bildeten die Basis für die Entwicklung der verschiedenen Chemosensorsysteme und deren Anwendungen. Dabei wurden sowohl diastereomere Mischungen von α, β-aquacyano Corrinoiden als zum ersten Mal auch isolierte Isomere untersucht.

Die Strategie zum Einsatz von hydrophobem Silica als Matrix zur Immobilisierung von Vitamin B12 und β-axial substituierten Derivaten führte zur grundlegenden Erweiterung der Koordinationschemie auf der α-orientierten (“unteren”) Seite natürlicher Cobalamine. Als Ergebnis dieser Untersuchungen wird ein biomimetisches Modell der „Base-off/Histidine-on“ Koordination vorgestellt, welches strukturelle Merkmale der aktiven Seite von cobalamin-abhängigen Enzymen wiedergibt. Solche Modelle spielen eine wichtige Rolle im grundlegenden Verständnis biologischer Prozesse.

Als Alternative zu optischen, corrin-basierten Chemosensoren wurden Metall-Indikator-Komplexe erfolgreich für den visuellen Nachweis von Zyanid und von weiteren biologisch wichtigen Anionen wie Phosphat und Oxalat entwickelt. Diese Sensorsysteme wurden durch ein systematisches Screening-Verfahren ausgewählt. Vorteile dieser Systeme sind hervorragende Farbwechsel und eine teilweise hohe Sensitivität.

Die prinzipielle Anwendbarkeit der entwickelten Chemosensoren wurde in Wasser und Vielkomponenten-Systemen wie Lebensmitteln, pflanzlichen Rohmaterialien, Zigarettenrauch, industriellem Abwasser und Blut überprüft.

The objective of this work is the development of rapid colorimetric detection methods for toxic cyanide and other biological anions to protect human health and the environment. Conventional tests are often time consuming and require laboratory equipment. Therefore, specific tests for toxic agents that can be used by non-specialists in resource-limited settings such as emergency situations or in tropical countries are desperately required. Currently, no rapid diagnostic tests exist for blood cyanide detection after poisoning by fire smoke so that patient treatment with an antidote is based only on symptoms.

Our studies focus on the development and application of selective and sensitive metal-based chemosensors. In particular, we are interested in corrin-based sensors for cyanide detection.

Ideally, the development of colorimetric methods for cyanide detection results in tests that are simple to perform, produce rapid visual readouts and require no laboratory equipment. Challenges are (i) complex sample media of biological fluids, (ii) low levels of detection that are necessary for highly toxic compounds and (iii) the selectivity of the intended methods.

For further improvements as well as a better understanding of the underlying reaction mechanism kinetic as well as thermodynamic studies are required.

Proof-of-principle studies are an additional important aim for possible applications.

Abbreviations

ACCa	Aquacyanocobyrinicacid
ACCbi	Aquacyanocobinamide
ACCbs	Aquacyanocobyrinicacid heptamethylester
AdoCbl	Adenosylcobalamin
AqCbl	Aquacobalamin
ASTM	International *American Society for Testing and Materials* (ASTM)
ATP	Adenosine triphosphate
B12	Vitamin B12, cobalamin
c-acid-cobester	C-acid aquacyanocobyrinicacid hexamethylester
Cbl	Cobalamin
CHES	2-(Cyclohexylamino)ethanesulfonic acid
CIElab	a color-opponent space with dimension ***L*** for lightness and ***a*** and ***b*** for the color-opponent dimensions specified by the International Commission on Illumination (French *Commission internationale de l'éclairage* = *CIE*)
CNCbl	Cyanocobalamin
CO	Carbon monoxide
COHb	Carboxyhemoglobin
Cobinamid	Aquacyanocobinamide
CSPE	Colorimetric solid phase extraction
DCCbi	Dicyanocobinamide
DCCbl	Dicyanocobalamin

DCCbs	Dicyanocobyrinicacid heptamethylester
Dmbz	Dimethylbenzimidazole
DRUV-vis	Diffuse reflectance spectroscopy in the ultraviolet and visible range
EDTA	Ethylendiaminetetraacetic acid
EPA	United States Environmental Protection Agency
HEPES	4-(2-hydroxyethyl)-1-piperazineethanesulfonic acid
HCN	Hydrogen cyanide
HPLC	High performance liquid chromatography
LCt_{50}	*Lethal concentration & time* – the vapour or gas exposure (usually mg per m^3) that causes death in 50% of the exposed population within 1 min
LCMS	Liquid chromatography–mass spectrometry
LD_{50}	*Lethal dose* – the dose (mg per kg of body mass) lethal to 50% of the exposed population
LED	Light emitting diode
LOD	Limit of detection
KCN	Potassium cyanide
KOH	Potassium hydroxide
MeOH	Methanol
PAN	Polyacrylnitril
SAM	Self-assembled monolayer
SPE	Solid phase extraction
WHO	World Health Organisation

List of Key Compounds

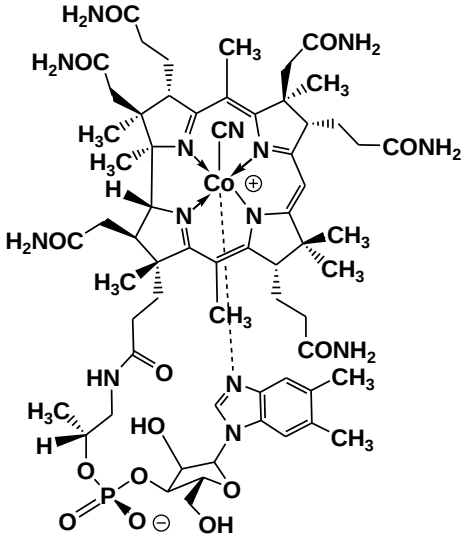

1, CNCbl, B12

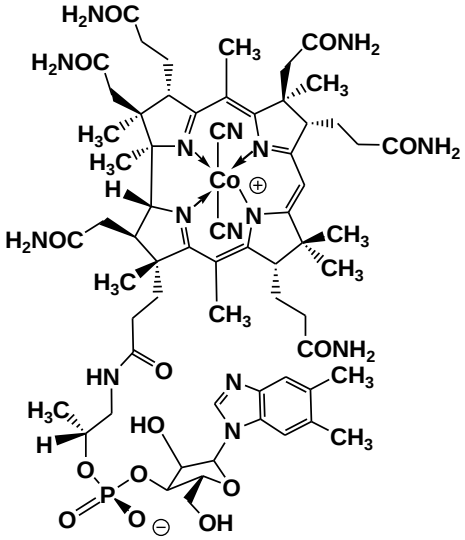

1-CN, DCCbl

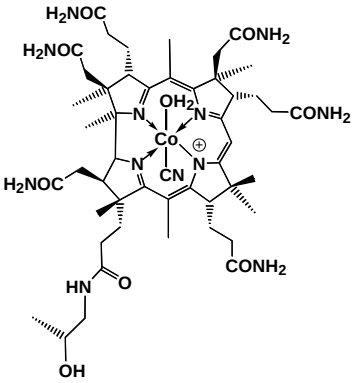

2$_{\alpha}$, ACCbi$_{\alpha}$

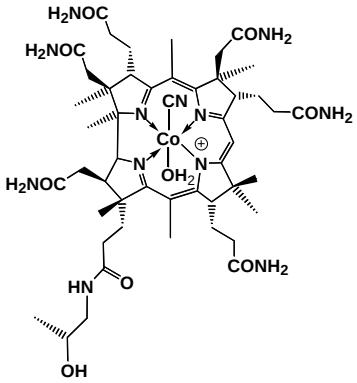

2$_{\beta}$, ACCbi$_{\beta}$

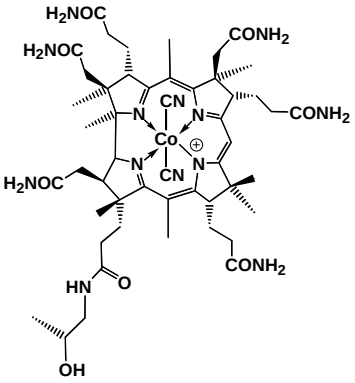

2-CN, DCCbi

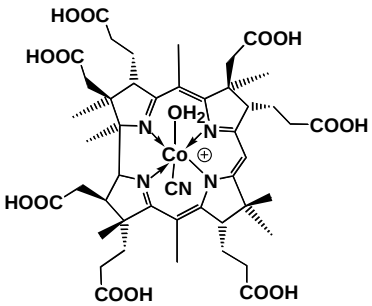

3$_{\alpha}$, ACCa$_{\alpha}$

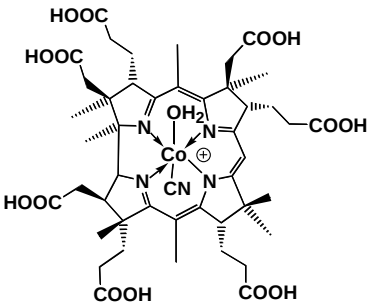

3$_{\beta}$, ACCa$_{\beta}$

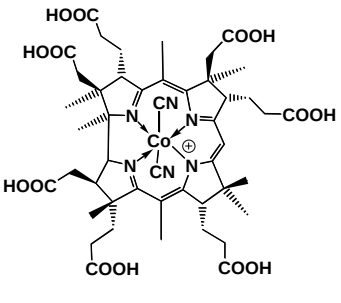

3-CN, DCCa

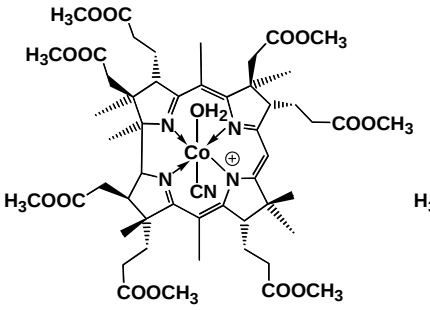

4$_{\alpha}$, ACCbs$_{\alpha}$

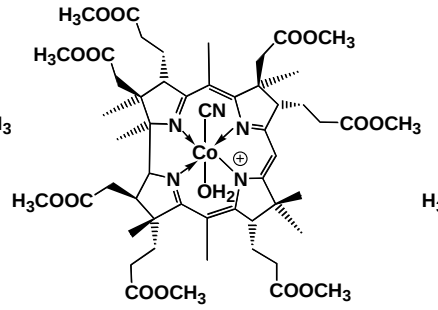

4$_{\beta}$, ACCbs$_{\beta}$

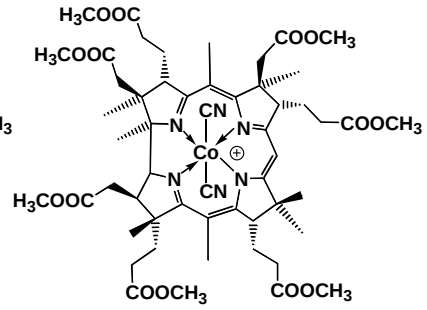

4-CN, DCCbs

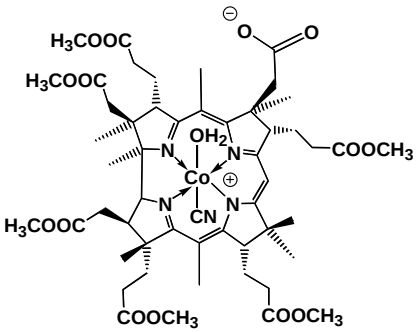

5$_{\alpha}$, c-acid-ACCbs$_{\alpha}$

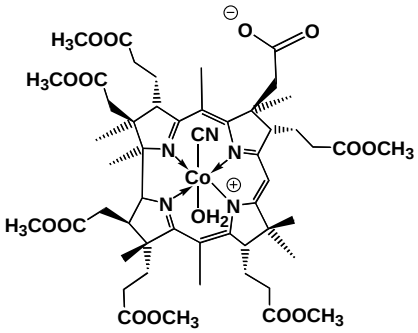

5$_{\beta}$, c-acid-ACCbs$_{\beta}$

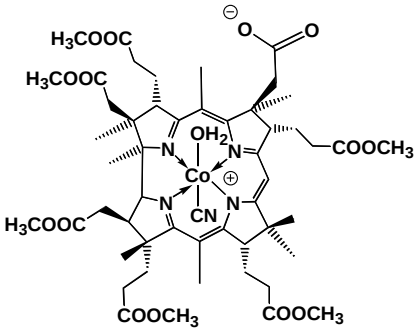

5-CN, c-acid-DCCbs

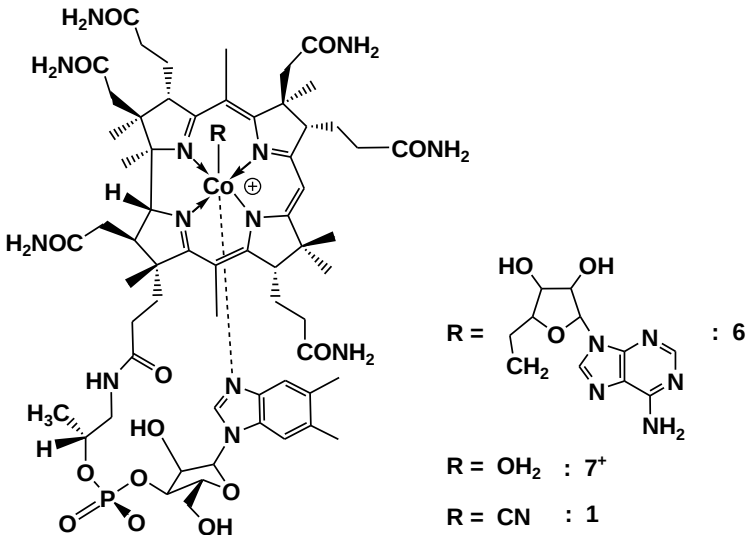

6, AdoCbl

7, AqCbl

1, CNCbl (B12)

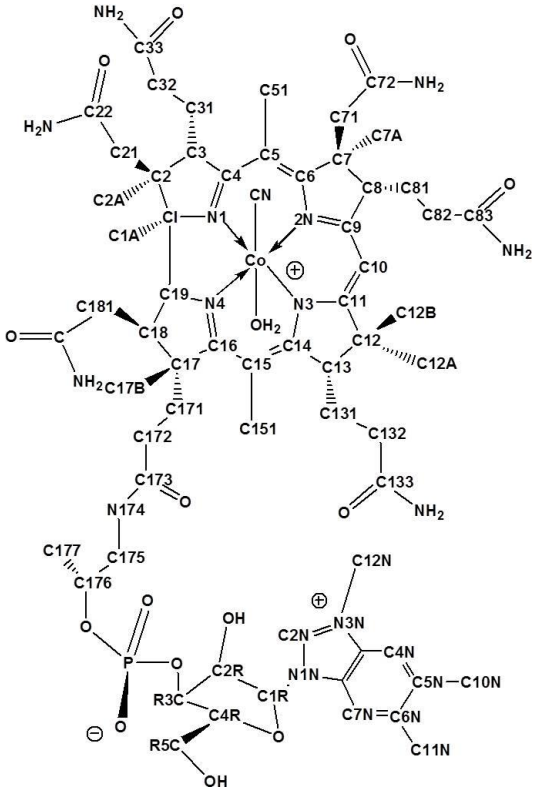

8

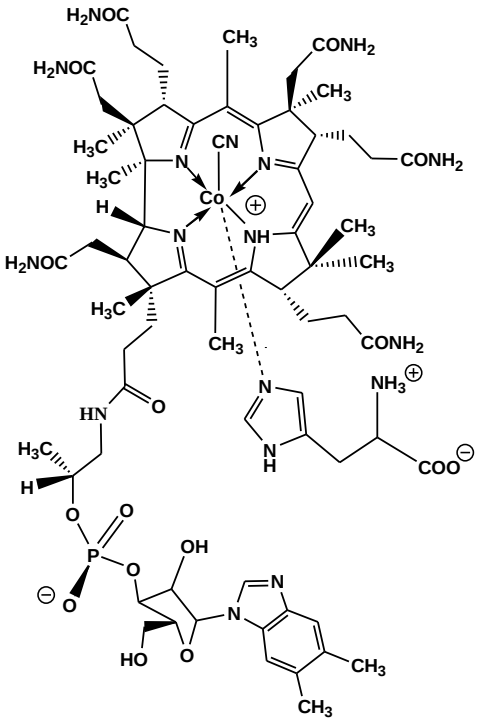

9

1 Introduction

Cyanide has a long history of precarious and productive use by mankind and offers a complex and fascinating chemistry. It occurs naturally in certain microorganisms and plants, but is also produced in bulk quantities for various important industrial applications. The high toxicity of this small negatively charged anion to almost all forms of life is a challenge in handling and control. Appropriate measures to monitor cyanide are therefore required to protect the environment and human health. In the last decades, the interest in cyanide management, transport, emissions, toxicity and detection attracted much attention from chemical research, industrial organisations, and regional and federal government agencies.[1-6] Straightforward colorimetric cyanide detection with the “naked-eye” based on a colour change of a chemosensor is desired for field applications by non-expert users without laboratory equipment. During this thesis we developed the first chemosensor for the rapid detection of endogenous cyanide in plants as well as of blood cyanide.

1.1 Chemistry of cyanide

The accidental discovery of *Prussian blue*, the first synthetic colour pigment, in 1704 in Berlin by the artist H. Diesbach initiated transition metal cyanide chemistry.[7] In 1782, hydrogen cyanide was identified by the Swedish pharmacist and chemist Carl W. Scheele (1742-1786). He isolated hydrogen cyanide as a flammable and water soluble gas by heating the dye *Prussian blue* with sulphuric acid.[7, 8] The acidity of the aqueous solution resulted in the names Berlin blue acid or prussic acid. Today it is known as hydrogen cyanide according to the Greek “kyanos”, meaning blue. Investigations of hydrogen cyanide by the French chemist Gay-Lussac (1778-1850) led to the realisation of oxygen free acids.[7]

The cyanide anion (CN^-) is isoelectronic to the small diatomic molecules and ions CO, NO^+, N_2, and C_2^{2-}, all characterized by a triple bond. Due to the negative charge, the cyanide group acts as the corresponding base to HCN, a colourless liquid

(Bp. 25.6°C) miscible with water. The relatively strong hydrogen carbon bond is responsible for a pKa value of 9.2 (at 25°C).[9]

Cyanide as an excellent σ-donor stabilizes d-metal ions particularly in higher oxidation states; nearly all transition elements form cyano-complexes.[10] The frontier orbitals of the negatively charged cyanide ion are energetically higher compared to those of its isoelectronic counterparts.[11] This property results in a better overlap of the highest occupied molecular σ-orbital with the lowest unoccupied d-orbital of the metal ion. However, the π*-acceptor orbitals are energetically too high for efficient back donation from the metal ion.[11] The cyanide anion can act as a terminal, monodentate ligand with carbon as the donor atom or as an ambidentate donor at both ends of the ion (e.g. in Ag(I) cyanide or *Prussian blue*). The cyanide ion is found at the strong field end of the electrochemical series and, therefore, most of the cyanide complexes are low spin species.[11]

Apart from thermodynamics, it is important to consider a wide variety of kinetic stability of metal-cyano complexes from inert to labile. Low spin Co(III) complexes with a d^6 configuration are regarded as typical inert transition metal ions compared to Co(II). The residence time of water in the inner coordination sphere of $[Co(H_2O)_6]^{3+}$ amounts to 10^5 s in contrast to approximately 10^{-6} s for $[Co(H_2O)_6]^{2+}$.[12] However, the nature of the coordinating ligands can dramatically influence these properties. The lability ratio of the Co(III) ion toward substitution at the axial position increases in the series of tetra-ammine, cobaloxime, porphyrin and corrin systems as follows 1: 10^4 : 10^6 : 10^9, corresponding to either an increasing extent of delocalization of the cis π-electron system or a decreasing size of the diameter of the macrocyclic cavity.[13, 14] It is suggested that both effects make the Co(III) ion softer, thus explaining the “Co(II)” like character in ligand substitution reactions at the axial positions.[15, 16] In contrast, interruption of the 13 atom, 14 π-electron delocalized system of the corrin ligand increases the hardness of the central Co(III) ion and reduces thereby its kinetic lability as demonstrated in a thorough recent study.[16-19]

Due to the highly covalent character of the metal-cyanide bond, a strong nephelauxetic influence and a strong trans-effect of the cyanide ligand are observed.[11, 16, 20] Both effects are extremely favourable for applications of

aquacyano-corrinoids as chemosensors for cyanide detection. Axially coordinating cyanide alters the electronic properties of the corrin ring and causes a colour change in the case of cyanide coordination. The trans-effect facilitates the substitution of the Co(III) bound water in aquocyano corrinoids, the basic reaction in colorimetric cyanide detection that have been investigated in this work.

Metal-cyanide complexes are often anionic with the general formula $M(CN)_x^{(x-n)}$ (n = oxidation state of the metal).[21] The stability of these compounds depends on the nature and oxidation state of the central metal ion as well as the pH of the solution, the mechanism of cyanide release and the temperature.[21] Sodium, potassium and calcium cyanide are highly soluble in water and therefore toxic.

According to the strength of the metal-cyanide bond, weak and strong metal-cyanide complexes are distinguished. Weak metal-cyanide complexes, such as $Cu(CN)_3^{2-}$, $Zn(CN)_4^{2-}$ and $Ni(CN)_4^{2-}$, dissociate under mildly acidic conditions (pH 4-6) and liberate hydrogen cyanide.[21] Strong metal-cyanide complexes such as $Fe(CN)_6^{3-}$, $Fe(CN)_6^{4-}$ and $Au(CN)_2^-$ complexes are rather stable even under mildly acidic conditions (pH > 2). Ferro- and ferri-cyanides decompose in aqueous solutions to release free cyanide when exposed to ultraviolet light.[22]

1.2 Cyanide groups in nature and biological systems

Hydrogen cyanide is believed to have been a key component in the atmosphere of the prebiotic period.[23] The Stanley Miller experiment in 1953 demonstrated the formation of HCN and organic compounds such as aldehydes from prebiotic earth atmosphere containing methane, ammonia, hydrogen and water.[24] Oro und Kimball demonstrated the polymerization of HCN to adenine.[25] Today, CN-groups are found in biological systems such as plants, microorganisms and animals of the phylum *Anthropoda*.[26]

[Fe]-only hydrogenases and [FeNi] hydrogenases, common in many microorganisms, are enzymes that catalyse the reversible splitting of dihydrogen into protons and electrons.[27] In the active site of [FeNi] hydrogenases, a dinuclear Ni-Fe centre is bound via four cysteinates to the enzyme. Surprisingly, the structure also revealed

the coordination of biologically uncommon ligands; three diatomic ligands, one CO and two CN-groups stabilize the iron additionally (see Figure 1, *left*).[27-29]

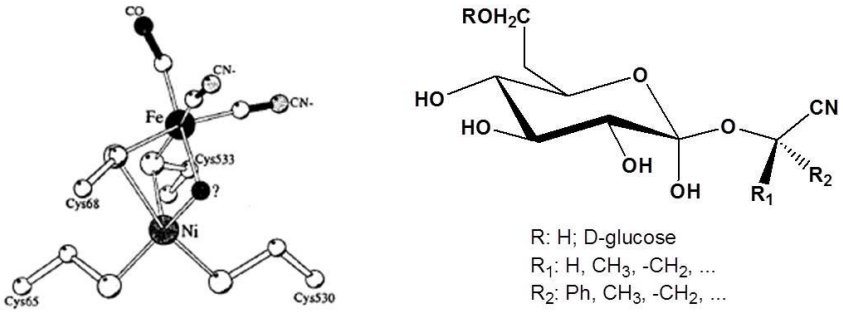

Figure 1. Structure of [NiFe] hydrogenase of *Desulfovibrio gigas*[29] (*left*) and a general structure of cyanogenic glycosides[26] (*right*).

More than 2650 plants and animal species from *Anthropoda* contain cyanogenic glycosides, derivatives of α-hydroxonitriles (cyanohydrins) that are stabilised by β-glycosidically bonded sugars (see Figure 1, right).[30] Cyanogenic glycosides are naturally synthesized from amino acids as their biogenetic precursors. The enzymatic liberation of cyanide (see 1.4.2) is mostly regarded as defence mechanism against herbivores and pathogens.[30] Additional functions as storage compounds for nitrogen and amino acids, which are utilized in growing seedlings, are approved.[30] Enzymes like oxidoreductases, transferases, hydrolases und lyases catalyse the reaction to formamide and ammonia, the oxidation to cyanate and thiocyanate or the reduction with nitrogenase to ammonia.[31, 32] The significant seed-germination stimulating influence of cyanide, released from the cyanohydrin glyceronitrile could be proven on various fire-responsive species from different continents.[33]

1.3 Toxicity of cyanide

1.3.1 Toxicity and symptoms

Cyanide is widely recognized as rapidly acting and lethal poison in form of gaseous hydrogen cyanide (HCN), as aqueous solution or as solid like common alkali metal salts. The lethal concentration of gas exposure per minute causing death in 50% of the exposed population (LCt_{50}) amounts to 2500 - 5000 mg·min/m^3.[7] The estimated LD_{50} doses of either intravenously administered cyanide or after skin contact are

between 1.0 and 2.5 mg/kg of bodyweight and 100 mg/kg of bodyweight, respectively, depending not only on the dose but also on (i) the chemical form of cyanide, (ii) the route and (iii) the speed of administration.[34]

Guideline	**Maximum concentration of cyanide [µg · L^{-1}]**
US EPA[35]	200
European Union[36]	50
Australia[37]	4
WHO[38]	70

Table 1. Guideline values of different organizations for the limits of maximal cyanide concentration in drinking water.[35-38]

There are different international or local guidelines for the maximum contaminant concentration of cyanide in drinking water; some of them are summarized in Table 1.[35-38] Signs and symptoms of acute cyanide poisoning reflect the deactivation of cell respiration particularly of the heart and the brain, i.e., organs that rely on continuous oxygen supply.[39, 40] Initial effects are hyperpnoea and tachycardia as an attempt to activate the respiration. Early neurologic manifestations include headache, giddiness and anxiety that are followed later by nausea, cardiac arrhythmias, coma seizure and respiratory depression up to death (see Table 2).[34, 41-45]

Symptoms	**Concentration in air (ppm)**
Smell	2 - 5
Maximum accepted working place concentration	10
Feeling of heat, vertigo, confusion	20 - 40 (light symptoms after some hours)
Nausea, vomitus	45 - 54 (tolerable 0.5- 1 hour)
Coma, drop in blood pressure, tachycardia, convulsion	100 - 200 (fatal after 0.5- 1 hour)
Apnoea, before cardiac arrest	300 (immediately fatal)

Table 2. Symptoms of HCN intoxication.[34, 41, 46, 47]

1.3.2 Pathopharmacology

In humans and animals hydrogen cyanide is readily absorbed following inhalation, oral and dermal exposure.[48] It is predominantly present as hydrogen cyanide (pKa of 9.2) at physiological conditions. Due to the small size of the molecule and the moderate lipid solubility it diffuses rapidly through the tissue. The high affinity of cyanide to the ferri form of iron (Fe(III)) results in binding mostly to methaemoglobin in the blood. Only approximately 1% of haemoglobin in blood, containing the ferrous form of iron (Fe(II)), is present as methaemoglobin.[49]

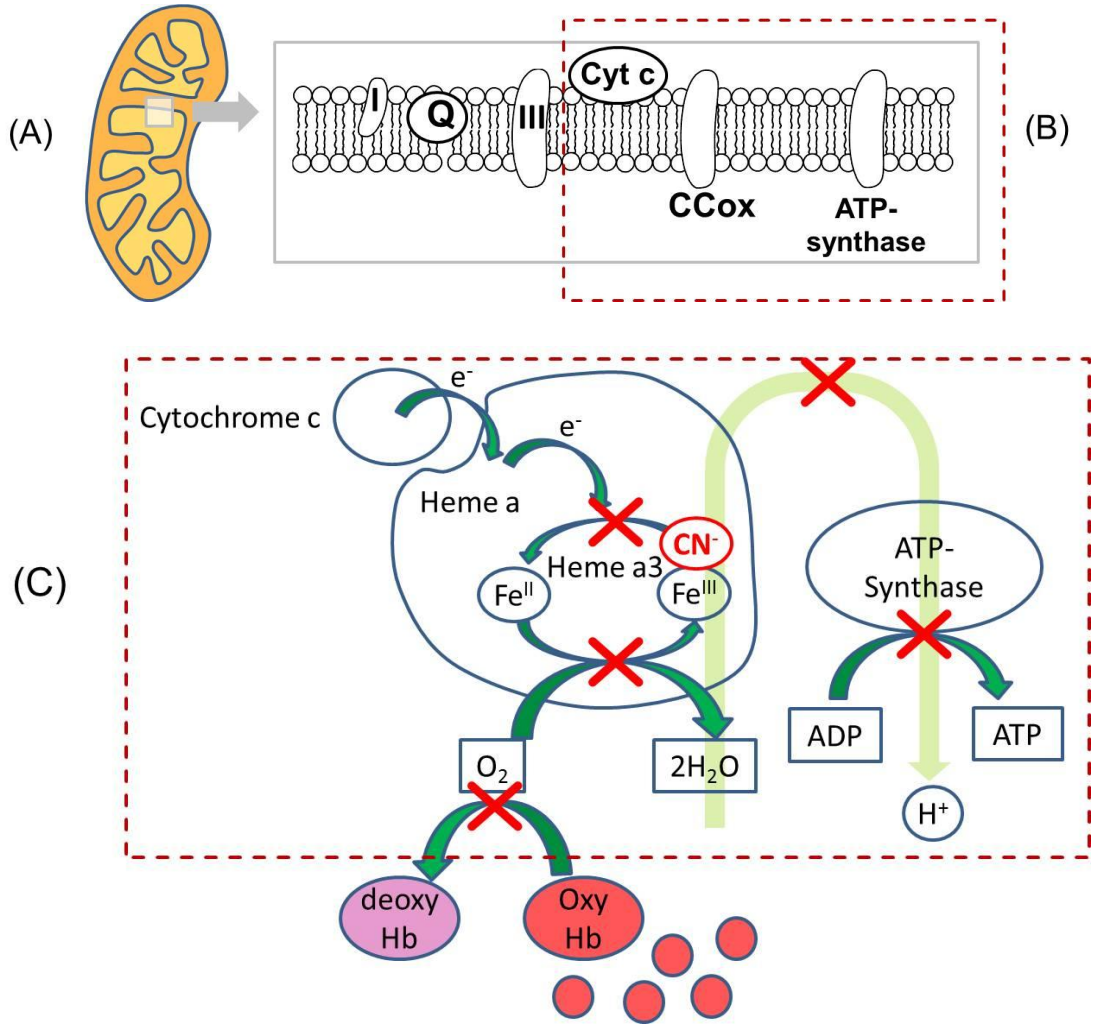

Scheme 1. (A) Scheme of mitochondria and (B) the electron transfer chain in the mitochondrial inner membrane with the enzyme complexes I, III, cytochrome c (Cyt c), cytochrome c oxidase (CCox) and ATP synthase. (C) Effect of cyanide on mitochondrial aerobic metabolism: inhibition of electron transport, redox activity of heme a3, proton pump and oxidative phosphorylation.[50]

Cyanide deactivates several enzymes. Most important is the inhibition of cytochrome c oxidase, the terminal oxidase of the respiratory chain located in the inner membrane of the mitochondria.[51] Cyanide binds with high affinity to the ferric ion of the heme a3 cofactor and blocks the binding site for dioxygen.[52] Therefore, the electron transfer for the reduction of oxygen to water is suspended and the iron remains in its ferri form. As a consequence, the proton pump from the mitochondrial matrix across the membrane, normally linked to the electron transfer, is also stopped. The proton gradient and the electro chemical potential at the membrane of the mitochondria that drives the protons back into the matrix via adenosine triphosphate synthase cannot be sufficiently established.[53] Oxidative phosphorylation, the production of ATP for the universal energy transport in the cells is interrupted, causing a depletion of intracellular ATP. The prevention of oxygen use causes an alteration from aerobic to anaerobic respiration resulting in acidosis, a lactic acid accumulation (see Scheme 1). Organs with high oxygen consumption such as the brain and the heart are affected the most. [34, 54, 55]

1.3.3 Diagnosis and antidotes

Currently there are four different effective antidotes against cyanide intoxication available; sodium thiosulfate, sodium or amyl nitrite, dicobalt EDTA ($Co_2(EDTA)(H_2O)_6$) and hydroxocobalamin.[50, 56-59] Thiosulfate serves as a sulphur source for the enzymatic formation of less toxic thiocyanate from cyanide. It acts relatively slowly and mainly in the blood and plasma. The most important side effects include nausea, vomiting and irritation. Sodium nitrite partly oxidizes the Fe(II)-haemoglobin to Fe(III)-methaemoglobin that eliminates cyanide from the system because of its higher binding affinity to cyanide than haemoglobin or cytochrome oxidase. Treatment is problematic in the case of a CO-intoxication with carbon monoxide (CO).[60] For fire victims with concomitantly blocked hemoglobin by CO, an additional reduction of the reversible oxygen carrier haemoglobin is undesirable. Vasodilation and hypotension are significant side effects. The antidote cobalt EDTA forms less toxic cobalt cyano-complexes in the blood, but has an enhanced cardiovascular risk. Hydroxocobalamin is administered as the most effective antidote in pre-hospital intervention, usually 5 g during 20 minutes.[61, 62] It detoxifies cyanide

by forming nontoxic cyanocobalamin (vitamin B12) that is renally excreted.[63] It has been approved in France as Cyanokit™ (Merck-Santé S.A.S.) in 1996.[64] In Switzerland it has been recommended to the emergency service since 2011.

Immediate administration of an antidote is of utmost importance in case of cyanide poisoning.[65] It is puzzling that no rapid tests for the detection of blood cyanide in emergency situations are currently available. The analysis of blood cyanide concentrations is based on either spectrophotometric detection after micro diffusion or on isotope-dilution gas chromatography-mass spectrometry (ID GC/MS) experiments.[66] Results become available only within approximately two hours, which is too long to be acceptable for treatments of cyanide poisoning in emergency situations. Alternatively, a serum lactate level higher than 8 mmol/L indicates cyanide poisoning but is not specific. Therefore, the initial diagnosis of cyanide poisoning still relies on the presented symptoms and the general clinical status of the patient.[65]

A simple and reliable method for the rapid identification of blood cyanide is highly desirable for first aid treatment of patients with acute cyanide poisoning by medical personnel.[65]

1.4 Sources of cyanide exposure

1.4.1 Historical cyanide exposure

Cyanide containing plants and pits have already been used in ancient civilizations as lethal poisons.[7, 8, 67] An Egyptian papyrus reports on the use of peach pits in judicial executions, the “penalty of the peach”.[8] The “cherry death” was one of the Roman methods of execution using cherry laurel leaves. The Greek physician Pedanius Dioscorides (circa 40-90 AD) refers to the poison of bitter almonds in his five-volume encyclopaedia “De materia medica”. The first detailed description of the intoxicating effects of bitter almond extract was published by the Swiss pharmacologist Johann J. Wepfer (1620-1695).[8] In the 19th century the application of cyanide contaminated bayonets was proposed in the Napoleonic War (1807-1814) and in the Franco-Prussian War (1870-1871).[68]

1.4.2 Natural occurrences

The most important natural sources of cyanide poisoning in humans and animals are plants and their seeds or pits. Over 2650 species of plants produce cyanogenic glycosides, including edible plants like cassava, sorghum, sweet potatoes, maize, millet, bamboo, lima beans, peas, soybeans, almond kernels, lemons, limes and seeds of peaches, apricots, prunes and flax.[30] More than 60 cyanogenic glycosides are known including linamarin and lotaustralin in cassava and lima beans, amygdalin in almonds, taxiphyllin in bamboo shoots and prunasin in stone fruits.[30] Usually they are termed with their trivial names according to the first reported natural source.

The toxicity of cyanogenic plants is based on the enzymatic hydrolysis of the cyanogenic glycosides by a corresponding beta-glycosidase.[69] Cell rupture during food preparation or consumption brings the spatially compartmentalized components into contact, activating the enzymatic hydrolysis (A) to sugars and a cyanohydrin that rapidly decompose to hydrogen cyanide and a ketone or aldehyde (B) (see Scheme 2). [70-72]

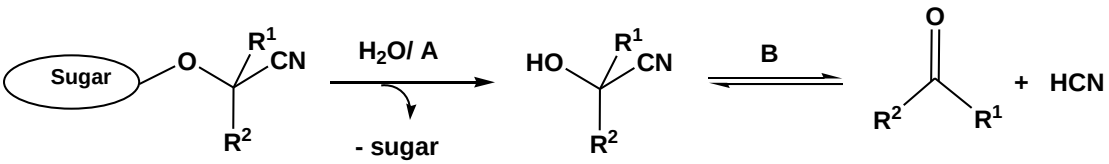

Scheme 2. General reaction scheme of the enzymatic hydrolysis of cyanogenic glycosides to a sugar and acetone cyanohydrine (A) that subsequently decomposes to a carbonyl compound and HCN (B).[71-75]

Cassava (*Manihot esculanta* Crantz), the sixth most important food crop globally, and sorghum (*Sorghum vulgare*) are staple foods for around 800 million people in Pacific Island countries, Latin America, Africa and regions of Asia.[76, 77] Cassava is increasingly popular due to its agricultural advantages that include good yields in poor soils without fertilizer, drought resistance and storability in the ground as food reserve for up to 3 years. The rising production of cassava from 2000 to 2010 in millions of tons is depicted in the diagram of Figure 2. Nigeria has the highest cassava production worldwide with approximately 40 million tons.

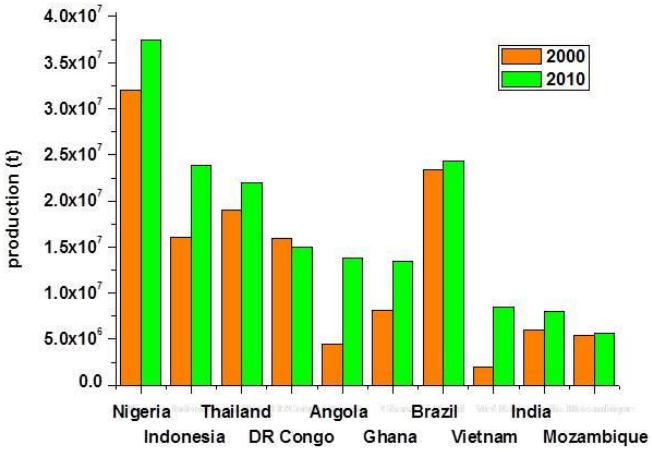

Figure 2. Production of cassava in tons in 2000 (orange) and 2010 (green) of the major cassava producing countries.[78]

Tubers and leaves are used for human and animal consumption, respectively. Cassava tubers are classified as “bitter” or “sweet” based on their content of cyanide. Sweet varieties contain 15-400 mg HCN/kg fresh weight; bitter cassava, which is more drought resistant and cheaper, has a content of 400-2000 mg HCN/kg fresh weight. The vitamin-packed leaves, consumed particularly in Africa, commonly contain 1000-2000 mg HCN/kg on dry matter basis.[77, 79, 80] Many different methods of proper processing of cassava have been developed in hundreds of years including soaking, fermentation, cooking, steaming, chipping, drying and roasting in varying order.[79, 81-85] Nevertheless, commercially available cassava products on the market often contain cyanide levels higher than the WHO-recommended safe level of 10 ppm.[86, 87] The cyanide contents of a selection of products of processed cassava are listed in Table 3. The lethal amount of a product containing 260 mg/kg of cyanide for a child of 20 kg body weight is in the range between 40 to 270 g, whereas an adult of 60 kg can consume up to 120 to 810 g.[88]

Product	Origin	Total cyanide [mg/kg]
Vegetable chips[88]	Australian and imported ingredients	26 (6)
Tapioca crisps (BBQ)[88]	Singapore	42 (8)
Cassava chips[88]	India	262 (34)
Frozen cassava roots, peeled, large pieces[88]	Vietnam	52 (7)
Tapioca flour, starch and pearls[88]	Thailand	<1
Gari[89]	Nigeria	25 (5)
Flour (soaking for 3 days)[90]	Zaire	32 (3)
Chinyanya (sun dried)[91]	Tanzania	133 (18)

Table 3. Total cyanide content of different commercially available products of cassava (three samples of each product were tested, standard deviation in brackets).

Inappropriate processing and release of cyanide during food preparation causes significant public health problems. Acute and chronic diseases are reported including konzo, an irreversible spastic paraparesis of the legs, endemic goitre and tropical ataxic neuropathy (TAN), a chronic condition of gradual onset that causes loss of vision, ataxia of gait, deafness and weakness.[92-98] Epidemics of such diseases often correspond to war and drought.[99]

Monitoring the cyanide content during food production or in cassava products before consumption is highly desirable. A simple test applicable by anybody without technical equipment could help to avoid food related diseases.[100]

Egan and Bradbury developed a picrate kit to detect cyanide in cassava products as well as urinary thiocyanate that correlates to cyanide uptake.[101-105] The kit is available free of charge for health and agriculture services and has been used to survey the cyanide content of cassava products. However, this picrate method takes at least 12 h at 30°C for cyanide detection and is, therefore, of limited applicability in field surveys.[88]

1.4.3 Anthropogenic sources

HCN and its alkali salts are basic chemicals used in metallurgy, electroplating, gold mining and as precursors for synthetic materials like cyanohydrin and adiponitrile that are processed to form synthetic fibres such as spandex, rayon and nylon. Cyanide based pesticides and insecticides are used for commercial mass fumigations (see Figure 3).[106]

The large annual industrial production (2.6 x 10^6 t in 2001) of cyanide include a potential risk of accidental or intended cyanide liberation during transportation, storage, commercial use or of careless handling.[107] The key sources of cyanide release into water and soils are wastes and discharges from metal mining, electroplating and cyanide fishing activities. Cyanide contaminations in soil (up to 10 g/kg) and in groundwater (up to 30 mg/L) occur around old spent aluminium smelting facilities and thousands of former gas plant sites.[108] Most dramatic is the accidental release of cyanide from gold mines with heap leaching operations.

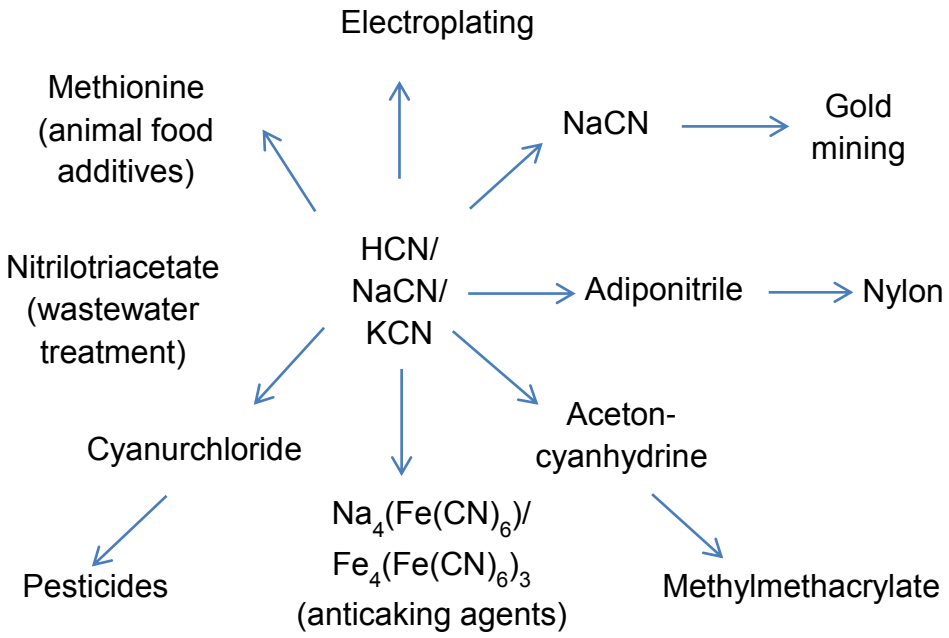

Figure 3 . Industrial products derived from hydrogen cyanide and its salts.[23, 107, 109-111]

In the period between 1990 and 2000 five examples of such discharges were reported. Well-known in Europe is the accidental release of 10^5 m^3 of free cyanide

containing tailing water from a gold mine near Baia Mare in Romania in 2000. This event is considered as one of the biggest ecological catastrophes in Europe ever.[23]

1.4.4 Iatrogenic sources

The sodium nitroprusside administered as an antihypertensive drug is an iatrogenic source of cyanide.[56, 58, 112] It is normally metabolized in the liver by the enzyme rhodanase to thiocyanate and subsequently excreted through the kidneys. Impaired renal function can lead to accumulation and poisoning of thiocyanate. Therefore, serial screening of renal function and methaemoglobin levels are required in nitroprusside therapy.

1.4.5 Smoke from fire

Cyanide poisoning in Europe and North America is most frequently caused by smoke inhalation from structural or enclosed space fires.[58] About 5'000 to 10'000 fire deaths and more than 23'000 injuries including those by 5'000 fire fighters are registered annually in the United States.[64] In 2006, 30 fire victims were reported in Switzerland and 510 in Germany.[113, 114] Between 60 and 80 % of these casualties are caused by smoke inhalation.[114] Carbon monoxide has historically been associated with morbidity and mortality after smoke inhalation.[115] In the last decades, studies in combustion and forensic chemistry demonstrated the influence of additional toxic gases generated in a fire.[106, 116] Carbon monoxide, hydrogen cyanide and lung irritants such as hydrochloric acid, sulphur and nitrogen oxides as well as ammonia are the most prevalent gases of about 5000 immediate toxic threats detected in fire smoke.[42] The constituents of the smoke depend on the burning material, oxygen supply, temperature and duration of the fire.[117] The incomplete combustion of nitrogen containing materials such as polyurethane, melamine, acrylonitrile, nylon, wool and silk generates hydrogen cyanide.[118] These materials are increasingly used in building construction, interiors and furnishings. A Swedish study investigated the contribution of CO and HCN in fire related deaths during the period 1992-2009 including data from 2303 fire victims.[114] In contrast to CO, data of blood cyanide levels are subject to post-mortem decay due to the instability of cyanide in blood. A temperature and concentration dependent rate of cyanide loss is

reported in various studies (84 % in 24 h at 25°C; $t_{1/2}$ = 12 min at initial cyanide concentration of 5 mg/L).[116, 119, 120] Nevertheless, in around 31% of the victim's blood cyanide concentrations above 0.5 µg/g were found, indicating significant HCN exposure. In 4 % of these cases life-threatening cyanide levels above 2 µg/g were reported. These data are consistent with the results of various studies showing the direct relationship between blood cyanide concentration and mortality.[121] A cumulative toxic effect of the combined exposure to cyanide and CO is suggested and complies with other studies where high but non-lethal COHb levels in addition to elevated cyanide levels of the victims were found.[116, 121, 122] It has also been observed that fire fighters and other victims of smoke inhalation associated cyanide poisoning tend to experience rapid incapacitation resulting in a lack of fight- or flight response that can indirectly cause death.[64]

Although smoke inhalation caused cyanide poisoning had been overlooked for a long time, today's emergency medical personnel and fire professionals are trained in the management of such patients in many countries.[58, 64, 106] The immediate administration of an antidote at the scene is the key to successful cyanide treatment after moving the victim from the source of exposure. Even though various methods for cyanide detection in blood do exist, no test for the rapid confirmation of cyanide poisoning is currently available. As a result, the treatment with an antidote is generally based on presumptive diagnosis far away from a medical facility, and provided by medical personnel with the limited resources of an emergency setting.

1.4.6 Terrorism and mass poisonings

Cyanide has been used intentionally as a poison in genocides, mass homicides, suicides and a weapon of war. The first large-scale production of cyanide as a chemical weapon started in 1915/1916 in France during World War I. Approximately $3.6 \cdot 10^6$ kg were produced by distilling concentrated aqueous solution of KCN with sulphuric acid.[7] But the application provided no military advantage. Concentrations of cyanide required to incapacitate or kill the enemy were not achieved due to the high volatility of cyanide and lacking cumulative effects. Starting in 1916, cyanogen chloride as a heavier and less volatile toxic gas that irritates the eyes and lungs was employed.[7, 123]

During the Holocaust, Zyklon B, a porous supporting material impregnated with HCN, was deployed in the gas chambers of the death camps. Even 50 years later, it could be detected in the walls of the crematoria.[124, 125]

But cyanide continues to be used as plentiful and readily available terrorist weapon. It requires no special handling skills, can kill quickly and is easily available.[126-128] The following examples of the last 20 years illustrate the danger and the dimension of deployment of cyanide to the civil population. A mass suicide of the members of the *Peoples Temple* in Jonestone, Guyana was performed with a grape flavoured drink enriched with potassium cyanide, resulting in the death of 900 children and adults.[129] In March 1995, cyanide was identified after a terrorist attack in the subway in Tokyo, Japan.[7] In 2002, an al-Qaeda's attempt to deploy cyanide to kill commuters on the London subway was prevented.[126]

1.5 Methods of cyanide detection

The various sources of possible cyanide exposure require safety monitoring to protect humans, animals and the environment from the adverse effects of natural or accidental cyanide release and exposure, or its intentional use as a poison.[23, 130]

1.5.1 Standard methods

Several methods have been standardized in the past decades to monitor cyanide in different matrices including water, air, soil, food or biological samples like blood and urine.[48] Complex or coloured samples require the liberation of hydrogen cyanide by acidification and absorption in basic aqueous solution before further analysis. Titration methods and spectrophotometric quantification, based on the *König reaction* and the argentometric titration, are legislated in German code DIN 38405-13 and EPA methods 9010-90.[131-133] The *König reaction* includes the oxidation of cyanide to cyanogen chloride and the following reaction with a pyridine/ barbituric acid mixture or isonicotinic acid/ dimethylbarbituric acid yielding in a blue polymethine dye that is visually detectable. The argentometric titration is based on the first method of cyanide determination with silver nitrate introduced by J. von Liebig.[134] An excess of silver can be detected by a colour reaction with an indicator or the precipitation of silver cyanide as shown in Scheme 3.

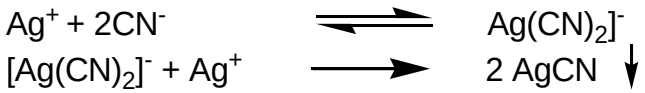

Scheme 3. Reaction for the coordination of cyanide to silver.[135]

Other certified standard tests include potentiometry with cyanide selective electrodes[132] and flow-injection amperometry.[136] Besides these certified methods, commercial short tests for workplace and personnel protection are also available and include the *Dräger test tubes* (see Scheme 4) and *Dräger gas detectors*[137] (product codes 6809150 and 68 10 887, Dräger, Lübeck) and the *Merckoquant Cyanid-Test* (product code 1.10044.0001, Merck, Darmstadt) based on the *König reaction*. Picric acid test kits for cyanide detection in food are available in particular in the tropical countries.[103]

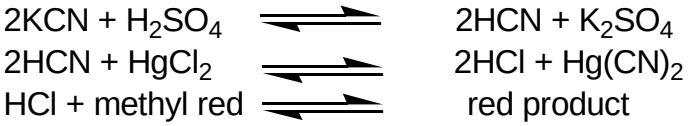

Scheme 4. Reaction scheme for the colorimetric cyanide detection in Dräger test tubes.[137]

All these methods are either time consuming or limited by disturbing anions and require technical equipment as well as trained personnel. Additional problems are the toxicity of the reagents and the explosiveness of picric acid. Often multistep sample pre-treatment, pre-concentration and organic solvents are necessary. Standard deviations in *Dräger test tubes* reach up to 30 % improved systems are therefore required.

New cyanide sensors and cyanide sensitive analytical methods have been established in the past ten years for special applications such as automatic industrial wastewater monitoring, food processing, and analysis in complex biological samples in particular in blood. More than 90 publications in the past 7 years reflect the development in optical methods including colorimetry, fluorimetry, near-infrared cavity ring down spectroscopy (NI-CRDS) and AAS, electrochemical methods like potentiometry and amperometry, mass spectrometry and gas chromatography.[138]

1.5.2 Colorimetric cyanide detection

Colorimetric methods are very useful for the detection of cyanide because of the simple visual confirmation of the presence or absence of the target analyte. Nearly 50% of all detection methods for the life threatening management used by first responder teams in the U.S. are colorimetric methods.[139] Semi-quantitative estimation is possible using colour charts; quantitative information can be received by spectroscopic measurements at appropriate wavelengths.[138, 140] Moreover, colorimetric identification of toxic substances is practicable even for the untrained population at relatively low cost.

Recent advances in colorimetric cyanide detection have been reviewed with respect to different aspects by Zelder and Männel-Croisé,[140] Xu et al.,[141] Cho et al.,[142] and Ma and Dasgupta.[138] The optical chemosensors take advantage of either the strong nucleophilicity of cyanide or the high binding affinity towards transition metal ions. The following strategies of bond formation between cyanide and the receptor can be distinguished; nucleophilic addition to an activated carbon or boron with C-C- or C-B-σ-bond formation, hydrogen bond formation (Scheme 5) and metal coordination.[140] The organic binding reactions rely on oxazine, pyrylium,[143] squaraine,[144] trifluoroacetophenone[145] and trifluoroacetamide derivatives,[146, 147] acridinium salts, and benzil or b-vinyl substituted calix[4]pyrrole systems[142]. Most popular is the nucleophilic attack of cyanide to an activated carbonyl group yielding in a cyanohydrin and causing an optical signal (Scheme 5., reaction A). Sessler et al. used the advantage of the catalytic effect of cyanide for the benzil-rearrangement (Scheme 5, reaction B) that promotes a high sensitivity with a limit of detection of approximately 1.7 µM.[148] Moreover, organically based receptors comprise the best-established standard methods of the *König reaction* (see 1.5.1) and the picric acid reaction (see 1.4.2).

One common drawback of these newly developed sensor systems is the need of organic solvents, whereas cyanide recognition is generally required in aqueous solution such as in biological samples or in water. Other issues concern the influence of water or pH on the sensitivity of the chromophores, in some cases low selectivity in

the presence of foreign anions or long reaction times (10 – 60 min) have been observed.[148]

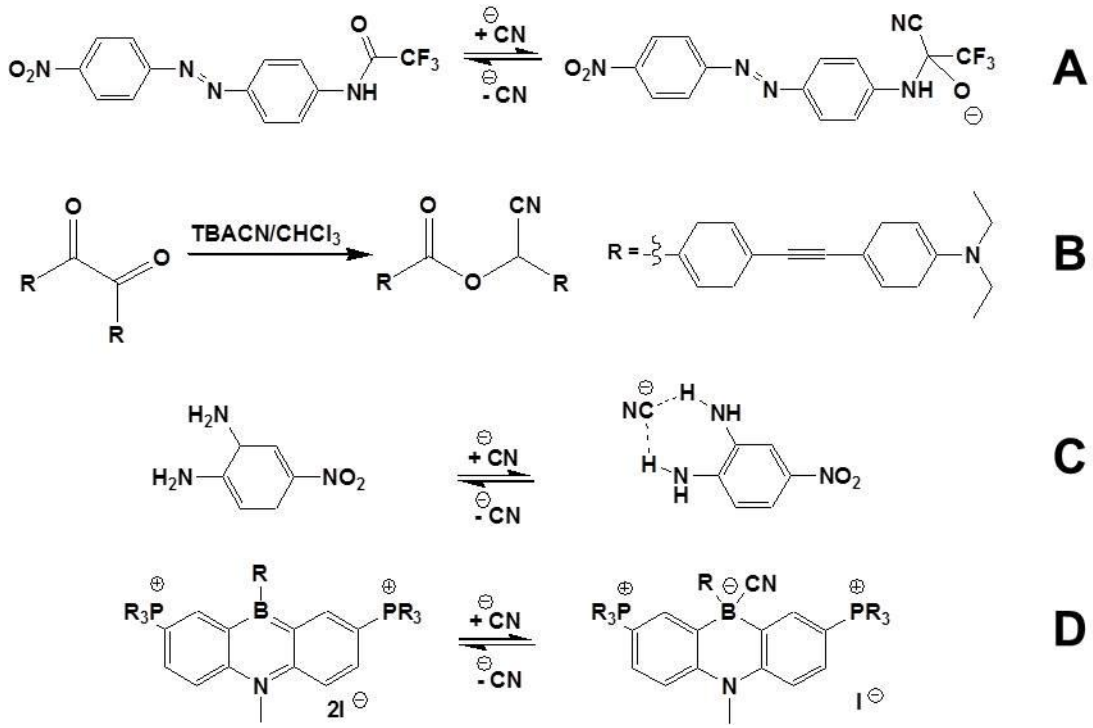

Scheme 5. Colorimetric cyanide sensors based on a covalently linked binding site to an activated carbon (reaction A, B) or a boron centre (reaction D). Hydrogen bonding based receptors (reaction C).

Hydrogen bonding interactions between receptors and cyanide are rather unselective. Incorporation of a sensor in nanostructured Al_2O_3 films demonstrates an innovative approach.[149] Cyanide coordination to a Lewis acidic boron centre has led to a variety of different sensors that allow the selective discrimination between cyanide and fluoride.[150-152]

The excellent binding properties of cyanide to transition metal ions make them suitable for cyanide sensing.[140] Three different approaches based on optical signalling chromophore complexes (i-iii) have been employed: (i) the direct formation of coloured metal-cyano complexes, (ii) the displacement of a transition-metal cyano-complex from an optical signalling organic subunit, and (iii) cyanide coordination to a metal-chromophore complex yielding a cyano-metal-chromophore complex (see

Scheme 6). Typical examples are (i) the formation of *Prussian blue*, (ii) the removal of copper from imidazole-functionalized polyfluorene to form a $[Cu(CN)_x]^{(1-x)}$ complex and (iii) the production of coloured dicyano corrinoids.[140, 141]

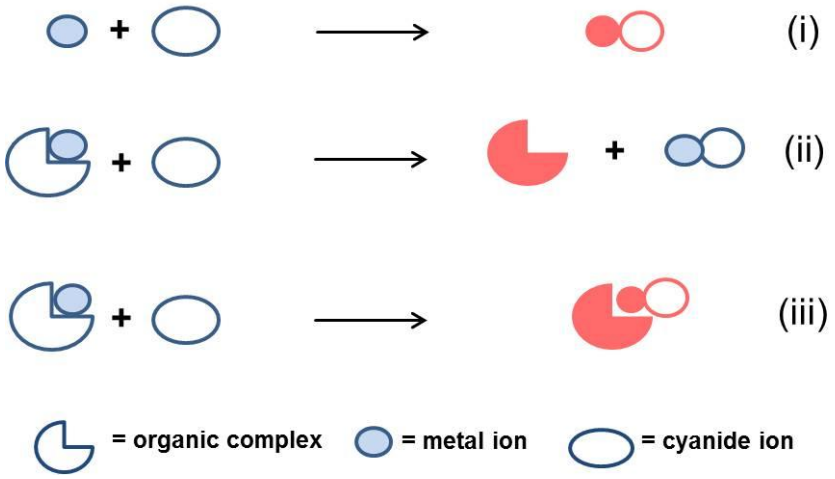

Scheme 6. Schematic presentation of three different approaches for colorimetric cyanide detection forming coloured metal-cyanide complexes (i), coloured organic compounds (ii), or coloured cyano-metal-chromophore complex (iii).

The formation of coloured transition metal complexes like *Prussian blue* (see Scheme 7) have been used for different spot tests.[130] However, the unspecific and/or little sensitive colorimetric response required further improvements and gave rise to the development of metal-based chemosensors.

$$Fe^{2+} + 6\ CN^- \longrightarrow [Fe(CN)_6]^{4-}$$
$$4\ Fe^{3+} + 3[Fe(CN)_6]^{4-} \longrightarrow Fe_4[Fe(CN)_6]_3$$

Scheme 7. Formation of *Prussian blue* from Fe(III)salts and hexacyanoferrat(II).[52]

Recently, the decomplexation strategy has attracted special attention. It utilizes the high binding affinity of cyanide to copper. The demetalation of various organic copper complexes by cyanide to thermodynamically more stable $[Cu(CN)_x]^{(1-x)}$ species is accompanied by a colour change of the organic dye.[153, 154] Li et al. employed that system to a fluorene polymer detecting as low as micro molar concentrations of cyanide (see Scheme 8).[154, 155] An alternative approach has been introduced by Lou et al. whereby the removal of cyanide from an organic dye is accompanied by a

colour change from yellow to blue.[156] The most important advantage of these systems as compared to the other examples is their application in pure water.

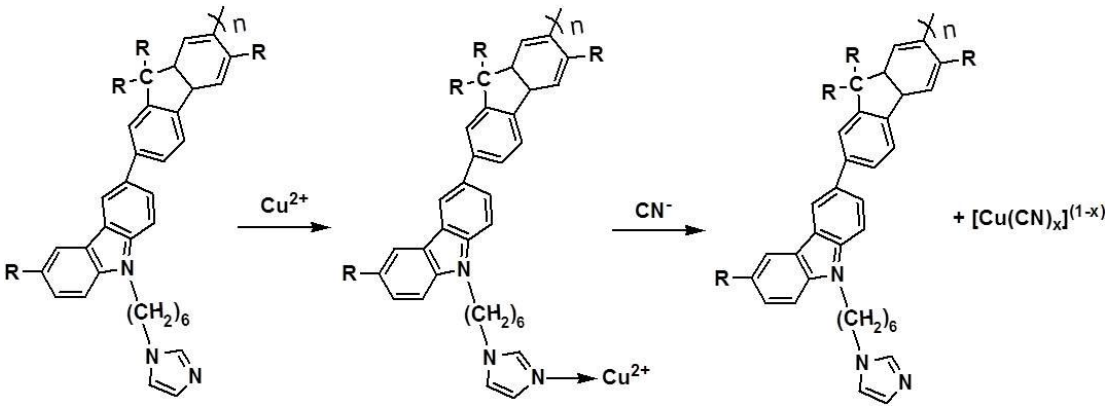

Scheme 8. Scheme of the displacement of Cu^{2+} from the organic complex to cyanide.[155]

Interferences are reported only for fluoride. Drawbacks include the interim formation of highly toxic dicyan gas from cyanide by the redox active Cu(II) ion. To avoid this dangerous side reaction, Cu(II) should be substituted by less redox active metal ions.

Cyanide coordination to metal complexes has been applied successfully for cyanide sensing using Zn-porphyrin-crown ether conjugates,[157] Ru(II)-cyanide complexes[158] and, most promising, corrinoids (see 1.5.3).[138, 140]

Although numerous approaches to new cyanide sensors are published, only few applications are reported. While in industrial waste water monitoring or process control, automatic sensor systems are increasingly employed, simple and safe short tests for direct cyanide monitoring in food, drinking water and blood are still a chemical challenge.[100]

1.5.3 Corrinoid based colorimetric cyanide sensing

The colour of metalloporphyrinoids and corrinoids is caused by HOMO to LUMO π to π* transitions of the porphyrin- or corrin ring.[159] The energy difference between the π and π* levels is influenced via the central metal ion by the donor/acceptor properties of the axial ligands of the central metal ion.[160, 161] Wertheman investigated the influence of different axial bound ligands in corrinoids by means of UV-vis

spectroscopy.[20] The nephelauxetic effect of cyanide as axial ligand causes a decrease in the π-π* energy differences compared to cobalt coordinated water and induces a shift of the UV-vis maxima to higher wavelengths, visible as a colour change from orange or red to violet.

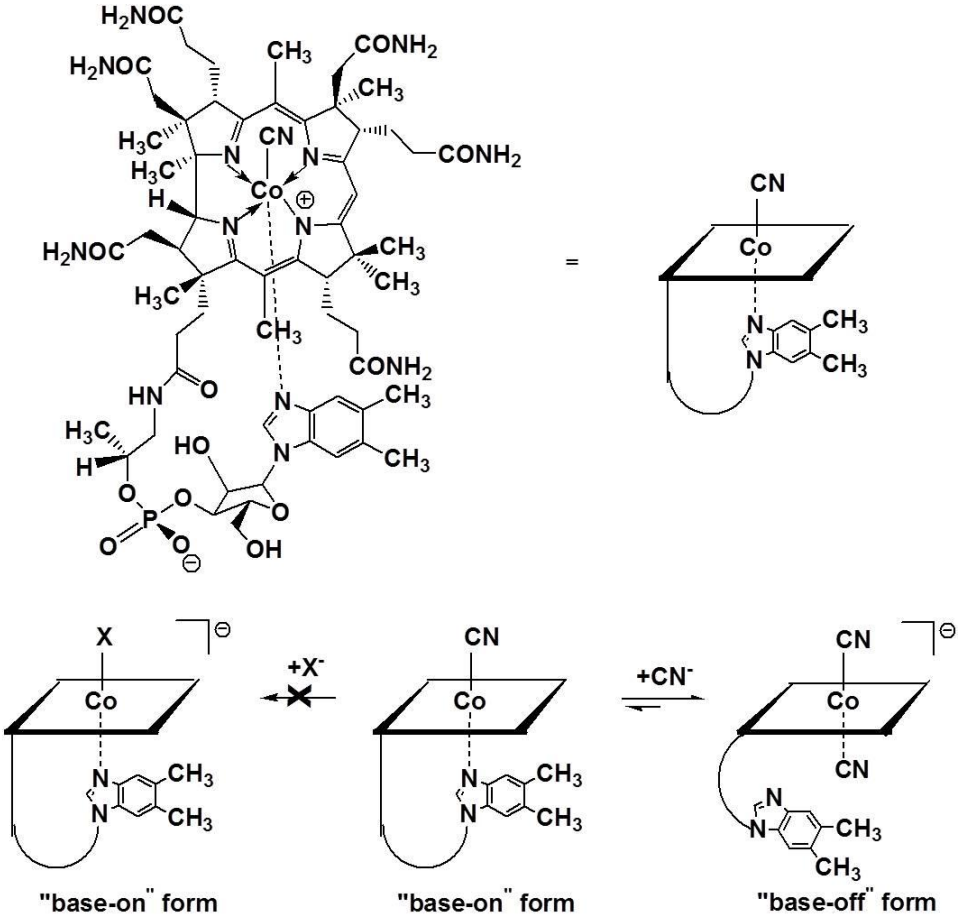

Scheme 9. Structural formula of vitamin B12 and the mode of cyanide binding.

The good selectivity and sensitivity of corrinoids toward cyanide and their applicability in pure water have promoted the use as chemical sensors for cyanide.[162-166] Pioneering incorporations of aquocyano-Co(III) derivatives into fibre optic chemical sensors or corrinoid functionalized polymers showed detection limits of 10 µM and 0.8 µM, respectively.[164, 167]

The most selective coordination of cyanide to corrinoids in water is achieved with vitamin B12 (see Scheme 9).[162] The nucleophilicity of cyanide is strong enough to substitute the intramolecular bound benzimidazole base, inducing a constitutional switch from the base-on to the base-off form (see Scheme 9). The resulting dicyano compound generates a bathochromic shift of the α-band in the UV-vis spectrum of 30 nm.[162] Long reaction times (10-20 min) and low sensitivity in the millimolar range are severe drawbacks.[162] The change to a slightly less polar solvent by addition of 5% methanol already leads to an increase in sensitivity.[162]

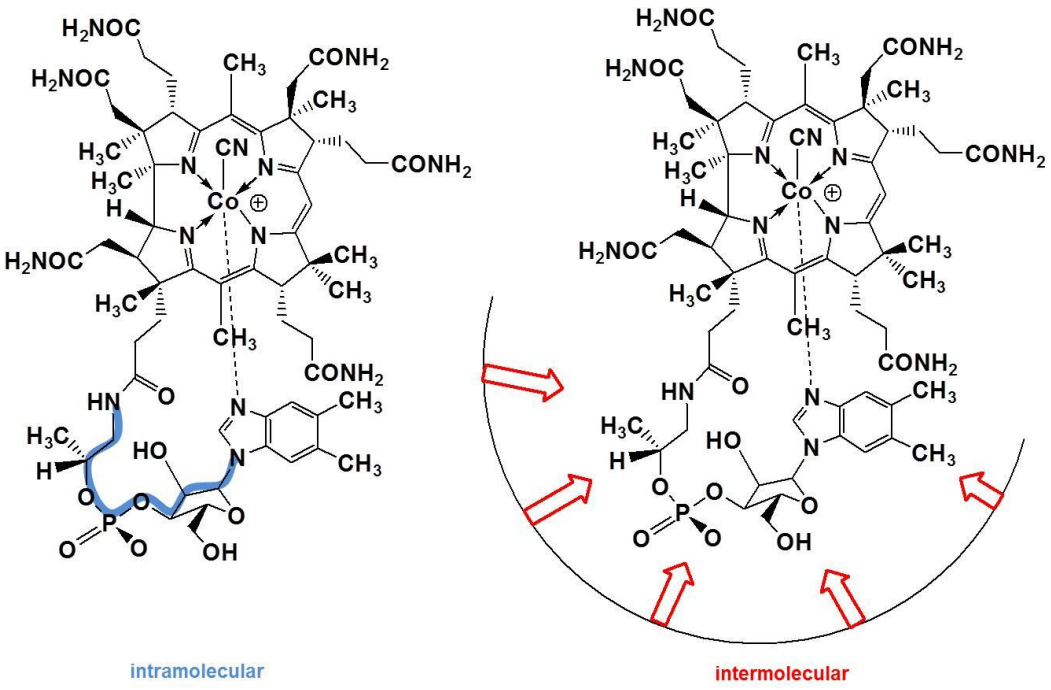

Figure 4. Scheme of the intramolecular alteration of the loop structure of vitamin B12, **1** (*left*) and intermolecular interactions between the corrinoid and the molecular environment.

The prominent properties of corrinoids including their high affinity and excellent selectivity toward cyanide, their water solubility and their occurrence in biological systems inspired us to detailed investigations and improvements of corrinoids for colorimetric cyanide monitoring. We assumed that the manipulation of the base-on/base-off properties should affect the sensitivity of vitamin B12 as chemical cyanide sensor. This is principally possible by alteration of the loop structure or by supramolecular interactions between the environment and corrinoid (see Figure 4).

The latter effect is often observed in biological systems for protein-B12 complexes and can lead to a significant stabilisation of the base-off form. Vitamin B12 proteins that regulate the base-on/base-off properties through intermolecular interactions inspired this work. We intended to use both of the above-mentioned strategies to control efficiently the selective and sensitive cyanide coordination to the metal centre.

1.6 Kinetics

To improve cyanide detection with corrin-based chemosensors, the understanding of the mechanism of cyanide coordination to the Co(III) centre, the influence of reaction conditions such as pH and temperature as well as the influence of molecular properties needs to be enhanced.

Primary kinetic studies of Reenstra et al.[168] focused on the investigation of aquacobalamin. A pH depending mechanism for the substitution of Co(III) coordinated water by cyanide is reported (reaction 1, Scheme 10). At pH values above 9 the addition of the cyanide anion via the carbon atom is the rate-limiting step, whereas at pH below 9 the addition of hydrogen cyanide via the nitrogen atom becomes more important.[168] At pH < 6 the increasing isomerisation to the carbon bound species is described (see Scheme 10, reaction 2).

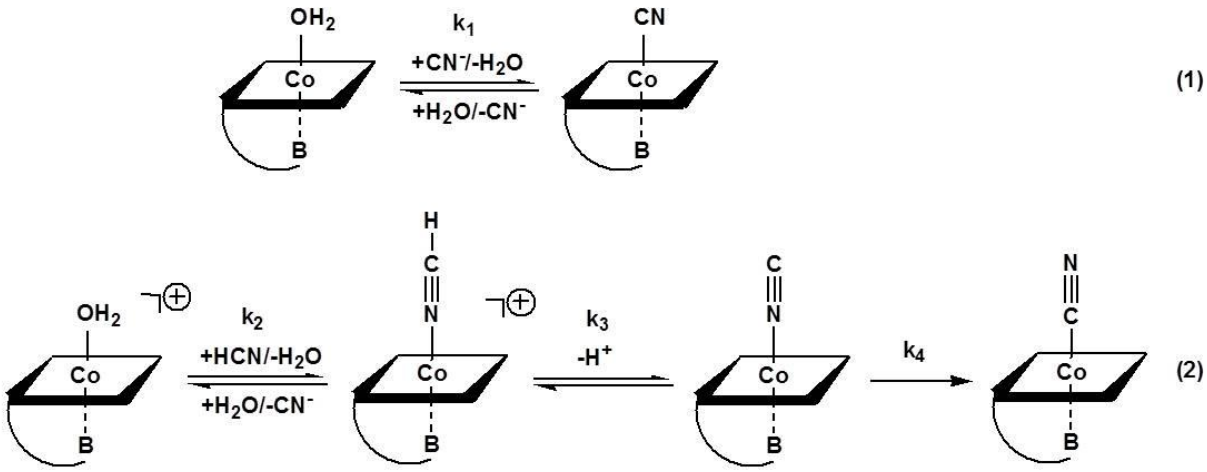

Scheme 10. Reaction scheme of the addition of hydrogen cyanide to aquacobalamin in solution and further reactions to cyanocobalamin.[168]

Investigations on aquacyanocobalamin under acidic conditions (pH < 2) with a protonated, dissociated Dmbz base showed the interesting effect of a cyanide catalysed isomerization of the axial bound water and cyano ligands coordinated to the α-(lower) or β-(upper) position of the corrin ring (see Figure 5).

Aquacyano corrinoids lacking the 5,6 dimethylbenzimidazole side chain exist as β-aqua, α-cyano and α-aqua, β-cyano diastereomers already at neutral conditions. The corresponding positions of the axial ligands above or below the plane of the corrin ring are presented in Figure 5.

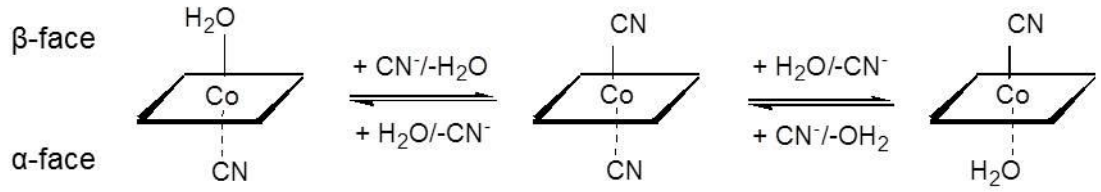

Figure 5. α-cyano, β-aqua (*left*) and α-aqua, β-cyano (right) diastereomers of corrinoids.

Substitution reactions at the axial positions of the central Co(III) in corrinoids are affected not only by the pH value but also by structural and electronic features of the corrin ring. The existence of aquocyano diastereomers and their possible isomerisation further complicates the determination of thermodynamic and kinetic parameters for the substitution of Co(III) bound water by different anions (see Scheme 11). While mixtures of isomers are already examined, measurements of isolated species are still missing. Challenges are the separation of the axial diastereomers, additional equilibria and in parts fast interconversion of the diastereomers in solution that complicates mechanistic studies.

The general reaction (3) in Scheme 11 represents the replacement of coordinated water by an exogenous ligand L. Marques et al. have proposed an additional partial conversion of aquacyano-corrinoids to the diaqua and dicyano forms for aquacyanocobester (reaction 4).[169] The cobalt bound water of the diaqua species is assumed to have a pKa of 5.9 as observed for comparable aquacyano corrin complexes. Thus, the aquahydroxo form should be present in small amounts under basic conditions (pH> 9) at which most cyanide detection reactions are performed (reaction 5). The Co(III) coordinated water in the latter species is labile for

substitution by exogenous ligands (reaction 6), but with a different rate constant than the aquacyano-species due to the smaller trans effect of OH^- as compared to CN^-. The negatively charged hydroxo group itself is inert to substitution. Under basic conditions the aquahydroxo species should be fractionally present as dihydroxo complex, which is inert (reaction 7).

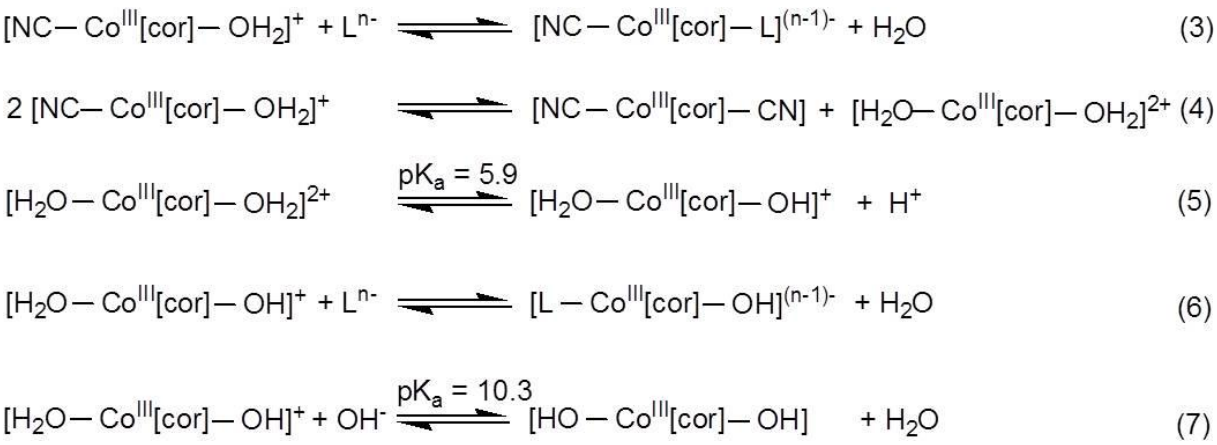

Scheme 11. (3) Ligand substitution of aquacyano corrinoids lacking the 5,6 Dmbz side chain, ([cor] = corrin ligand), (4) additional equilibrium between the aquacyano complex and the dicyano and diaqua species, (5) acid dissociation for the diaqua species, (6) ligand substitution of aquahydroxo corrinoid, (7) pH dependent formation of the dihydroxo corrinoid.

Various kinetic and mechanistic investigations of substitution reactions on corrinoids have been carried out in the last three decades.[168-173] However, we investigated the kinetics and the mechanism of cyanide coordination to corrin-complexes as employed in cyanide detection with stopped-flow technique. This method is convenient to follow very fast substitution reactions in order to yield a more detailed insight in the mode-of-action of our corrin-based chemosensors for cyanide.

2 Results and discussion

2.1 Colorimetric cyanide detection in water

Incomplete corrinoids were employed for the visual and the spectrophotometric detection of cyanide in water. Detection is based on the substitution of Co(III) bound water with cyanide accompanied by a change of colour. Different functionalities in the corrinoid side chains influence the substitution at the metal centre. The results led to the optimisation of sensitivity and selectivity of cyanide versus potentially interfering anions. Conditional binding affinities at different pH values were determined and completed the investigations.[174]

2.1.1 Influence of the corrin side chains

Inspired by the highly selective, but rather insensitive detection of cyanide with vitamin B12 in water, we decided to explore incomplete corrinoids lacking the 5,6-dimethylbenzimidazol side chain as more sensitive chemosensors.[162] Aquacyanocobinamide **2** (ACCbi), aquacyanocobyrinic acid **3** (ACCa), and aquacyanocobester **4** (ACCbs) were chosen and applied as mixtures of axial diastereomers (see Figure 6).

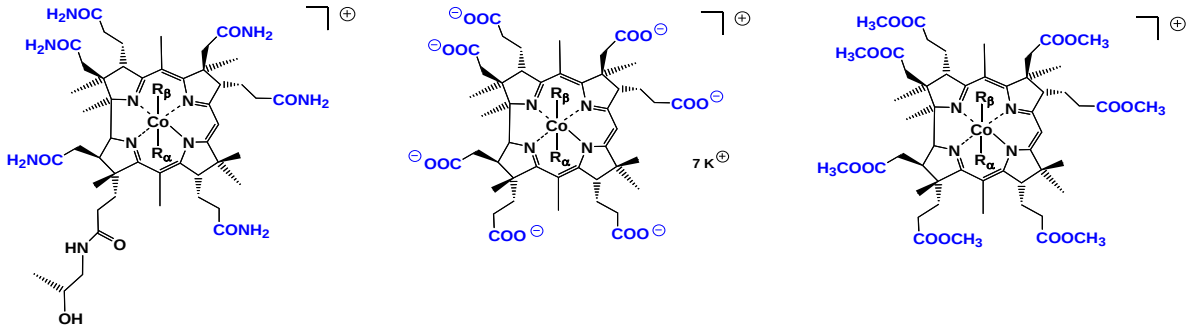

2 **3** **4**

Figure 6. Structural formula of α-cyano, β-aqua (R_α = CN, R_β = H_2O) and α-aqua, β-cyano (R_α = H_2O, R_β = CN) corrinoids; aquacyanocobinamide **2** (ACCbi), aquacyanocobyrinic acid **3** (ACCa) and aquacyanocobester **4** (ACCbs).

The substitution of axial bound water by cyanide causes a bathochromic shift of the α-, β- and γ-bands (for ACCa from 525 nm, 497 nm and 353 nm to 578 nm, 426 nm and 366 nm) accompanied by a change in colour from orange to violet (see Figure 7).[174]

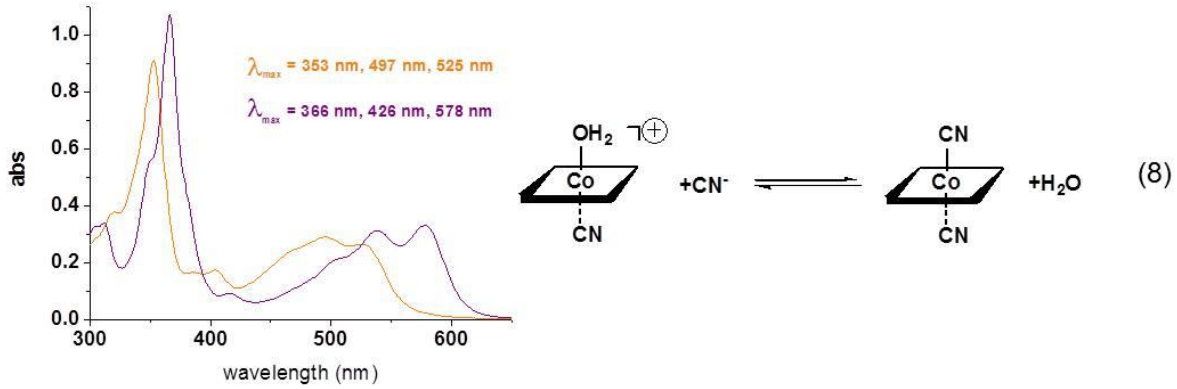

Figure 7. Substitution reaction of Co(III) bound water of aquacyano-corrinoids with cyanide to dicyano-corrinoids (right) and related UV-vis spectra of ACCa.

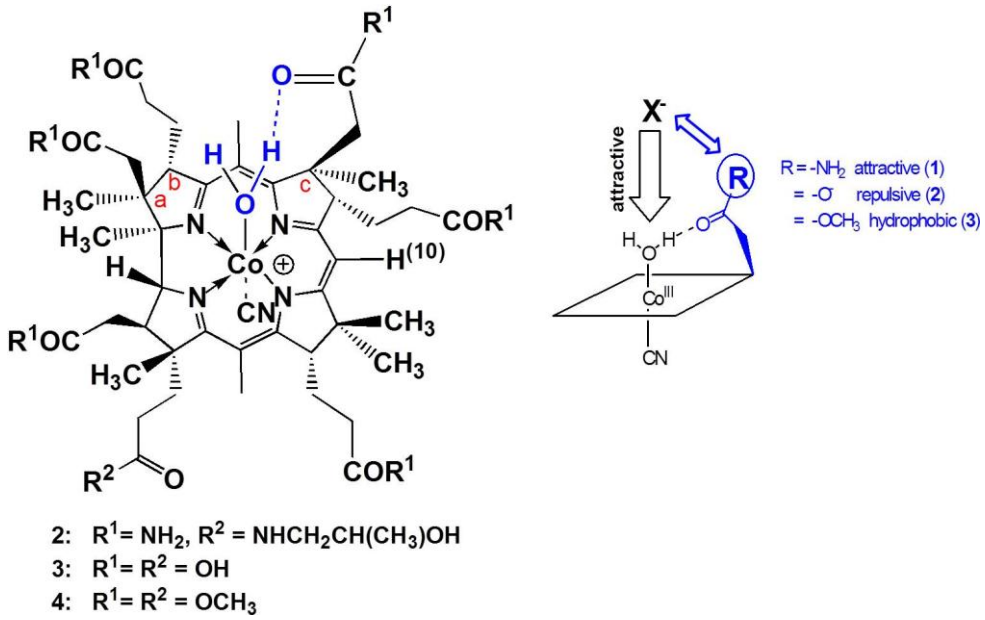

2: $R^1 = NH_2$, $R^2 = NHCH_2CH(CH_3)OH$
3: $R^1 = R^2 = OH$
4: $R^1 = R^2 = OCH_3$

Figure 8. General formula of corrinoids **2** to **4** (*left*) and proposed interaction between the incoming anion X^- and the inwardly oriented c-side chain of the corrinoids (*right*).[174]

An important advantage of these corrinoids is the fast substitution of Co(III) bound water by cyanide within a few seconds compared to the substitution of the intramolecular bound Dmbz-base in vitamin B12 which takes approximately 15

minutes.[161, 166, 175] Different functionalities of the corrinoid side chains were expected to influence this reaction by interaction between the incoming anion and the inwardly oriented c-side chain of the corrinoid. A hydrogen bond between the β-axial water and the carbonyl oxygen of the c-side chain is known from the X-ray structure of β-aquacobalamin.[176, 177] The proposed model in Figure 8 (right) represents the suggested interaction between the incoming anion X^- and the inwardly oriented c-side chain; the potential attractive interaction via the amid nitrogen, electrostatic repulsion via carboxylate and hydrophobic interaction via the ester group.

First we delimited the appropriate pH range of the substitution reaction (see Figure 9) by monitoring the UV-vis spectra between pH 7 and 11 of the aquacyanocorrinoids. No influence of pH is observed up to pH 9.5. However, a bathochromic shift of the

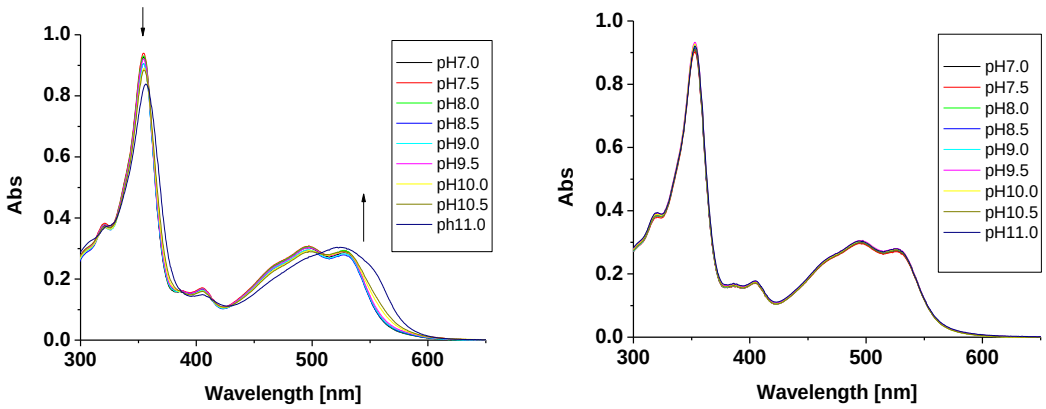

Figure 9. UV-vis spectra of ACCbi (left, 40 µM) and ACCa (right, 40 µM) in the pH range from 7.0 to 11.0. UV-vis spectra of ACCbs are analogous to the spectra of ACCbi.

UV-vis absorptions of corrinoids ACCbi and ACCbs in basic solution at pH above 9.5 indicate a deprotonation to the hydroxocyano corrinoids (Figure 9, *left*; reaction 7).

$$[H_2O-Co^{III}[cor]-CN]^+ + OH^- \rightleftharpoons [HO-Co^{III}[cor]-CN] + H_2O \qquad (7)$$

In contrast, aquacyanocobyrinicacid (ACCa) is not deprotonated up to pH 11 (see Figure 9, right). We assume that the negatively charged carboxylate shields the Co(III) bound water from deprotonation. The conditional binding affinities for cyanide to ACCbi and ACCbs at pH 7.5 and pH 9.5, respectively, acquired by UV-vis titration

experiments, are within the range of 1.35 x 10^6 M^{-1} to 2.73 x 10^6 M^{-1} (see Appendix I) Significantly lower by an order of magnitude are the binding constants for compound ACCa, presumably controlled by the electrostatic repulsion of the c-acetate side chain and cyanide.[174]

The selectivity of cyanide binding to the central Co(III) has been investigated with the following fourteen anions F^-, Cl^-, Br^-, I^-, SCN^-, NO_3^-, HCO_3^{2-}, $C_2O_4^{2-}$, SO_4^{2-}, $H_2PO_4^-$, ClO_4^{2-}, CH_3COO^-, OCN^-, $EDTA^{2-}$ in the presence and absence of cyanide.[174] All fourteen anions were tested up to a concentration of 4 mM, the anions F^-, Cl^-, Br^-, I^-, SCN^-, OCN^- up to a concentration of 300 mM. A 250 times excess of one or several of these anions (or even all) is tolerated by the chemosensors as indicated by the absence of a change in colour. Notably, the UV-vis spectra of ACCa (Figure 10, left) or low concentration of the dicyano-form (10 µM, Figure 10, right) are not affected by the addition of these anions up to a concentration of 4 mM at pH 7.5.

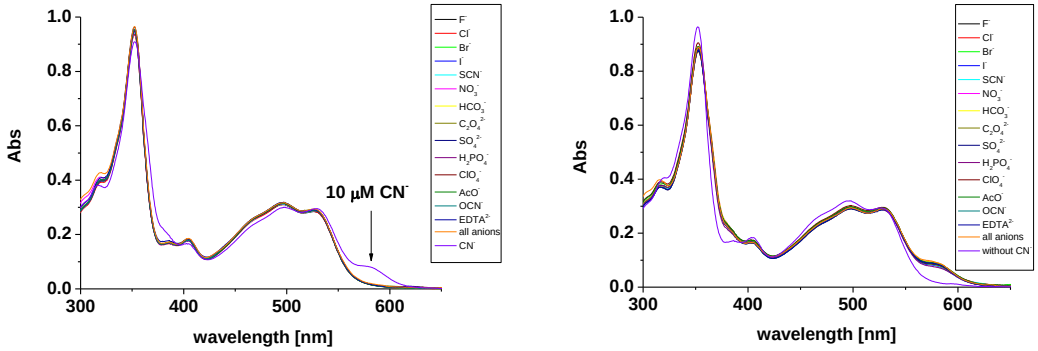

Figure 10. UV-vis spectra of aqueous solutions of ACCa (40 µM; [HEPES] = 20 mM; pH= 7.5 ± 0.1), in the presence of one of the following anions F^-, Cl^-, Br^-, I^-, SCN^-, NO_3^-, HCO_3^{2-}, $C_2O_4^{2-}$, SO_4^{2-}, $H_2PO_4^-$, ClO_4^-, CH_3COO^-, OCN^-, $EDTA^{2-}$ (4 mM), all fourteen anions or CN^- (10 µM) (*left*) and in the presence of CN^- (10 µM) (*right*). On the right, one spectrum without any added anion is given as a reference.

Table 4 presents the limits of tolerance at pH 7.5 and pH 9.5 using the corrinoid sensors **2** to **4**. The tolerance of ACCa against SCN^- is as high as 200 mM in contrast to the fifty times less sensitive chemosensors ACCbi and ACCbs. The results are in agreement with the differences in the conditional binding constants of SCN^- to ACCa

(0.35 M^{-1}), that are 157 and 347 times lower than the values of ACCbi (55.09 M^{-1}) and ACCbs (121.35 M^{-1}) at pH 7.5.

[mM]	**B12**	**2** (ACCbi)				**3** (ACCa)				**4** (ACCbs)			
	pH 7.5/ pH 9.5	pH 7.5		pH 9.5		pH 7.5		pH 9.5		pH 7.5		pH 9.5	
2.5													
3									OCN^-	SCN^-		SCN^-	OCN^-
4		SCN^-		SCN^-									
5					OCN^-						OCN^-		
20			OCN^-				OCN^-						
300	$EDTA^{2-}$					SCN^-		SCN^-					

Table 4. Interference of the indicated anions at the declared concentration in the absence of cyanide (grey fields = interference; white fields = no interference; [chemosensor] = 40 µM, [HEPES] = 20 mM (pH 7.5), [CHES] = 20 mM (pH 9.5)).

We assume that the high selectivity of aquacyanocobyrinicacid up to a factor of 30 is caused by the electrostatic repulsion between SCN^- and the negatively charged c-side chain. Thiocyanate and cyanate are disturbing anions in millimolar concentrations; fluoride interferes in molar concentration whereas the sensitivity toward cyanide is still 10^5 times higher.

The lowest concentration of cyanide identifiable by the “naked eye” was appraised by a good discrimination in colour by three different persons. The chemosensors **2** to **4** allow the visual detection of cyanide in water for concentrations as low as 10 µM at pH 9.5 (see Table 5) in 5 seconds. This is much better than the detection with vitamin B12 (c~ 0.12 mM, t~15 min).[162]

Chemosensor (40 µM)	**pH 7.5**		**pH 9.5**	
	µM	**g/L**	µM	**g/L**
2 (ACCbi)	10	$2.6 \cdot 10^{-6}$	10	$2.6 \cdot 10^{-6}$
3 (ACCa)	10	$2.6 \cdot 10^{-6}$	10	$2.6 \cdot 10^{-6}$
4 (ACCbs)	30	$7.8 \cdot 10^{-4}$	10	$2.6 \cdot 10^{-6}$
1 (CNCbl)[162]	250	$6.5 \cdot 10^{-3}$	120	$3.1 \cdot 10^{-3}$

Table 5. Sensitivity of the chemosensors **2** to **4** and vitamin B12 (detection limits identifiable by the naked eye).

2.2 Kinetics of the cyanide substitution reaction

The significant influence of the side chains of incomplete aquacyano corrinoids in anion coordination inspired us to investigate the reaction mechanism. Kinetic studies about the coordination of cyanide to isolated axial diastereomers of cobinamide and c-acid-cobester are discussed below and represent the basis for a current master's project in our research group. We demonstrated a difference in the reaction rate of water substitution by cyanide on the α ("lower")- and β ("upper")-face of these "incomplete" corrinoids.

2.2.1 Mixture of diastereomers

Before studying isolated diastereomers, we investigated the kinetics of the substitution of Co(III) bound water by cyanide in a mixture of α-aqua, *β*-cyano- ($ACCa_\beta$) and *β*-aqua, α-cyanocobyrinicacid ($ACCa_\alpha$) (see Scheme 12). A molar ratio of the axial diastereomers $ACCa_\beta$ and $ACCa_\alpha$ in solution of 1:1.2 between 15 and 45 °C was determined from the integrals of the corresponding two singlets of the H10 position in the ^{1}H NMR spectrum.[73]

The stopped-flow measurements were performed under pseudo first-order conditions at pH 9.5 with an excess of cyanide of 10 to 50 times. The absorption vs. time traces for three different wavelengths are shown in Figure 11, each wavelength at two different concentrations of cyanide. The decrease of the absorption at 353 nm

corresponds to the consumption of the complexes $ACCa_{\alpha}$ and $ACCa_{\beta}$, whereas product formation can be followed at increasing absorptions at 367 nm and 578 nm.

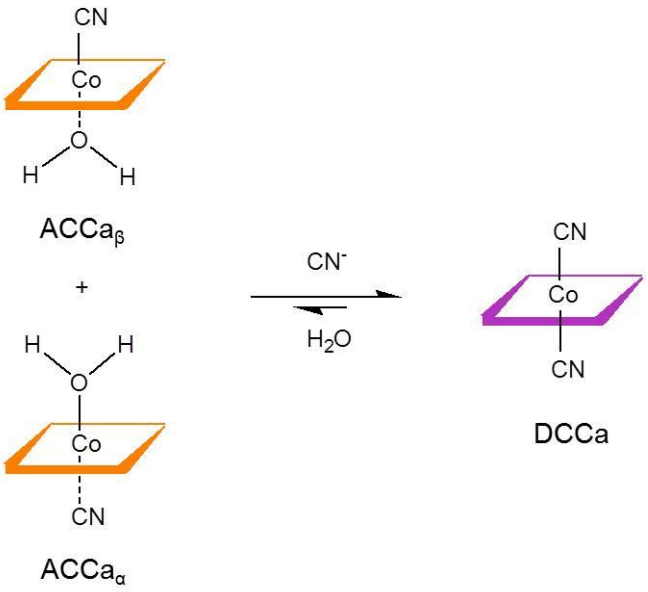

Scheme 12. Proposed mechanism of the reaction of α-aqua, *β*-cyano ($ACCa_{\beta}$) and *β* -aqua, α-cyano ($ACCa_{\alpha}$) diastereomers with cyanide to the dicyano product.[73]

After only 2 seconds the reaction is nearly completed. The traces could be fitted with a biexponential function $y = y_0 + A1 \cdot e^{-ki/t1} + A_2 \cdot e^{-kii/t2}$, that is reasonable for a parallel reaction of two different diastereomeric substrates into one product (see Scheme 12).

The pseudo first order rate constants $k_{obs,i}$ and $k_{obs,ii}$ values were obtained from the bifunctional fit using the program origin 8. The second order rate constants k_i^{II} and k_{ii}^{II} were determined from the slope of the k_{obs} values versus cyanide concentration for seven different temperatures (see Figure 12). The two second-order rate constants k_i^{II} (4200 ± 50 M^{-1} s^{-1}) and k_{ii}^{II} (15600 ± 400 M^{-1} s^{-1}) differ by a factor of 3.7 at 25 °C and a pH of 9.5.

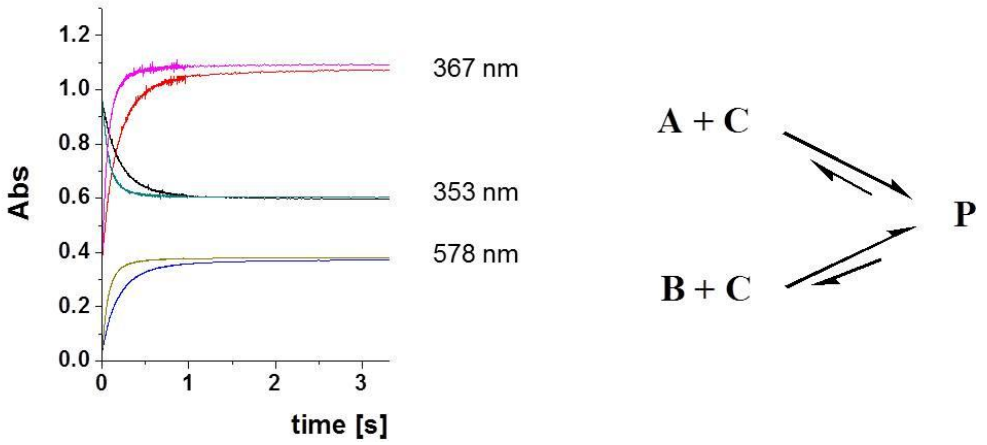

Figure 11. (*left*) Typical absorption *vs.* time traces at 367nm, 353 nm and 578 nm (each at 20 and 50 times excess of CN^-) recorded during the stopped-flow measurement. (*right*) General scheme of the conversion of two different species A and B with the same reactant C to product P, as the only species.[73]

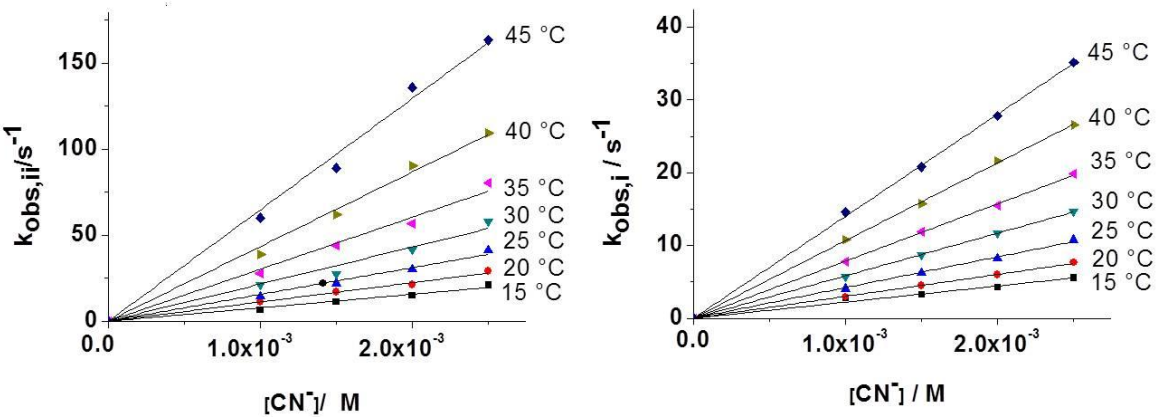

Figure 12. Plot of $k_{obs,i}$ (left) and $k_{obs,ii}$ (right)[73] vs. concentration of cyanide for the reaction depicted in Scheme 12 at different temperatures. Experimental conditions: pH = 9.5 ([CHES] = 20 mM, [ACCa] = 40 μM).

We assigned k_i^{II} and k_{ii}^{II} to the different substitution rates at the α- and β-sites of the corrin system (see chapter 4.,

Table **20**).[73] However, an unambiguous assignment of k_i^{II} and k_{ii}^{II} to the substitution at the α- or β-site of the corrin ring is not possible from this study.

On the other hand, biphasic kinetics can also be explained by the partial formation of the aquahydroxo complex as discussed by Chemaly et al. for related aquacyano-

corrinoids as outlined in chapter 1.6 (reactions 3 to 7).[169] In this case, the two different rate constants k_i^{II} and k_{ii}^{II} derive from cyanide coordination to the major aquacyano and the minor and slower reacting aquahydroxo species, respectively. This assumption includes that the rate constants of water substitution by cyanide at the α- and β-faces are similar and not distinguishable by stopped-flow experiments.

We determined the activation parameters $\Delta H^{\ddagger}$ and $\Delta S^{\ddagger}$ (see Table 7) from the temperature dependence of the second order rate constants according to equations in Figure 13, right. The corresponding Eyring plots are shown in Figure 13, left. The negative activation entropy of $ACCa_i$ can be correlated to an associative reaction mechanism. In contrast, a dissociative interchange mechanism for ligand substitution is suggested for ACCbi.[173]

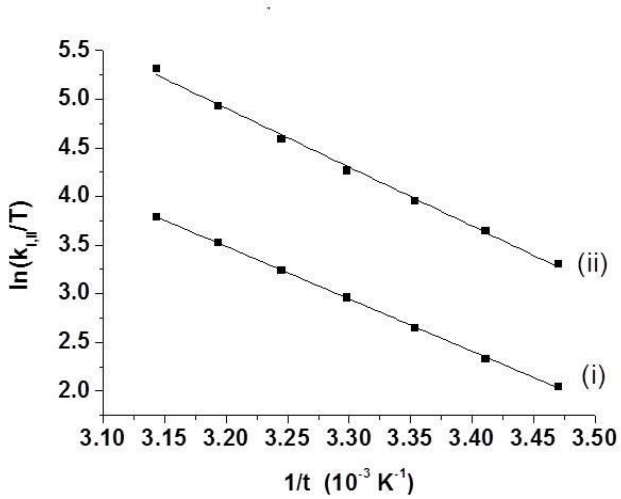

$$k = \frac{k_B T}{h} \; e^{\frac{-\Delta G^{\ddagger}}{RT}}$$

$$\ln\left(\frac{k}{T}\right) = \frac{-\Delta H^{\ddagger}}{RT} + \ln\left(\frac{k_B T}{h}\right) + \frac{\Delta S^{\ddagger}}{R}$$

Figure 13. Eyring plot for the reactions of the mixture of the aquacyano diastereomers ACCa (i) and ACCa (ii) with cyanide, as depicted in Scheme 12.[73]

In order to discriminate between the reactions on the α- and β-faces of the complexes, which are presumably responsible for the biphasic kinetics, we decided to separate the two aquacyano diastereomers of the corrinoids. With the separated compounds we determined the kinetic rate constants by stopped-flow measurements.

2.2.2 Investigations of isolated diastereomers

For mechanistic investigations of cyanide coordination to isolated aquacyano corrinoids with a defined configuration at the metal centre, it was attempted to

separate all three mixtures of aquacyano corrinoids **2** – **4** into their axial diastereomers.

All attempts to separate the diastereomers of aquacyanocobester (ACCbs) on a C18 column using different water methanol gradients failed. Only mixtures with a ratio of nearly 6:1 of the diastereomers could be obtained, suggesting a fast equilibrium of the two species. A time dependent increase of isomerisation was detected by HPLC. A conversion of aquacyano- to dicyanocobester up to 10% was observed in the presence of light. To avoid this undesired side reaction, all experiments with aquacyanocobester were carried out in the dark.

The separation of the axial diastereomers of aquacyanocobyrinic acid (ACCa) was also not successful. However, we were able to isolate one diastereomer of the c-acid-aquacyanocobester derivative c-acid-ACCbs. This derivative is particularly interesting for proving the proposed influence of the c-acid side chain in the substitution of Co(III) bound water by different ligands (see chapter 2.2.3).

α-Aqua, β-cyano- (ACCbi$_\beta$) and α-cyano, β-aqua- (ACCbi$_\alpha$) cobinamide were also successfully synthesized from the corresponding dicyano complex and separated by preparative reverse-phase C18 chromatography. The diastereomers were characterized by LCMS$^+$, UV-vis and ^{1}H NMR spectroscopy. The α- and β-isomers were identified by comparison of the ^{1}H NMR shifts of the protons H3, H10 and H19 with those of a peptide B12 derivative according to a previous investigation of group[178].

The stopped-flow measurements with ACCbi$_\alpha$ and ACCbi$_\beta$ at pH 9.5 as well as the subsequent calculations were performed as described earlier in chapter 2.2.1. This time and in contrast to investigations with the diastereomeric mixtures, the kinetic data could be fitted with a monoexponential function $y = y_0 + A \cdot e^{-k/t}$ for cyanide coordination at low temperatures (5 – 15°C) (see Figure 14, A, C). For measurements above 15°C, the experiments were more precisely described with a biphasic fit (see Figure 14, B, D). This effect can be assigned either to an equilibrium between the axial diastereomers or the formation of the aquahydroxo complex.

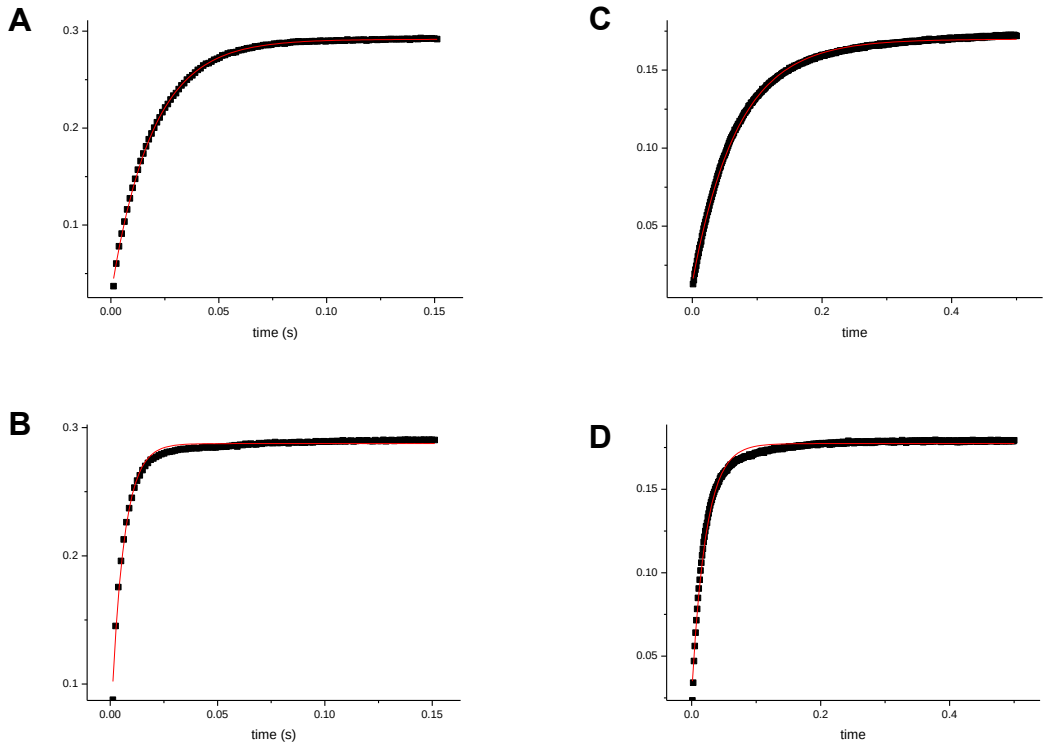

Figure 14. Monoexponential fit of the change of the relative absorbance vs. time at 580 nm of $ACCbi_{\beta}$ at 5°C (A) and 20°C (B), and of $ACCbi_{\alpha}$ at 5°C (C) and 20°C (D); [CN^-] = 0.5 mM, [CHES] = 20 mM, pH 9.5).

The second order rate constants $k_{ACCbi\alpha}{}^{II}$ and $k_{1\beta}{}^{II}$, monoexponetially fitted, are presented in Table 6.At a low temperature of 5 or 10°C, the reaction rate of $ACCbi_{\beta}$ is 4 times faster than of that of $ACCbi_{\alpha}$. This behaviour can be explained by stabilisation of the β-axial coordinated water in $ACCbi_{\alpha}$ through hydrogen bonding with the inwardly oriented c-side chain (see Figure 8). The latter has been observed earlier for aquacobalamins.[176, 177] It was also realized that the reaction rate as a function of temperature is different for the two species. With increasing temperature, the quotient $k_{ACCbi\beta}{}^{II}/k_{ACCbi\alpha}{}^{II}$ decreases from 4.0 (5°C) to 2.7 (30°C). As seen in Table 6, the influence of the temperature is more pronounced for the α-cyano diastereomer. This may be caused by a destabilisation of the hydrogen bond with increasing temperature or by isomerization of the β-cyano species to the α-cyano species. In order to investigate in addition the pH dependence of the kinetic data, measurements at pH 9.0 were carried out. The results showed that the second order rate constants

$k_{\alpha}^{II}{}_{ACCbi}$ and $k_{\beta}^{II}{}_{ACCbi}$ are 2.0 and 1.7 times slower at pH 9.0 and 25°C than at pH 9.5. We attribute this effect to the available content of free cyanide.

T (°C)	$k_{\alpha}^{II}{}_{ACCbi}$ [$M^{-1}s^{-1}$] 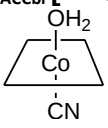	$k_{\beta}^{II}{}_{ACCbi}$ [$M^{-1}s^{-1}$] 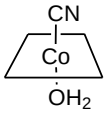	$k_{\beta}^{II}/k_{\alpha}^{II}$
5	$2.51 \cdot 10^4$	$1.02 \cdot 10^5$	4.04
10	$3.57 \cdot 10^4$	$1.44 \cdot 10^5$	4.05
15	$5.61 \cdot 10^4$	$2.04 \cdot 10^5$	3.63
20	$8.08 \cdot 10^4$	$2.81 \cdot 10^5$	3.47
25	$1.15 \cdot 10^4$	$3.60 \cdot 10^5$	3.14
30	$1.49 \cdot 10^5$	$4.06 \cdot 10^5$	2.72

Table 6. Monoexponential fit of the changes of the relative absorbance vs. time at 580 nm of $ACCbi_{\beta}$ at 5°C (A) and 20°C (B), $ACCbi_{\alpha}$ 5°C (C) and 20°C (D); ((CN^-) 0.5 mM, CHES 20 mM, pH 9.5).

At pH 9.0, the mixture contains 35% HCN and 65% CN^- (pK_a of HCN = 8.74), whereas at pH 9.5 it contains 85% CN^-. The second order rate constant of the measurement with a mixture of $ACCbi_{\alpha,\beta}$ was reported by Baldwin et al.[172] to have a comparable value of $k_1^{II} = 2.1 \cdot 10^5$ $M^{-1}s^{-1}$ (pH 9.5, 25°C). This data is in good agreement with the average value of $k_{\alpha}^{II}{}_{ACCbi}$ and $k_{\beta}^{II}{}_{ACCbi}$ from our studies ($2.38 \cdot 10^5$ $M^{-1}s^{-1}$).

The activation parameters $\Delta S^{\ddagger}$ and $\Delta H^{\ddagger}$ for $ACCbi_{\alpha}$ and $ACCbi_{\beta}$, presented in Table 7, were determined from the Eyring plots. The activation enthalpies $\Delta H^{\ddagger}$ are in a similar range for the substitution at the α- and β-position of the same corrinoid. The negative activation entropy of $ACCbi_{\beta}$ at pH 9.5 shows the tendency to an associative activated reaction mechanism and correlates to the less increasing rate constants for the β-cyano isomer ($ACCbi_{\beta}$) with increasing temperature.

It is puzzling that activation entropy and enthalpy at pH 9.0 differ markedly from the values measured at pH 9.5. A master's thesis is currently conducted in our group with the objective to enhance our understanding of this observation.

corrinoid	$\Delta H^{\ddagger}$ [kJ/mol]	$\Delta S^{\ddagger}$ [J/mol K]
ACCa (i), pH 9.5	45 ±1	-25 ±1
ACCa (ii), pH9.5	50 ±2	4 ±5
ACCbi$_{\beta}$, pH 9.5	37.7 ±3	-12.4 ±2
ACCbi$_{\alpha}$, pH 9.5	48.9 ±4	15.6 ±2
ACCbi$_{\beta}$, pH 9.0	87.1 ± 4.1	73 ± 10
ACCbi$_{\alpha}$, pH 9.0	94.4 ± 5.0	81 ± 13
c-acid-ACCbs	2.42	47.2

Table 7. Activation parameters for the coordination of CN^- to different α**,** β- aquacyano corrinoids in mixtures of (ACCa(i) and ACCa(ii)), as isolated isomers ACCbi$_{\alpha}$ and ACCbi$_{\beta}$ at different pH values and c-acid-ACCbs.

In summary, for the first time kinetic studies of cyanide coordination to isolated axial diastereomers of aquacyano corrinoinds were examined. It has been demonstrated different substitution rates for the upper and lower position of the Co(III) center of aquacyanocobinamide, ACCbi$_{\alpha}$ and ACCbi$_{\beta,}$ at low temperatures.

2.2.3 Investigations of c-acid-α-cyano, *β*-aquacobester

The synthesis of c-acid-cobester was performed as described in literature.[179] We isolated the α-cyano, *β*-aqua product c-acid-ACCbs$_{\alpha}$ as the only product suggesting thermodynamic preference due to the stabilisation of the β-coordinated water by a

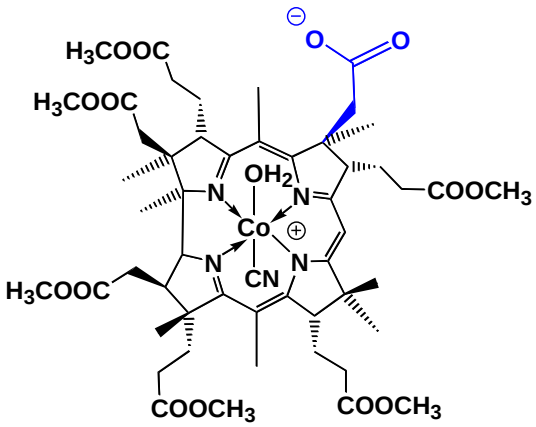

Figure 15. Structural formula of c-acid aquacyanohexamethylcobester **5** (c-acid-ACCbs$_{\alpha}$).

hydrogen bond. The stopped-flow measurements of the substitution of Co(III) coordinated water with cyanide were conducted under the same conditions as for corrinoids ACCbi and ACCa at pH 9.5. The kinetic data, obtained between 5 and 30°C, were fitted properly with a monoexponential function (see Figure 46, chapter 4). The substitution rates of c-acid-ACCbs$_{\alpha}$ ($k_{5\alpha}^{II}$) are presented in Table 22 in the Experimental part. The second order rate constants $k_{5\alpha}^{II}$ ($5.95 \cdot 10^4$ $M^{-1}s^{-1}$ at 30°C) are 2.5 (30°C) times slower than that of $k_{\alpha}^{II}{}_{ACCbi}$ ($1.49 \cdot 10^5$ $M^{-1}s^{-1}$ at 30°C), suggesting a stronger influence of the hydrogen bond via the carbonyl oxygen in c-acid-ACCbs$_{\alpha}$ as compared to the hydrogen bond via the amid nitrogen of ACCbi$_{\alpha}$. Alternatively, electrostatic repulsion because of the negative charge of the carboxylate could also cause this effect. Significant differences between the second order rate constants and the activation parameters of c-acid-ACCbs$_{\alpha}$ and a mixture of ACCbs$_{\alpha,\beta}$ reported by Marques et al.[169] (see chapter 4, Table 21) are not observed. Furthermore, an additional second order rate constant k_2^{II} which corresponds to a secondary equilibrium (eq. 5) could not be observed in our experiments. A comparison between different corrinoids shows, that the substitution rates of a mixture of ACCa-isomeres, c-acid-ACCbs$_{\alpha}$ and ACCbi$_{\alpha}$ are increasing in the ratio ACCba$_{\alpha,\beta}$: c-acid-ACCbs$_{\alpha}$: ACCbi$_{\alpha}$ = 1 : 2.9 : 7.2 (20°C, see Table 20 and Table 22). The lowest reaction rate is obtained for the mixture of α-,*β*-aquacyano diastereomers of ACCa. It can be assumed that the four downward oriented side chains additionally shield the α-face against substitution. Further experiments to verify the results and to exclude additional pH dependent equilibria are planned and integrated into our current research topics. Crystallization of all the complexes, unfortunately, has not yet been successful.

2.3 From base-on to base-off cobalamins on a hydrophobic surface

An immobilisation strategy has been developed that (i) extends the coordination chemistry of cobalamins and (ii) improves the sensitivity in cyanide detection. The following approach is based on the manipulation of the base-on/base-off properties of the nucleotide side chain by the molecular environment in order to influence sensitivity and selectivity of the coordination of cyanide to cobalt-centre of cobalamins. In contrast to the strong intramolecular coordination of the Dmbz base in

aqueous solution, an enormous stabilisation of their base-off forms through absorption on hydrophobic surfaces was observed. Reminiscent to the binding to proteins, this process is controlled by the nature of the (“upper”) β-bound ligand. The new immobilisation strategy allows the synthesis of (‘‘lower’’) α-face modified B12 derivatives that cannot be obtained under homogenous aqueous conditions. Based on this strategy, the first biomimetic base-off/histidine-on coordination complex of B12 was synthesised.

2.3.1 Immobilisation of cobalamins on hydrophobic silica

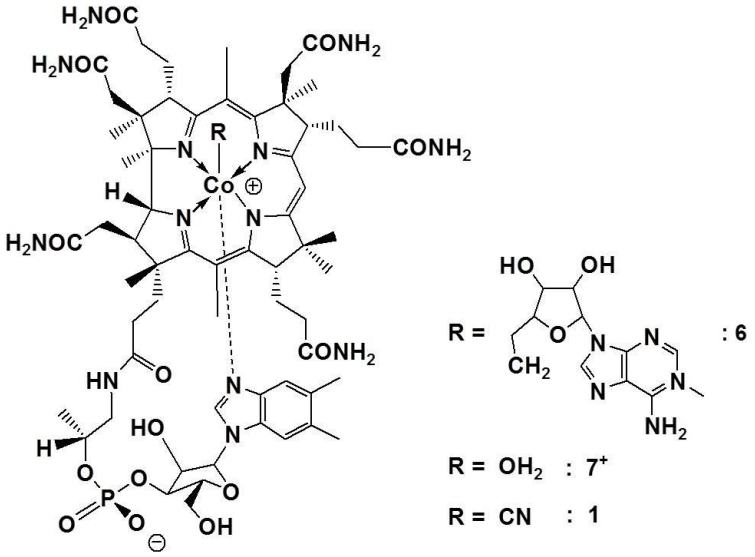

Figure 16. Structural formula of coenzyme B_{12} (AdoCbl; **6**), aquaB_{12} (AqCbl; $\mathbf{7^+}$), vitamin B_{12} (CNCbl; **1**).[180]

A series of three biologically relevant cobalamins with the β-axially bound ligands 5`-deoxyadenosyl, aqua and cyano (**6**, **7** and **1**) was immobilised on C18-alkyl modified silica.[180] The (“upper”) β-coordinated ligands control the strengths of the nucleotide-metal coordination at the opposite face and thus the intramolecular dissociation of the Dmbz base in solution. Increasing stabilisation of the Dmbz coordination is correlated to decreasing $pK_{base\text{-}off}$ values in the series from AdoCbl to CNCbl and AqCbl (see Table 8 and Table 9). This molecular switch of cobalamins with the Dmbz base either coordinated (base-on) or protonated and dissociated from the cobalt centre (base-off) of the corrin macrocycle is represented in Figure 17.[181]

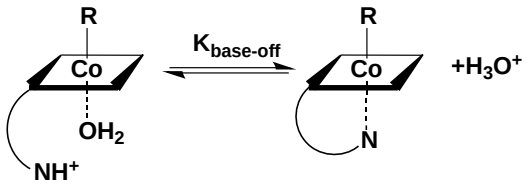

Figure 17. The base-on/base-off equilibrium of cobalamins includes protonation of the dissociated base and ligand exchange at the metal centre.[181]

Adenosylcobalamin (AdoCbl) with a $pK_{base\text{-}off}$ of 3.7 is present in water at neutral conditions predominantly in its nucleotide coordinated base-on form.[182] An aqueous solution of AdoCbl (pH 6.5) was manually pressed through a *silica C18ec* column (1 mL) and absorbed as $AdoCbl_{C18}$ (C18 for ''*silica C18ec*'') on the surface of the white silica material. An immediate change of color from red AdoCbl to yellow $AdoCbl_{C18}$ was observed. The diffuse reflectance spectrum of $AdoCbl_{C18}$ is consistent with the UV-vis spectrum of the base-off AdoCbl in water at pH 2 (see Figure 18, left). A blue shift of 67 nm compared to the base-on form of AdoCbl in water (pH 6.5) is observed. This result suggests that $AdoCbl_{C18}$ is present in the base-off constitution. As seen from Figure 18 (*right*) the DRUV-VIS spectra of immobilised $AdoCbl_{C18}$ are not pH dependent between pH 2 and 10. The experiments were performed by passing water of different pH through the column and spectra were taken after 24 h.

In contrast, a complete base-off to base-on transition with a $pK_{base\text{-}off}$ of 2.9 was observed for immobilised AdoCbl on unmodified silica ($AdoCbl_{Silica}$) without indication of any additional equilibrium (see Figure 18, *right*). This significant difference in behaviour between immobilised $AdoCbl_{C18}$ and $AdoCbl_{Silica}$ supports the assumption that the base-off form of $AdoCbl_{C18}$ is stabilised by attractive interactions between the nucleotide linker and the alkyl modification of the surface of the solid.[180] The pH-independent formation of a base-off $AdoCbl_{C18}$ species that is unable to switch back to its base-on form differs from the behaviour in solution and on non-modified silica suggesting that hydrophobic interactions between the solid support and the dissociated nucleotide linker (base-off) are strongly favoured compared to interactions with the structurally more compact base-on form.[180]

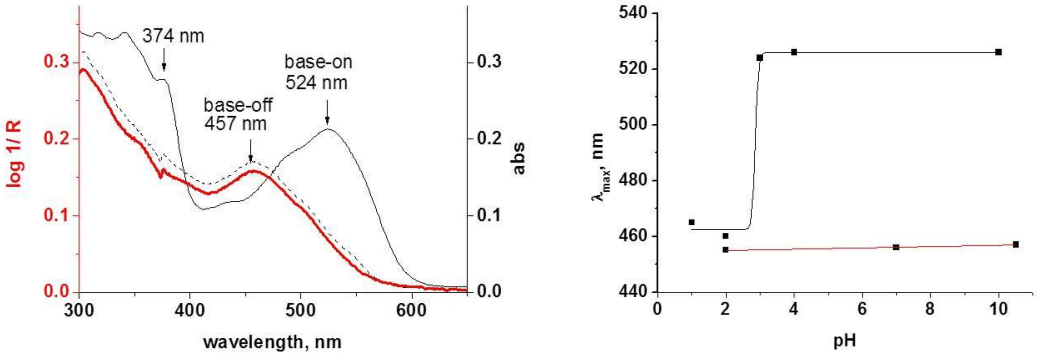

Figure 18. (*left*) Diffuse reflectance spectrum of $AdoCbl_{C18}$ (red) at pH 10 in comparison to the UV-vis spectra (black) of AdoCbl in water in its base-off (pH 2; dotted line) and base-on (pH 7.5; solid line) forms, respectively. (*right*) pH-dependence of the absorbance maxima of the α/β band of Ado-Cbl_{C18} (red line) or $AdoCbl_{Silica}$ on unmodified silica (black line; $pK_{base\text{-}off}$ = 2.9).[180]

The dissociated Dmbz base is encapsulated within the C18 alkyl chains of the solid support (see Scheme 13).[180] A similar constitutional change is observed during cofactor binding in enzymes such as glutamate-, or methylmalonylcoenzyme A mutase, whereas the dissociated nucleotide linker is embedded into a hydrophobic binding pocket of the protein.[183-185]

In the series of the investigated cobalamins **1**, **6** and **7**, β-axially cobalt(III)-coordinated water induces the strongest intramolecular coordination of the trans-coordinated Dmbz base to the metal centre.[181] The $pK_{base\text{-}off}$ value of -2.4 of aquacobalamin reflects a 10^6-fold preference of the base-on form compared to AdoCbl ($pK_{base\text{-}off}$(AqCbl) - $pK_{base\text{-}off}$(AdoCbl) = 6.1).[181] Therefore, AqCbl remains base-on during immobilisation at neutral conditions. Though, pH dependent blue shifts of the reflection maxima were observed under acidic conditions indicating the base-on/base-off transition.

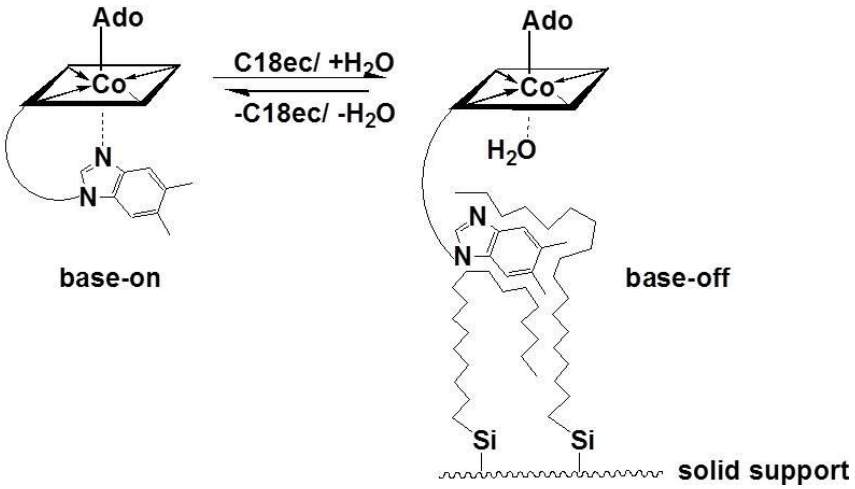

Scheme 13. Proposed model for the base-on to base-off switch of AdoCbl while being immobilised on the solid support. The base-off constitution (*right*) is stabilised by encapsulation of the Dmbz base between the alkyl chains of the C18-alkyl material.

A $pK_{base\text{-}off}$ value of 2.5 for $AqCbl_{C18}$ was determined from the blue shift of the γ-band (see Figure 19) that correlates to a 10^5-fold preference of the base-off form within the solid-support compared to the behavior in water ($pK_{base\text{-}off}$ ($AqCbl_{C18}$) - $pK_{base\text{-}off}$ (AqCbl) = 4.9, see Table 8).[180]

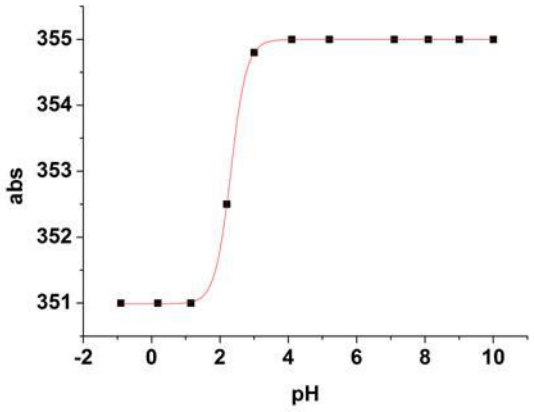

complex	$pk_{base\text{-}off}$
AdoCbl in water	3.7
$AdoCbl_{Silica}$	2.9
$AdoCbl_{C18}$	no base-on form is observed
AqCbl in water	-2.4
$AqCbl_{C18}$	2.5

Figure 19. (*left*) pH-dependence of the absorbance maxima of the γ-band of aqua-Cbl immobilised on C18ec (silica $AqCbl_{C18}$; $pK_{base\text{-}off}$ = 2.5).

Table 8. (*right*) $pk_{base\text{-}off}$ values of AdoCbl[181] and AqCbl[181] in water or immobilised on silica or silica C18ec and treated with aqueous solution of different pH values. All values were determined from the shifts of the γ-band of the DRUV-VIS or UV-vis spectra.

Obviously, in spite of the strong intramolecular coordination of the Dmbz-base in AqCbl, the base-off form is stabilised by the hydrophobic surface of silica C18ec as well.

Vitamin B12 (CNCbl) shows in water a base-off to base-on transition between pH 0 and 1 with a $pK_{base\text{-}off}$ value of 0.36 (see Table 9) and a red shift of the α- and β-bands ($\Delta\lambda_{max}$ ~ 20 nm; Figure 20, blue solid and grey dotted lines). This $pK_{base\text{-}off}$ value lies between the values of AdoCbl and AqCbl. Investigations on $CNCbl_{C18}$ reflect this middle position concerning the stabilisation of the intramolecular Dmbz coordination as well. In pH dependent experiments, even at basic conditions up to pH 10, only an incomplete base-off/base-on transition is observed.[181] The diffuse reflectance spectra of $CNCbl_{C18}$ present only one broad absorption at 528 nm (Figure 20; blue and grey lines).

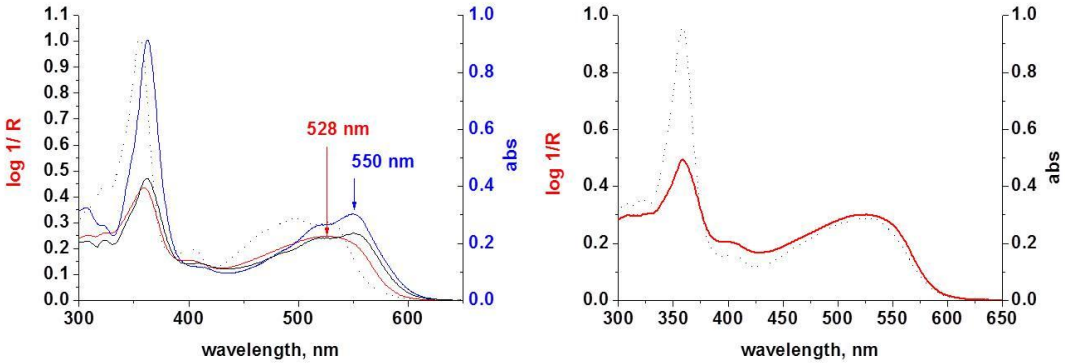

Figure 20. (*left*) DRUV-vis spectra of $CNCbl_{C18}$ (pH 9; red) in comparison to $CNCbl_{Silica}$ (pH 7.5; black) and UV-vis spectra of CNCbl in water in either the base-off (pH -0.5; grey, dotted line) or base-on form (pH 7.5; blue); UV-vis spectrum of base off CNCbl. (*right*) DRUV-vis spectrum of $CNCbl_{C18}$ pH 9, red) and UV-vis spectrum of base-off CNCbl (pH 0.3; grey, dotted line).

The DRUV-vis maxima of $CNCbl_{C18,}$ after treating the column with water in the range from pH 6 – 13 (24 h), are consistent with the UV-vis maxima of CNCbl at pH = 0.3 in water. At this pH value (pH = pKa = 0.3), a one to one mixture of the base-on and base-off forms of CNCbl is present in solution.

It can be assumed that $CNCbl_{C18}$ (after flushing the column with water in the range from pH 6 – 13) exists as well in two configurations which are discriminated in their base-on/base-off constitution. The base-off species is stabilised by hydrophobic interactions between the nucleotide loop and the C18-chains of the alkylated silica surface and remains pH independent in the base-off form. A coexisting second species shows an acid induced dissociation of the Dmbz base between pH 2 and 4. The pH dependent shifts of the γ-band of $CNCbl_{C18}$, in comparison to the values of the pH titration of CNCbl in water led to the assumption that a complete switch back to base-on $CNCbl_{C18}$ is not possible (see Figure 21 left, red and blue lines).

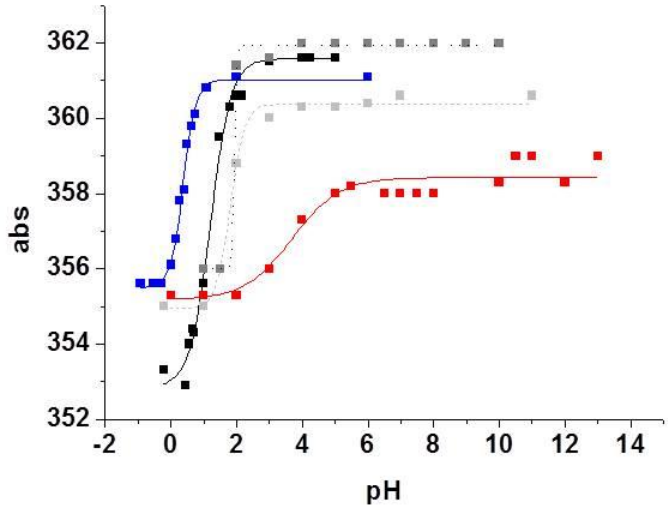

complex	$pk_{base-off}$
CNCbl in water	0.36
$CNCbl_{Silica}$	1.87
$CNCbl_{TLC}$	1.80
$CNCbl_{paper}$	1.93
$CNCbl_{C18}$	3.70

Figure 21. (*left*) pH dependent shifts of the γ-band of CNCbl immobilised on silica C18ec ($CNCbl_{C18}$; red line), on silica ($CNCbl_{Silica}$; black line), on silica TLC plates ($CNCbl_{TLC}$; light grey, dashed line), on filter paper ($CNCbl_{paper}$; dark grey dotted line), and in water (blue line).[180]

Table 9. (*right*) $pK_{base-off}$ values of CNCbl in water or immobilised on different materials upon storing in water of different pH. All values were determined from the shifts of the γ-band of the DRUV-VIS or UV-vis spectra.

Reference experiments with $CNCbl_{Silica}$ (CNCbl immobilised on non-modified silica) at pH 3-8 show that the diffuse reflectance spectra agree with the UV-vis spectra of base-on CNCbl with two distinct maxima for the α-, and β-bands at 527 nm and 550 nm, respectively.[180] An example is presented for $CNCbl_{Silica,}$ immobilised at pH 7.5 (see Figure 21, black line). Figure 21 left shows the pH dependent shifts of the γ-

band of $CNCbl_{C18}$ and $CNCbl_{Silica}$ treated with water at increasing pH in comparison to the values of the pH titration of CNCbl in water.

Only a small shift of the base-on/ base-off transition to less acidic conditions is observed for $CNCbl_{Silica}$ compared to the $pK_{base\text{-}off}$ values of the pH titration of CNCbl in water. (see Table 9 and Figure 21, black line). Additional pH dependent immobilisation studies were performed on Silica TLC plates and on filter paper. CNCbl was immobilised by dipping the solid support into the aqueous solution. As expected for non-hydrophobic surfaces, the pH dependent shifts of the γ-band of these species also demonstrate the base-on/base-off conversion in the same range as in the measurements with silica columns (1 mL ; see Figure 21, grey dashed line and grey dotted line). The corresponding $pK_{base\text{-}off}$ values are shown in Table 9.

In summary, immobilisation of AdoCbl, AqCbl and CNCbl on alkyl modified silica C18ec altered significantly the base-on/base-off properties of the intramolecularly coordinated Dmbz base of the immobilised species as demonstrated with pH dependent measurements and in comparison with studies in solution. A stabilisation caused by hydrophobic interaction between the nucleotide loop and alkyl chains of the silica surface is assumed.

2.3.2 Base-off cobalamin as precursor for new synthetic pathways

The easier accessibility of base-off cobalamins under weakly acidic up to basic conditions extends the coordination chemistry at the (‘‘lower’’) α-face of natural Cbls through immobilisation and offers new possibilities in vitamin B12 chemistry. This was demonstrated with the design of biomimetic complexes of Cbl-protein assemblies.

In follow-up studies, two different strategies were pursued to probe the altered nucleotide binding of immobilised cobalamins: methylation of $CNCbl_{C18}$ at the N3 position of the Dmbz base with methyl iodide, and substitution of the α-face coordinated water ligand (see Scheme 14). The methylated $CNCbl_{C18}$ was eluted from silica C18ec and characterised with ^{1}H-NMR spectroscopy and LCMS spectrometry.

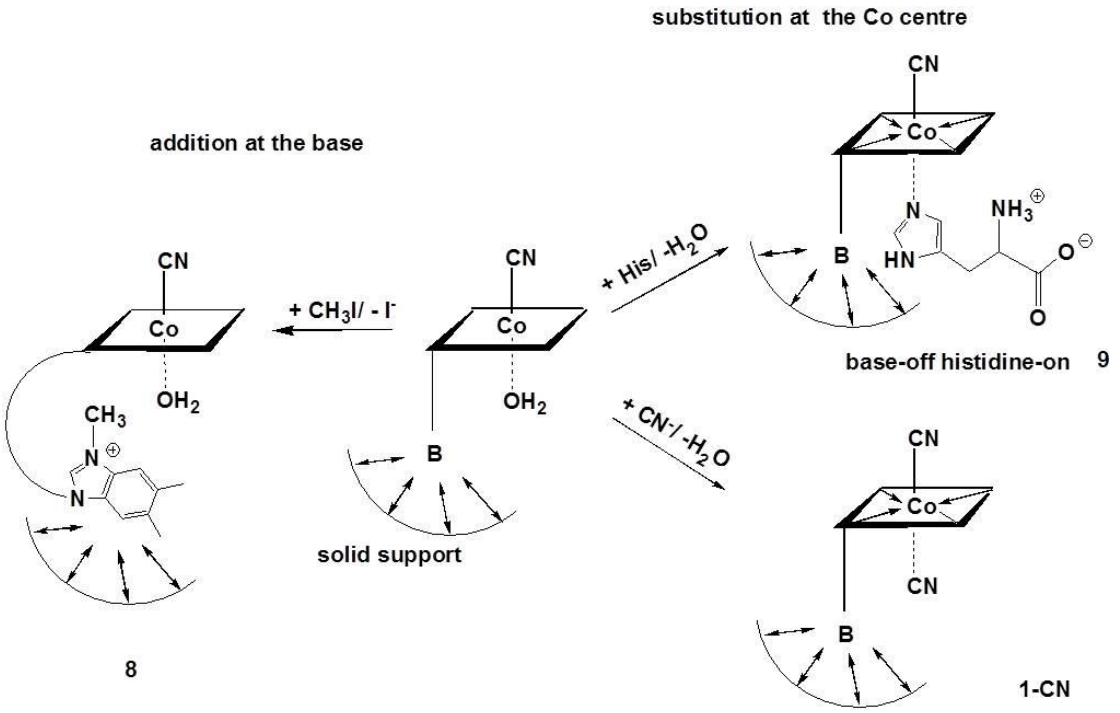

Scheme 14. Synthesis scheme of **8**, **9** and **1-CN** from immobilised base off $CNCbl_{C18}$.

Figure 22 shows the low field shifts of the ^{1}H-NMR signals of B2, B4, B7 of the dissociated methylated Dmbz base the ribose proton R1 and the proton in H 10 position.[180]

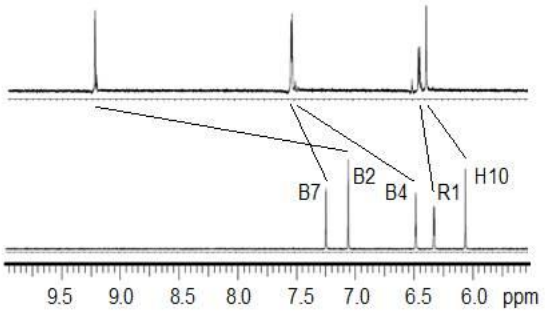

Figure 22. Low-field region of the ^{1}H NMR spectra of **8** (top) and CNCbl (bottom); characteristic signals of the base (B2, B4, B7), the corrin ring (H10) and the ribose (R1) are indicated.[180]

The low field shift of the proton in the H(10) position of the corrin ring, which is highly sensitive the binding of the axial ligands to Co(III) reflects also the altered binding

mode of the Dmbz base. An additional singlet (3 Hs) at 1.06 ppm indicates the methylated N3 nitrogen compared to correlated signals of CNCbl.[180]

A control experiment was performed in solution. An aqueous solution of vitamin B12 (1 mM; 2 mL) and methyl iodide (2 mL) was stirred for 7 days at 30 °C. The reaction was periodically tested with LCMS, but compound **8**$^{+}$ was not observed. In agreement with earlier studies in solution, base-on CNCbl was not methylated under homogenous conditions because of the protection of the N3 position of the Dmbz base by metal-coordination.[186]

As the second strategy (see Scheme 14) the substitution of the α-coordinated water under basic conditions was assessed. Histidine as a ligand is apparently not sufficiently nucleophilic to substitute the intramolecularly bound Dmbz base in solution.[183, 185] Coordination to base-off Cbls is also not possible under acidic conditions because of protonation of the histidine ligand. In contrast to these limitations under homogenous conditions, treatment of $CNCbl_{C18}$ with a saturated aqueous solution of histidine resulted in a base-off/histidine-on Cbl_{C18} complex. The characteristic maxima at 550 nm and 527 nm of the DRUV-vis spectrum of the latter can be assigned to the α-coordination of histidine to base-off $CNCbl_{C18}$ (see Figure 23).

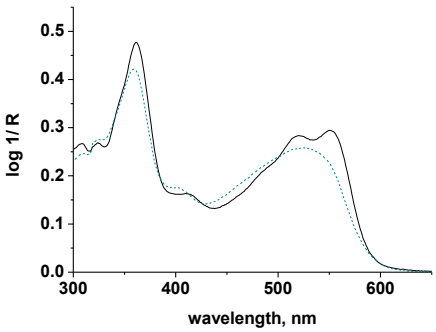

Figure 23. Spectrophotometric changes experienced by immobilised CNCbl (**1**$_{SP}$; *dotted line*) after addition of histidine (**9**$_{SP}$; *solid line*).[180]

The discrimination between histidine-on and benzimidazole-on coordination to Co(III) is not possible, but it is more plausible than to an imidazole-induced switch from

base-off Cbl_{C18} to its base-on form.[180] The base-off/histidine-on coordination presents a biomimetic binding-motif of cobalamin-protein complexes that has not yet been observed in non-biological environments.[185]

The results from immobilised corrinoids further motivated us to study the cyanide substitution of the α-coordinated water. The less strongly coordinating Dmbz base let us expect a higher sensitivity and a faster reaction time than is found for CNCbl in solution. The cyanide-detection experiments were performed in a two-step procedure

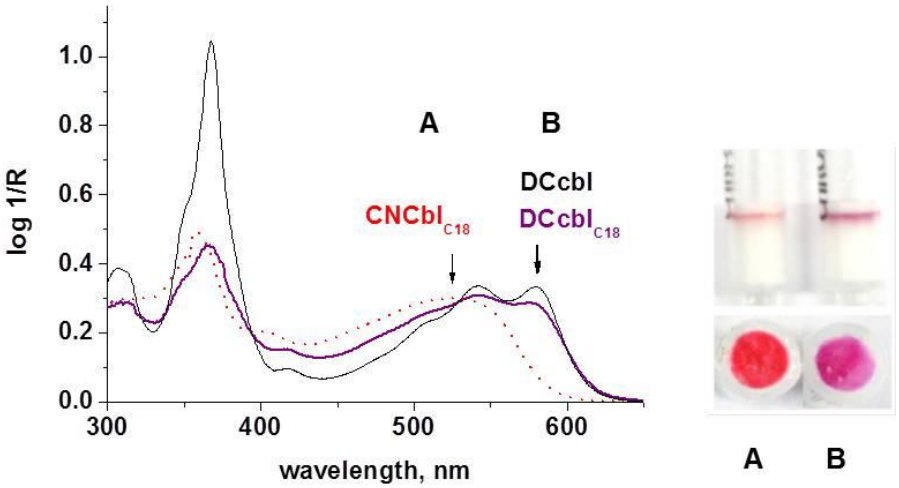

Figure 24. *A:* Spectrophotometric changes experienced by immobilised CNCbl (**1**$_{SP}$; *dotted line*) after addition of cyanide (B: DCCbl$_{SP}$; *solid line*) and DCCbl as reference.

with *chromabond columns* (1 mL). First, CNCbl was immobilised on the top of the white silica C18ec. Afterwards, aqueous solutions containing different cyanide concentrations were passed through the column. This method allowed for the rapid visual detection of cyanide concentrations as low as 1.0 mg/L (1 ppm) at pH 7.5. The observed color change from red to violet took 1 minute (see Figure 24, right).[180] The reflection spectrum of $DCCbl_{C18}$ with the maximum of the α-band at 583 nm is comparable to the absorbance maxima of DCCbl under homogenous conditions (Figure 24, left).[162]

These results were the basis for more detailed investigations of the use of immobilised vitamin B12 and incomplete corrinoids for cyanide detection.

Applications of immobilised corrinoids for analytical purposes are the subject of chapter 2.6.5 and 2.6.6.

2.4 Colorimetric cyanide detection with immobilised incomplete corrinoids

Colorimetric solid phase extraction with immobilised corrinoids has been developed as a new technique for the rapid, effective and economic optical detection of cyanide in complex samples. Concentrations as low as 0.05 mg/L, the limit of detection for cyanide in drinking water according to the guidelines of the WHO, can be visually detected. Quantifications are possible with diffuse reflectance spectroscopy or with a handheld spectrophotometer using the color detection system of the CIELab values. The parallel optical detection of CN^- and SCN^- is achieved with a newly developed anion detection kit. The two anions are often present simultaneously in biological samples.

2.4.1 Colorimetric cyanide detection with immobilised aquacyano-corrinoids

The excellent applicability of immobilised vitamin B12 for cyanide sensing was encouraging for studying immobilised incomplete corrinoids **2** to **4** as well. A series of different alkyl modified silica (*C4, C8, C18RP* and *C18ec*) were tested in regard to their adsorption properties of the corrinoids on the top of the material.

First, a series of different alkyl modified silica (*C4, C8, C18RP* and *C18ec*) were tested with respect to their absorption properties for the corrinoids on the top of the material.[187] Absorption on alkyl modified silica is based on hydrophobic interactions. *Silica C18ec* with the longest alkyl chains and therefore the highest degree of hydrophobic surface was found to be most suited for the immobilisation of ACCbi and ACCbs. It was demonstrated that the nature of the side chain of the corrinoid macrocylce is very important for efficient immobilisation. Converting the seven hydrophobic ester side chains of ACCbs to negatively charged carboxylates in ACCa leads instead to a favoured immobilisation on basic aluminium oxide (Alox N).

The three steps of immobilisation, (i) of ACCbi and ACCbs on silica C18ec columns (1 mL), (ii) passing the cyanide containing sample solution through the column, and

(iii) removing the coloured silica layer for spectroscopic measurements were performed as described for vitamin B12 in chapter 2.3.1 and more detailed in chapter 4. The formation of the immobilised dicyano-product corresponds to the reaction between the corrinoid and cyanide in solution and is described in Scheme 12 and Scheme 14 (formation of 1-CN). The coloured complex on the top layer of the silica C18 matrix material was investigated with DRUV-vis spectroscopy. Measurements in dependence of increasing cyanide concentrations show an increasing reflection of the α-band at 583 nm. Figure 25 shows the plot of the maximum of log 1/R at 583 nm of $DCCbs_{C18}$ versus cyanide concentration. Quantitative determinations are possible in the linear range between 0 and 0.075 mg/L at pH 7.5 and between 0 and 0.2 mg/L at pH 9.5.[187]

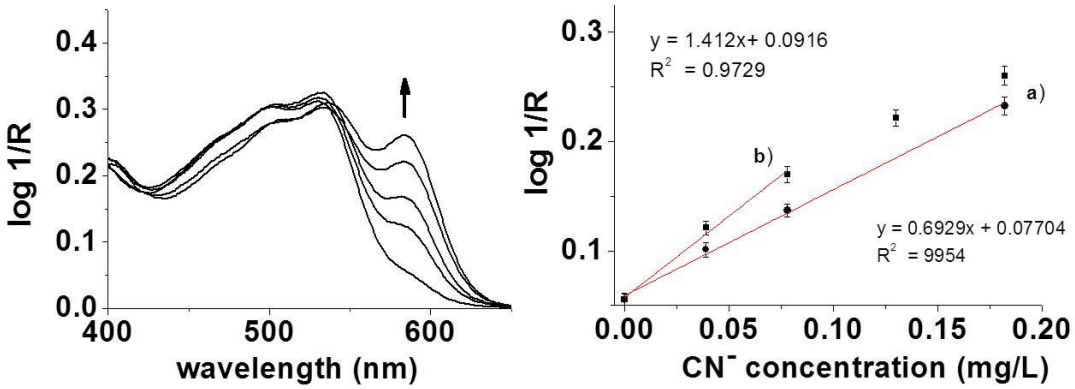

Figure 25. *(left):* DRUV-vis spectra of $ACCbs_{C18}$ (20 nmol) as reference and after passing solutions (5 mL, [CHES] = 20 mM, pH 9.5) of CN^- (0.04 mg/L, 0.08 mg/L, 0.13 mg/L and 0.18 mg/L) through the C18ec-column. *(right):* Calibration curve for the quantification of CN^- at 583 nm and pH 7.5 (a) or pH 9.5 (b).[187]

Visual comparison between the colour of the immobilised chemosensor before and upon passing the sample solution through the column allows the qualitative identification of cyanide that is desirable for the development of a cyanide detection kit (see Table 10).

In addition, colour specific L*a*b* values of the CIELab-system were measured with a hand-held spectrophotometer CM-2900d (see Table 10). The differences in colour in

comparison to $ACCbs_{C18}$ as reference are reported as ΔE values in Table 10. Colour differences of ΔE > 2 are correlated to univocal visual discrimination.[188]

$c(CN^-)$ mg/L		0.04	0.08	0.18
pH 9.5				
ΔE	Ref.	17.3 ± 0.2	20.5 ± 0.2	31.4 ± 1.3
pH 7.5				
ΔE	ref.	8.0 ±0.2	15.2 ± 0.2	17.9 ± 0.7

Table 10. (*From left to right*) Top views on $ACCbs_{C18}$ as reference (20 nmol, orange) and after passing solutions (5 mL, [CHES] = 20 mM, pH 9.5, [HEPES] = 20 mM, pH 7.5) of increasing concentration of CN^- through the column. Corresponding ΔE values are given (CIELab system, ref. = reference).[187]

A distinct colour change from orange to dark red can be visually observed when solutions (5 mL) of concentrations as low as 0.04 mg/L of cyanide passed the column (Table 11, entries 1 and 2). This observation correlates to ΔE values that are four and eight times above ΔE = 2. This result proves that the colorimetric solid phase extraction is suited for the control of drinking water with the WHO's guideline value of 0.05 mg/L.[38]

In comparison to the detection under homogenous conditions we found for $ACCbs_{C18}$ a seven-fold improved sensitivity (Table 11; entries 1 *vs* 3, 2 *vs* 4), which results from the extraction and simultaneous concentration of cyanide as $DCCbs_{C18}$ on the solid support from a larger sample volume. This is indicated by comparable detected quantities of cyanide per quantity of chemosensors $ACCbs_{C18}$ or ACCbs (RQ, Table x; entries 1 *vs* 3, 2 *vs* 4). Compared to the detection of cyanide with $CNCbl_{C18}$, the

sensitivity of $ACCbs_{C18}$ is approximately 25 times higher at pH 7.5 (Table 11; entries 1 *vs* 5). This behaviour can be explained by the lack of the Dmbz "protecting group" that causes a fully exposed and better accessible metal centre in $ACCbs_{C18}$. Although less sensitive than the incomplete chemosensors, the effects of the hydrophobic C18 material on the sensing properties of B12 are much more pronounced. For $CNCbl_{C18}$, an enormous benefit of a 130 times higher sensitivity (Table 11, entries 7 *vs* 5) and a 13 times lower quantity of cyanide per quantity of chemosensor compared to the detection of cyanide with CNCbl under homogenous aqueous conditions is observed.[180] This strong "hydrophobic" effect is only obtained for $CNCbl_{C18}$ and not for the incomplete corrinoids supporting the justification of the remarkable increase in sensitivity of $CNCbl_{C18}$ with a destabilisation of the coordinating Dmbz base within the hydrophobic solid-support (see chapter 2.3.1). In incomplete corrinoids such an effect is not possible because there is no Dmbz-base.

Entry	Chemosensor	pH	$c_{(CN)}$ [mg/L][c]	$n_{(CN)}$ [nmol]	RQ[d]
1[b]	$ACCbs_{C18}$	7.5	0.04	7.5	0.375
2[b]	$ACCbs_{C18}$	9.5	0.04	7.5	0.375
3[a]	ACCbs	7.5	0.3	10	0.25
4[a]	ACCbs	9.5	0.3	10	0.25
5[180][b]	$CNCbl_{C18}$	7.5	1.0	200	10
6[180][b]	$CNCbl_{C18}$	9.5	0.3	50	2.5
7[162][a]	CNCbl	7.5	130	5000	125
8[162][a]	CNCbl	9.5	13	500	12.5

Table 11. Minimum concentration of visually detected cyanide with CNCbl and ACCbs under homogenous or heterogeneous conditions at pH 7.5 or 9.5; ([a] [CNCbl] = [ACCbs] = 40 nmol, V = 1mL, [d] $[CNCbl_{C18}] = [ACCbs_{C18}]$ = 20 nmol, V = 5 mL, [HEPES] = 20 mM (at pH 7.5), [CHES] = 20 mM (at pH 9.5), [c] > 10% over the minimum visually detectable concentration of cyanide, [d] RQ: Ratio of quantities, $RQ = n_{[CN]}/ n_{[CS]}$, CS: chemosensor).

The selectivity of $ACCbs_{C18}$ was assessed like in the tests under homogenous conditions for the fourteen anions F^-, Cl^-, Br^-, I^-, SCN^-, NO_3^-, HCO_3^{2-}, $C_2O_4^{2-}$, SO_4^{2-},

$H_2PO_4^-$, ClO_4^{2-}, CH_3COO^-, OCN^- and $EDTA^{2-}$ (0.1 M; 5 mL; [CHES] = 20 mM, pH 7.5 and 9.5).[174] Most perturbing for the visual detection of cyanide with $ACCbs_{C18}$ were concentrations of 35 mg/L of SCN^- (>0.6 mM; 5 mL) and 42 mg/L OCN^- (>1 mM; 5 mL).[174] The interference of these anions under CSPE conditions is higher compared to that under homogenous detection and may be caused by the larger sample volume of the former (5 mL in CSPE vs. 1 mL in homogenous conditions). An additional interference from iodide is observed with concentrations above 3 mM (381 mg/L). The iodo-, thiocyanato-, and cyanato$CCbs_{C18}$ complexes of the interfering anions can be identified by means of the DRUV-vis spectra as shown in Figure 26. The maxima of these $XCCbs_{C18}$ spectra are in good agreement with the maxima of the UV-vis spectra in dichloromethane (see chapter 4, Table 18).

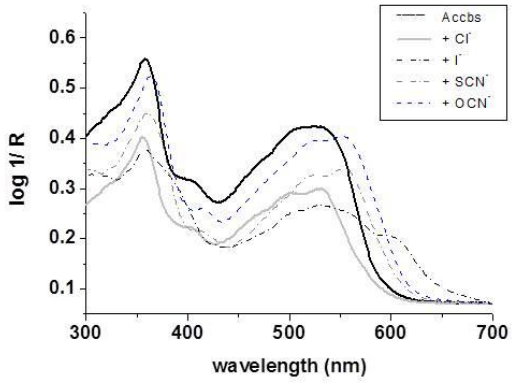

	ACcbs	+ Cl^-	+ I^-	+ SCN^-	+ OCN^-
ΔE	ref.	0.8 ± 0.2	31.7 ± 0.2	22.3 ± 0.1	20.2 ± 0.2

Figure 26. *(left):* DRUV-vis spectra of $ACCbs_{C18}$ (20 nmol) and after passing solutions (0.5 mL, [HEPES] = 20 mM, pH 7.5) of chloride, iodide, thiocyanate or oxalate (0.1 M) through the column. (*right*)*:* Corresponding photographs of top views of the columns and corresponding ΔE values (CIELab system, ref. = reference = $ACCbs_{C18}$).

The corresponding colour changes and the spectrophotometric ΔE values for passing high concentrations of these anions through the column (100 mM) are shown in Figure 26. The spectrum of chloroCCbl shows no shift of the absorbance maxima compared to ACCbs and is only given as an example for non-interfering anions.

As seen in this study, the selectivity of $ACCbs_{C18}$ is limited which also restricts its applicability in cyanide sensing in practical situations. In particular, biological samples

often contain SCN^- in addition to CN^-. For such cases a special detection kit was developed as described in chapter 2.4.2.

An important economic and ecological advantage of the silica C18ec material is the regeneration of the $DCCbs_{C18}$ containing matrix. Washing the columns with 0.1-1% of diluted aqueous acids (3 mL) and then with water (20 mL) results in back-formation of $ACCbs_{C18}$, visible as the orange color.[187] During this process, $ACCbs_{C18}$ and $CNCbl_{C18}$ remain adsorbed on the top of the filter material. A series of ten subsequent runs of cyanide detection and regeneration showed no apparent loss of sensitivity or alteration of the quality of immobilised $ACCbs_{C18}$ and $CNCbl_{C18}$. We assume that many more consecutive tests are possible with this system.

2.4.2 Alternative matrix materials

As alternative materials for cyanide sensing EmporeTM SPE columns (EC-SPE, 1 mL, product number 4115,) and EmporeTM extraction discs (*C18*, diameter of 47 mm, product number 2215) were tested. These materials contain a C18ec impregnated polymer. Immobilisation of the chemosensors on EmporeTM SPE columns already led to an unfavourable colour change to violet (λ_{max} = 580 nm). As a result these products were not investigated further. However, self-made discs from EmporeTM extraction discs impregnated with CNCbl or ACCbs were assessed using a self-made filter holder device (see Figure 27).

A highly sensitive detection of the violet dicyano product was observed but the surface of the polymer disc becomes saturated with the chemosensor already at the very small cyanide concentrations of 0.06 mg/L (see Figure 27, left). The linear range for quantitative determinations of the cyanide concentration is, therefore, also too small for practical applications. (see Figure 27, right). However, the method is most promising for the qualitative cyanide detection in low concentrations near the limit of the allowed cyanide concentration in drinking water (0.05 mg/L).[38]

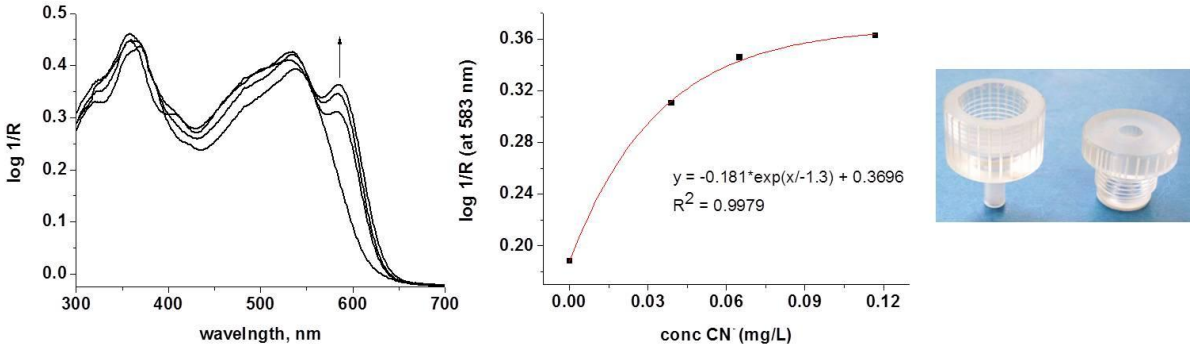

Figure 27. *(left)* DRUV-vis spectra of $ACCbs_{C18}$ (20 nmol) and $ACCbs_{C18}$ (20 nmol) after passing solutions (0.5 mL, [CHES] = 20 mM, pH 9.5) of CN^- (0.04 mg/L, 0.065 mg/L, 0.12 mg/L) through an Empore disc; (*centre*) plot of log 1/R at 583 nm versus cyanide concentration pH 9.5 (exponential fitted); (*right*) photograph of the self-made filter holder.

ACCa, containing seven acid side chains, was successfully immobilised on Alox N/UV_{254} TLC plates. Test strips (15 x 5 mm) were produced by dipping the material into an aqueous solution of ACCa (1 mM, 2 sec), thus absorbing the chemosensor as $ACCa_{TLC}$. Initial studies of soaking the test stripes into cyanide containing sample solutions showed that the reaction of $ACCa_{TLC}$ to $DCCa_{TLC}$ was completed after ten minutes. Figure 28 shows test stripes after subsequently soak with increasing concentrations of cyanide (0 - 2.08 mg/L). A color change from orange to violet indicated the formation of $DCCa_{TLC}$. With $ACCa_{TLC}$ it is possible to identify cyanide concentrations as low as 1 mg/L with visual detection.

RP-18 HPTLC plates immobilised with ACCbs were slightly more sensitive for cyanide detection than $ACCa_{TLC}$ but still much less sensitive than C-SPE with a visual detection limit as low as 0.04 mg/L of cyanide.

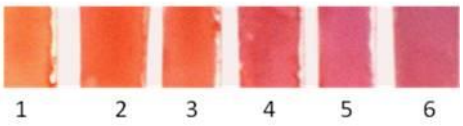

Figure 28. (*From left to right):* $ACCa_{TLC}$ after soaking for 10 minutes in sample solutions ([CHES] = 20 mM, pH 9.5) with increasing concentrations of cyanide (0, 0.26 mg/L, 0.52 mg/L , 1.04mg/L , 1.56 mg/L and 2.08 mg/L).

2.4.3 Visual detection kit for the simultaneous sensing of cyanide and thiocyanate

A detection kit was developed for the selective visual sensing of multiple analytes. Cartridges connected in series with different immobilised chemosensors allow the spatially separated detection and extraction of different anions (see Scheme 15).[187] As a proof-of-concept we demonstrated the visual discrimination between cyanide and thiocyanate, a typical issue for urine samples of persons with chronic cyanide poisoning.[105, 189] In the detection zone of the first cartridge which is loaded with $CNCbl_{C18}$, cyanide is selectively detected visually by the colour change from red to violet as described in chapter 2.4.1. An additional layer of highly concentrated $CNCbl_{C18}$ in the second cartridge, i.e. the “extraction cartridge”, removes potentially excessive, interfering cyanide. Complete cyanide removal from the sample solution is verified with a consecutively arranged small test zone of $CNCbl_{C18}$. The final detection zone is in the third cartridge and contains $ACCbs_{C18}$ for the detection of thiocyanate.

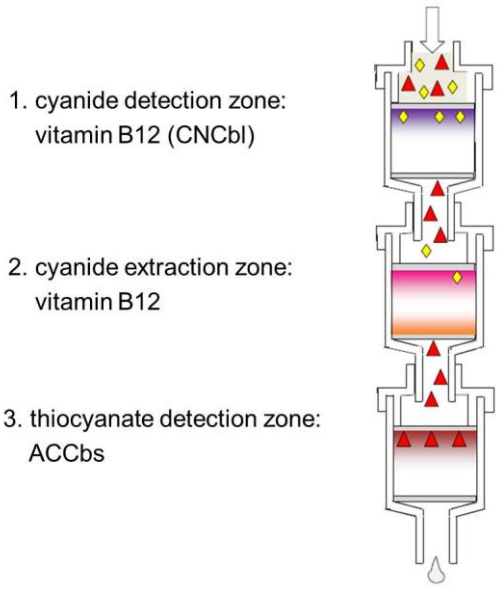

Scheme 15. Scheme of the detection kit for simultaneous anion proof; cartridge 1: cyanide detection zone containing $CNCbl_{C18}$, cartridge 2: cyanide extraction zone containing $CNCbl_{C18}$, cartridge 3: thiocyanate detection zone containing $ACCbs_{C18}$.[187]

Detailed information about the detection procedure and the concentrations used is provided in the Appendix VII.

It may be concluded that immobilised aquacyano corrinoids provide an improved sensitivity for cyanide detection from aqueous solution even below the WHO's guideline value for cyanide in drinking water of 0.05 mg/L.[38] The identification of cyanide is possible with the naked eye or may be supported with a hand-held spectrophotometer. Quantifications are indicated up to 0.2 mg/L but this is in principle adjustable via the amount of immobilised chemosensor. Most promising for the detection of multiple analytes in complex samples is the strategy of connecting cartridges in series with separate extraction and detection zones. In a proof-of-concept, the simultaneous detection of cyanide and thiocyanate was demonstrated. Practical demonstrations are presented in chapter 2.6.5.

2.5 Optical screening of metal-based chemosensors for the detection of cyanide and other biologically important anions

In this section an alternative approach to search for highly sensitive and selective chemosensors for the colorimetric detection of cyanide and other biologically important anions is presented. The detection mode is based on the decomplexation of a transition metal-indicator complex by the anion of interest which is associated with a colour change. In a microarray screening of metal indicators, transition metal ions and anions, novel chemosensors for the detection of cyanide, phosphate and oxalate were identified. The most promising systems were studied in more detail.

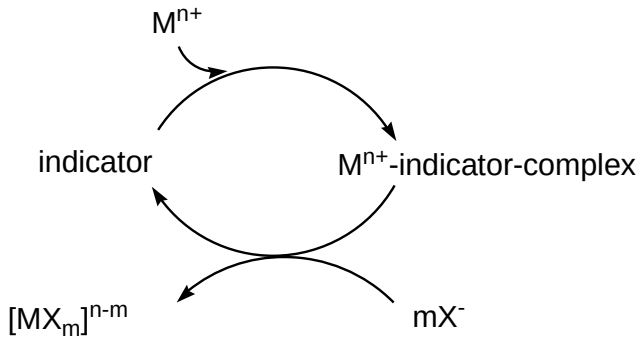

Scheme 16. Schematic overview of the optical screening procedure for the identification of anion-chemosensors from mixtures of commercially available indicators and metal ions ($M^{2+/3+}$) tested with different anions.

Among various approaches designed for cyanide detection, decomplexation of copper chromophore complexes with cyanide is one of the rare systems that are operable, just as corrinoids, in aqueous solution.[141, 153, 190, 191] We tested this interesting method in a microarray screening for a multitude of metal indicators, transition metal ions and anions.[192] A general overview of the two step procedure is presented in detail in Scheme 16.

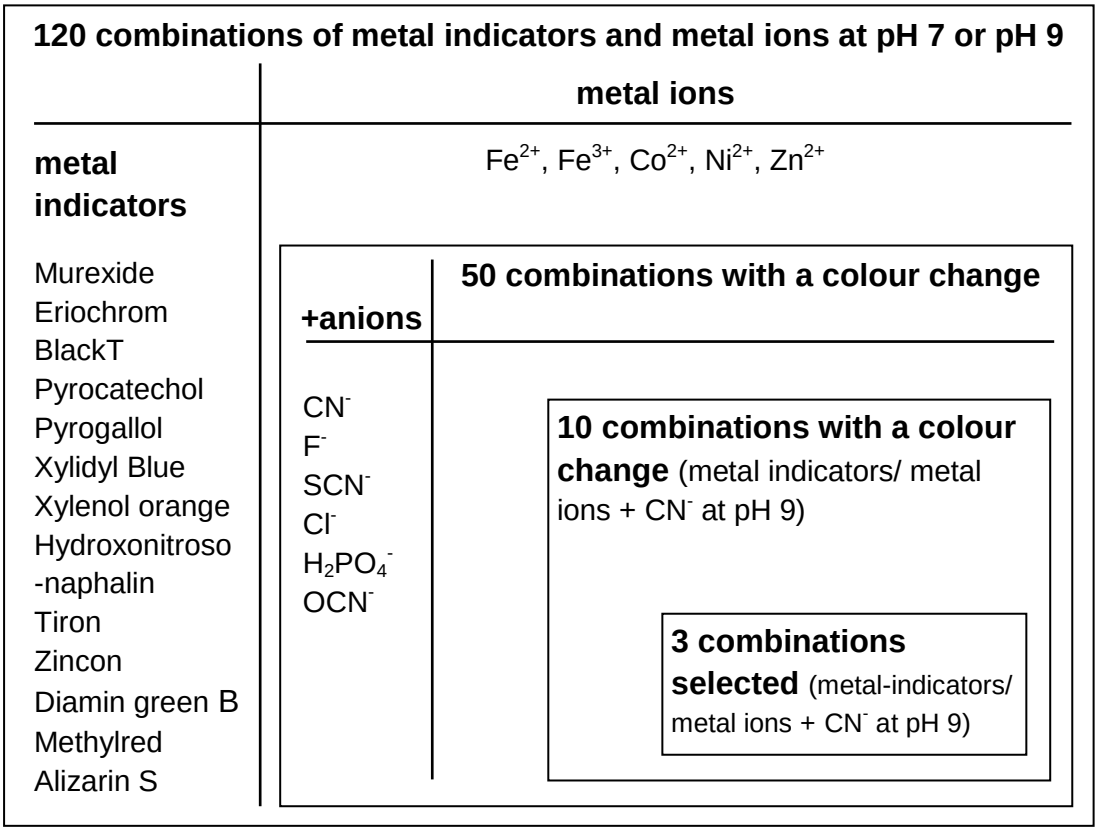

Scheme 17. Master-detail-screen of 120 combinations of 12 metal indicators (50 µM) and 5 metal ions (50 µM) applied in the first round at pH 7 or pH 9; the 50 selected combinations of metal indicators (50 µM) and metal ions (50 µM) applied in the 2nd round; the ten selected combinations of metal indicators (50 µM) and metal ions (50 µM) that showed a change in color after adding cyanide (3 mM) in water (pH 9.0 ± 0.1).[192]

The reaction cycle corresponds to the well-known complexometric titration developed by Schwarzenbach at the University of Zurich; in a first step a solution of a complexometric indicator forms with transition-metal ions a metal ion-indicator complex that causes a colour change of the solution.[193] In a second step, positively

tested anions coordinate to the metal with higher stability constants, thereby releasing the free indicator and reversing the solution to the initial colour. At first, we focused on the selection of chemosensors for cyanide detection. A detailed schedule of the overall screening process is presented in Scheme 17.

In the first round, twelve commercially available metal indicators such as murexide and eriochrome T (50 µM) were tested with equimolar amounts of Fe^{2+}, Fe^{3+}, Co^{2+}, Ni^{2+} or Zn^{2+} at pH 7 or pH 9.[192] A colour change was observed for 50 metal-indicator complexes of the 120 possible combinations. In the second screening round, these fifty selected metal-indicator complexes were tested with six different solutions of anions in relatively high concentrations (3 mM). Besides cyanide, five of the most interfering anions in cyanide detection were employed.[141, 174]

A successful reaction cycle with a colour change back to the colour of the free indicator was observed for ten of this metal-indicator/cyanide systems at pH 9 within a few seconds at room temperature. Of these systems, the three with the most pronounced colour changes from yellow to pink and from blue to colourless, were investigated in more detail (see Table 12 and Figure 30): murexide/Ni^{2+} (or Co^{2+}) and zincon/Zn^{2+} at pH 9.[192] This way it was possible to identify a novel highly sensitive cyanide indicator system, i.e. the Ni^{2+}-murexide complex, with a limit of detection (LOD) for cyanide that lies below the Maximum Contaminant Level (MCL) of 0.2 mg/L (7.7 µM) of the U.S. Environmental Protection Agency (EPA) (see Table 12).[1, 192]

The selectivity of the three systems was tested with the 13 anions F^-, Cl^-, Br^-, I^-, SCN, NO_3^-, CO_3^{2-}, $C_2O_4^{2-}$, SO_4^{2-}, $H_2PO_4^-$, ClO_4^-, AcO^- and OCN^- at pH 9 in water ([CHES] = 20 mM, see Figure 47 and Figure 48).[192] Decomplexation of the murexide-(Co^{2+}/Ni^{2+}) systems are only observed for oxalate and phosphate in concentrations that are 100 times and about 10^3 times higher than cyanide, respectively. An excellent selectivity with no interference with any of the tested anions has been demonstrated by the less sensitive zincon/Zn^{2+} system.

metal indicators	metal ions[a]	VD_{vis} [µM]	LOD [µM]	colour change	$interferent_{vis}$/ [mM]
Murexide	Ni^{2+}	40 (1.4 mg/L)	6 (0.16mg/L)	yellow>pink	$C_2O_4^{2-}$ /0.5 PO_4^{3-} /3
Murexide	Co^{2+}	60 (1.6 mg/L)	14	yellow>pink	$C_2O_4^{2-}$/0.1 PO_4^{3-} /1.5
Zincon	Zn^{2+}	250	65	blue>colourless	-

Table 12. Characteristic data of the selected metal-based sensors with the most pronounced colour changes ([a][M^{2+}] = 20 µM, [murexide] = 36 µM, [zincon] = 40 µM; pH 9.0 ± 0.1).[192]

Titration experiments with the three selected indicator/M^{2+}/cyanide systems were performed in order to follow the stepwise conversion from the free indicator to the indicator/metal complexes and its subsequent decomplexation by the addition of cyanide.

Murexide (H_5L) exists at pH 9 as purpureate anion (H_4L^-) indicated by a UV-vis absorbance maximum at λ_{max} = 522 nm (see Figure 29).[194] The stepwise titration (62 µM) with Co^{2+} (0 - 70 µM) in water ([CHES] = 20 mM; pH 9.0) shows a clear conversion to the murexide/Co^{2+} complex without any side reactions indicated by an isosbestic point at 505 nm.[192]

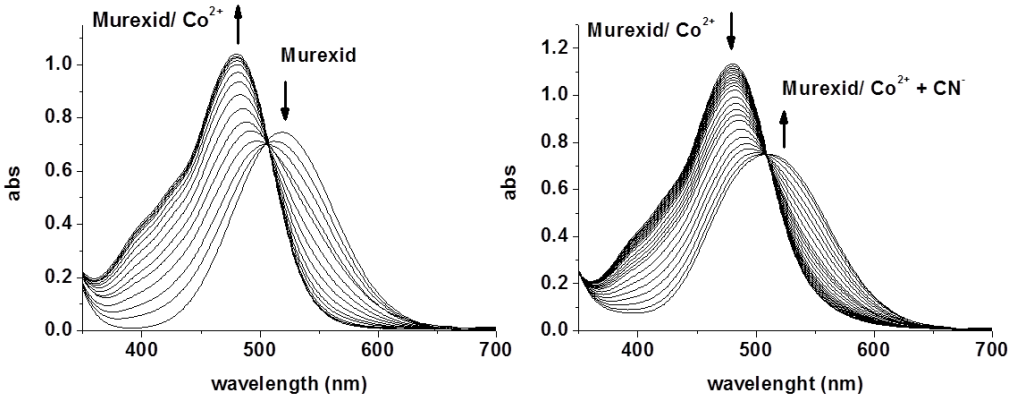

Figure 29. (*left*) UV-vis spectra of the titration of murexide (62 µM) with Co^{2+} (0- 70 µM) in water ([CHES] = 20 mM; pH 9.0 ± 0.1). (*right*) UV-vis spectra of the titration of a mixture of murexide (62 µM) and Co^{2+} (55 µM) with increasing amounts of CN^- (0 - 310 µM) in water ([CHES] = 20 mM; pH 9.0 ± 0.1).

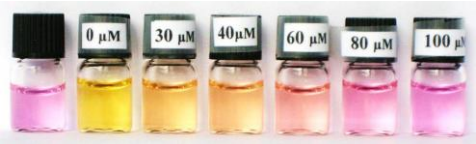

Figure 30. *From left to right:* Murexide (36 µM) in water, a mixture of murexide (36 µM) and Ni^{2+} (20 µM) in water without additional cyanide (second vial) as well as increasing amounts of CN^- (30 - 100 µM) at pH 9 ([CHES] = 20 mM).[192]

The absorbance maximum of the yellow-orange $(Co^{2+}\text{-}H_4L)^+$ complex is hypochromically shifted ($\Delta\lambda_{max}$ = 42 nm) compared to the free murexide. Corresponding experiments for the murexide/Ni^{2+}/CN^- -system are described in the publication in the Appendix IV.[192]

In addition, the metal to ligand ratios of the M^{2+} purpureate complexes of 1:1 were verified using the method of continuous variations.[195] The plot of the UV-vis absorption at 476 nm versus the molar fraction of murexide suggests the formation of a $(M\text{-}H_4L)^+$ complexe as it is representatively shown in Figure 31 for $(Ni\text{-}H_4L)^+$.[192]

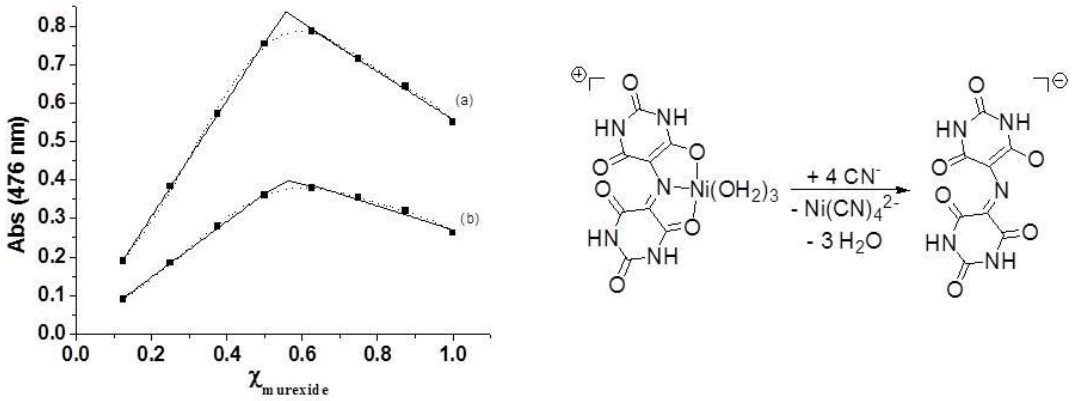

Figure 31. Jobplot diagram and reaction scheme for the formation of a $(Ni\text{-murexide})^+$ complex $(Ni\text{-}H_4L)^+$.

The UV-vis absorption spectra of the stepwise titration of a solution of zincon (40 µM, λ_{max} = 620 nm) with Zn^{2+} (20 µM) also indicate a straightforward complexation with an isosbestic point at 531 nm. The hypsochromic shift of the absorption maximum of

$\Delta\lambda_{max}$ = 133 nm during the titration reflects the excellent visually detectable colour change from yellow to blue as seen in the photographs of the solutions (see Figure 32). The Zn^{2+}/zincon complex demonstrates its suitability as a chemosensor for cyanide with outstanding properties with respect to selectivity and colour change. The remaining drawback of its relatively low sensitivity may possibly be improved with an immobilisation on the appropriate solid-phases and by using the method of colorimetric solid phase extraction as described above for CNCbl (Chapter 2.3.1).

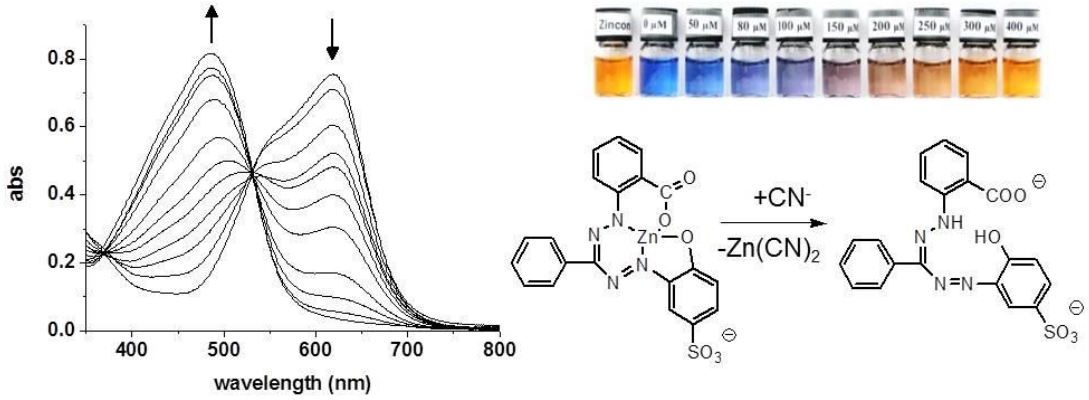

Figure 32. (*left*) UV-vis spectra of a mixture of zincon (40 µM) and Zn^{2+} (20 µM) in water ([CHES] = 20 mM; pH 9.0 ± 0.1) with increasing amounts of CN^- (0 - 0.5 mM). (*right top*) pictures (*from left to right*) of zincon (40 µM) and zincon/Zn^{2+} (40 µM/ 20 µM) with increasing concentrations of CN^- (0 - 400 µM) in water ([CHES] = 20 mM; pH 9.0 ± 0.1). (*right bottom*) Reaction scheme for the decomplexation of the (Zn-zincon)$^{2-}$ complex.[192]

The successful analysis of cyanide with the displacement method offers the possibility to extend such systems to multiple anions. A representative second screening procedure focused on other biologically important anions like phosphate and oxalate. Such anions are routinely tested during blood analysis. Increased levels of the oxalate are linked to inborn metabolic diseases such as primary hyperoxalury or the intestinal disease *Morbus Crohn* and analysed in clinical settings using enzymatic tests or ion chromatographic methods. The procedure was applied in the same manner as for the first screening. This time, 36 combinations were tested (see Table 24 in chapter 4) whereby cations such as calcium or magnesium with a high affinity towards the selected anions had been selected. In the two step process two other novel sensor systems were identified: calcon/Ca^{2+}- and an eriochrom

black T/Mg^{2+} system. Optical detection of micromolar concentrations of phosphate at pH 12.3 and millimolar concentrations of oxalate at pH 9.0, respectively, has been achieved.[192] Both decomplexation reactions are accompanied by a colour change from violet to blue (see Table 13 and Figure 33).

indicator/ metal ion	**analyte**	**OD** [µM]	**LOD** [µM]	**interf. [mM]**
Calcon/ Ca^{2+} (pH 12.3)	HPO_4^{2-}/ PO_4^{3-}	80 (8mg/L)	24 (3 mg/L)	CO_3^{2-} [0.5] OCN^- [0.4]
Eriochrom black T/ Mg^{2+} (pH 9.0)	$C_2O_4^{2-}$	1000 (88mg/L)	95 (8.4 mg/L)	HPO_4^{2-}[2] PO_4^{3-} [2]

Table 13. 'Naked eye' screening of colorimetric metal-based chemosensors for phosphate and oxalate (margin of error in brackets).[192]

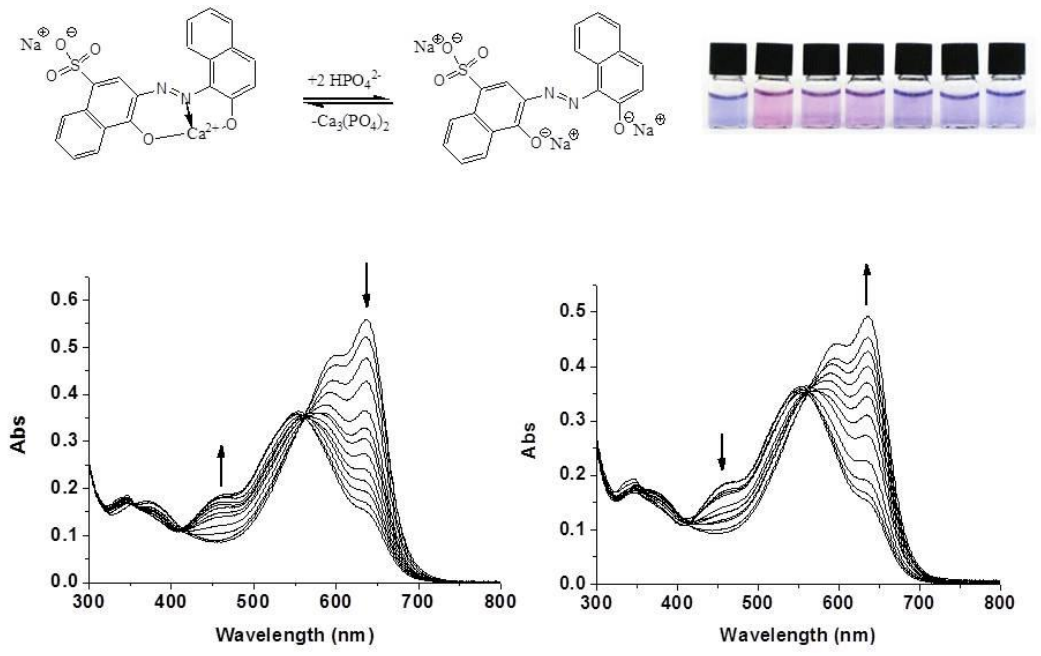

Figure 33. (*top left*) reaction scheme of the formation of the Ca^{2+}/calcon complex; (*left*) UV-vis spectra of the titration of calcon (40 µM) with Ca^{2+} (0 - 120 µM) in water (pH 12.3); (*right*) UV-vis spectra of the titration of the Ca^{2+}/calcon complex with increasing amounts of HPO_4^{2-} (0 - 500 µM); (*top right*) photographs of corresponding solutions (*from left to right*) with calcon, Ca^{2+}/calcon and increasing concentrations of HPO_4^{2-} (0 - 400 µM, pH 12.3).[192]

The UV-vis absorptions of the titration of calcon (40 µM) with Ca^{2+} (0 - 120 µM) at pH 12.3 correlate very well with the spectra for the decomplexation of the Ca^{2+}/calcon complex under addition of increasing amounts of HPO_4^{2-} (0 - 500 µM, see Figure 33). The limits of detection determined either by the naked eye or with UV-vis spectroscopy are relatively high compared to the limits of detection of these anions in drinking water (PO_4^{3-}: 6.95 mg/L) but in the range of concentration limits in blood or urine (PO_4^{3-}: 76 – 49 mg/L (blood); 460 - 1850 mg/d (urine)). Applications in simple and fast colorimetric medicinal surveys, therefore, are possible in principle.

In summary, a two-step 'naked-eye' screening procedure for the identification of selective metal-based chemosensors for biologically important anions from commercially available metal-indicators and metal ions has been successfully developed. The chemosensors allow the optical detection of either micromolar cyanide or phosphate as well as millimolar oxalate in water. An excellent colour change is observed for the Ni^{2+}/murexide system meanwhile the best selectivity was tested with the Zn^{2+}/zincon system. Compared to the identification of cyanide with corrinoids using CSPE, the analytical procedure is more complex as it relies on different solutions. Introducing CSPE to this method could improve the sensitivity. Applications in food safety control have been illustrated in chapter 2.5.8.

2.6 Applications

In the wide range of possible applications of colorimetric cyanide detection we focussed on three primary contexts: (i) the detection of cyanide in food, mainly in cassava, (ii) in blood and (iii) in industrial wastewater. All of these targets are in need of quick and simple methods for cyanide detection as the first step to remedy or manage cyanide contamination. Qualitative analyses and quantifications of the cyanide content in cassava, during food processing, as well as in wastewater samples are presented below. But first we report our investigations of the enzymatic liberation of endogenous biological cyanide.

2.6.1 Study of enzymatic liberation of cyanide at a biological interface

The enzymatic release of cyanide in cassava is a two-step process. After cell rupture the cyanogenic glycoside linamarin is enzymatically hydrolysed by linamarase (A) to glucose and acetone cyanohydrin (see Scheme 18.).[70, 196] In a second step, the cyanohydrin decomposes spontaneously to HCN and acetone in an environment of above pH 4 (B).[197] Acetone cyanohydrin can also be decomposed by hydroxynitrile lyase, an additional enzyme expressed in low levels in the roots.[198] It is generally assumed that the linamarase activity is the rate limiting factor in cyanide liberation.[71, 72]

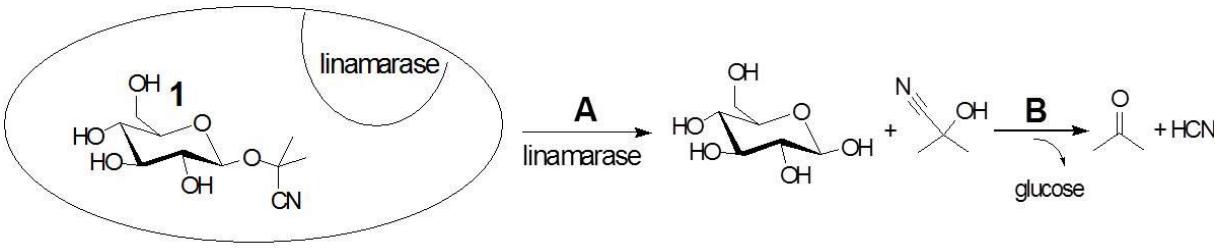

Scheme 18. Scheme of the linamarase catalysed hydrolysis of linamarin to sugar and acetone cyanohydrin (A) that subsequently decomposes to acetone and HCN (B).[71, 73]

Extracts of ground cassava roots from a supermarket in Zurich were analysed with the chemosensors ACCa and ACCbs at pH 9.5. Preliminary experiments were carried out to verify the selective binding of liberated cyanide to ACCa and ACCbs by ^{1}H NMR and UV-vis spectroscopy. The spectra of the isolated dicyano compounds from the cassava extract are in agreement with the spectra of synthesised DCCa and the commercially available product DCCa, respectively.[73] In particular, the singlet of the proton at H (10) position (see chapter 2.1.1, Figure 8), that is highly dependent on the nature of the axially coordinated ligands, indicates the clear formation of the dicyano product.[20, 182]

The diffuse reflectance maxima of colourless samples of ground cassava spiked with ACCa (λ_{max} = 353, 497, and 527 nm) shifted to longer wavelengths (λ_{max} = 365, 534, and 578 nm) indicating the formation of DCCa. These data correspond to those of ACCa and DCCa conducted under homogeneous conditions (see Figure 34). The diffuse reflectance maxima of colourless samples of ground cassava spiked with

ACCa (λ_{max} = 353, 497, and 527 nm) shifted to longer wavelengths (λ_{max} = 365, 534, and 578 nm) indicating the formation of DCCa. These data correspond to those of ACCa and DCCa conducted under homogeneous conditions (see Figure 34).

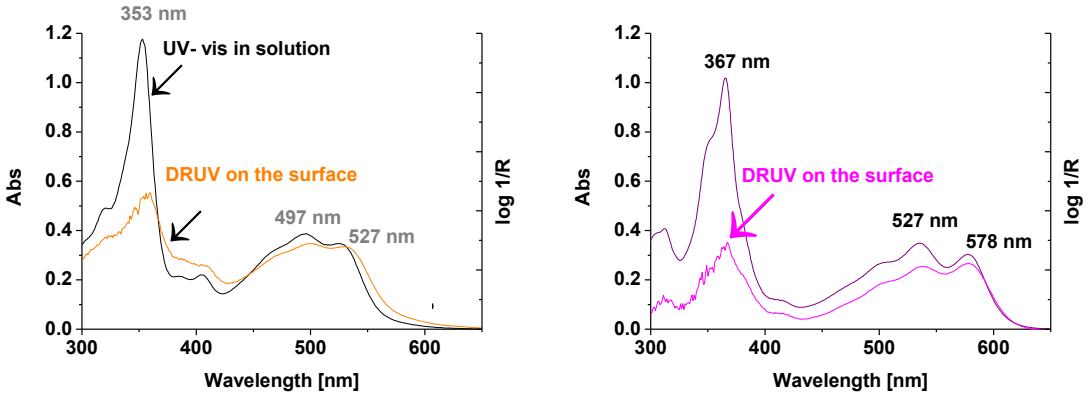

Figure 34. Comparison between UV-vis spectra recorded from ACCa samples in water and DRUV-vis spectra of ACCa (*left*) and DCCa (*right*) on a cassava surface.

The diffuse reflectance maxima of colourless samples of ground cassava spiked with ACCa (λ_{max} = 353, 497, and 527 nm) shifted to longer wavelengths (λ_{max} = 365, 534, and 578 nm) indicating the formation of DCCa. These data correspond to those of ACCa and DCCa conducted under homogeneous conditions (see Figure 34).

The enzymatic release of cyanide from linamarin was studied on a freshly cut slice of cassava with a defined size.[73] First, the maximal concentration of cyanide liberated from the whole surface of the slice during 2 h was quantified to be 1.8 µg/kg. For the following measurements, an excess of ACCa relative to the maximal concentration of released cyanide was evenly applied to the surface of the cassava slice. The formation of the violet coloured complex on the surface of the cassava slice was monitored by diffuse reflectance spectroscopy. Figure 35 (*left*) presents the DRUV-vis spectra recorded every 2 minutes over a period of 1 h. The formation of the dicyano-complex from ACCa and cyanide is fast (2 sec) compared to the enzymatic liberation of cyanide. It suggests that the time depending increase of the dicyano product reflects the rate of the enzymatic liberation of cyanide on top of the cassava surface.[73]

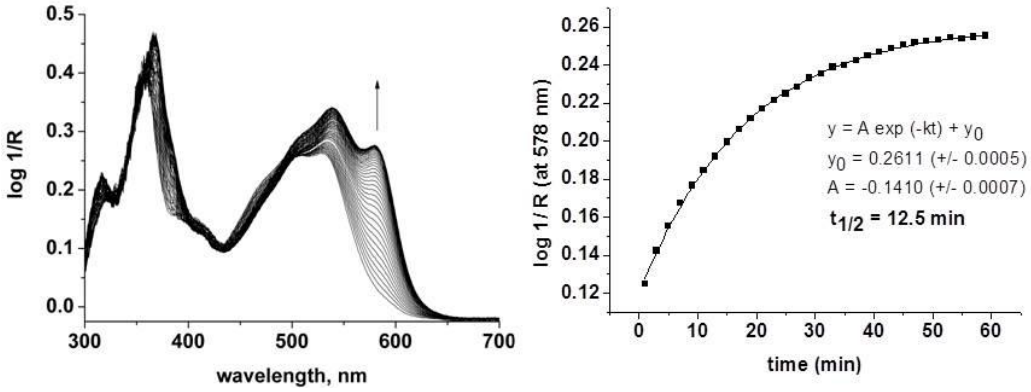

Figure 35. (*left*) DRUV-vis spectra recorded every 2 minutes for the reaction of ACCa (56 nmol) with enzymatically-liberated cyanide on the surface of a standardised slice of cassava (Ø = 15 ± 0.2 mm; thickness 2 ± 0.2 mm; m = 0.4 ± 0.04 g). (*right*) corresponding kinetic trace at for the absorbance at λ_{max} = 578 nm.[73]

The corresponding kinetic trace at 578 nm in Figure 35 (right) can be described as a first order kinetic with a half-live period of 12.5 (± 0.2) min. The results show that the time of complete cyanide release during soaking of a cassava extract, which is one way to remove cyanide during food preparation, is approximately 60 minutes.

2.6.2 Cyanide quantification

Rapid detection of the content of total cyanide in cassava tubers after enzymatic release has been compared to detection after acid hydrolysis, one of the standard procedures described by Haque and Bradbury (see chapter 4, acid hydrolysis methodology).[104, 199] Freshly peeled, ground and homogenised quantities of cassava roots were stored for 60 minutes in sealed tubes for hydrolytic cleavage of linamarin by endogenous enzymes. After dilution of the extract with water and centrifugation, the supernatant solution was used for spectrophotometric detection of cyanide with chemosensor ACCa at pH 9.5 ([CHES] = 20 mM). The content of cyanide was estimated by means of a calibration curve that was obtained from cyanide titration of an aqueous solution of ACCa (40 µM; cyanide 2-45 µM, CHES 20 mM, pH 9.5).[73] The results of analysis from the two independent methods are summarised in Table 14. The cyanide levels were found to vary between different tubers as well as along the length of the tuber. The content of cyanide in all samples was below 300 mg/kg

which is typical for sweet cassava.[81] The results of analysis using ACCa either after enzymatic- or acid hydrolysis are in good agreement. The cyanide content in finely ground flax seed was also determined (n = 2). This was done directly in the supernatant aqueous solution of the centrifuged sample.

Sample	Cyanide [mg/kg fresh weight] (enzymatic hydrolysis)	Cyanide [mg/kg fresh weight] (acid hydrolysis)
Cassava 1	122± 3	125± 9
Cassava 1	187± 5	184± 9
Cassava 2	265± 5	259± 10
Flax seed	72± 5	93± 8

Table 14. Contents of total cyanide of different cassava samples and flax seed. The data are averaged values from at least two measurements.[73]

The cyanide levels obtained for flax seed with the two methods differ by 21 mg/kg. It is possible that the concentration of endogenous enzyme is insufficient for the enzymatic cleavage of the cyanogenic glycoside. With the acid method the total cyanide is detected. It appears that, compared to established picric acid tests, corrin-based chemosensors represent a much faster and more straightforward non-toxic alternative for the determination of endogenous cyanide in food, particularly in cassava.

2.6.3 Cyanide detection during food processing

The immediate detection of endogenous cyanide with corrin-based chemosensors is advantageous for the subsequent removal of cyanide during cassava processing. Two common processing methods, boiling and a combination of soaking and filtration have been compared.[81] Samples were taken during processing and the decrease of cyanide content was tracked visually by the colour change from orange (ACCa) to violet (DCCa) and additionally acquired by means of the UV-vis absorbance data. Figure 36 (*right*) represents the percentage decrease during stirring and boiling (100 °C) of ground cassava (1 g) in water (8 mL). In the first 10 min, 45% of cyanide

is released, but further boiling has only a minor influence. The denaturation of the enzyme at higher temperature as well as coagulation of the starch is presumably responsible for this effect. In comparison, washing and filtration of the same quantity of ground cassava removes cyanide more efficiently.[73]

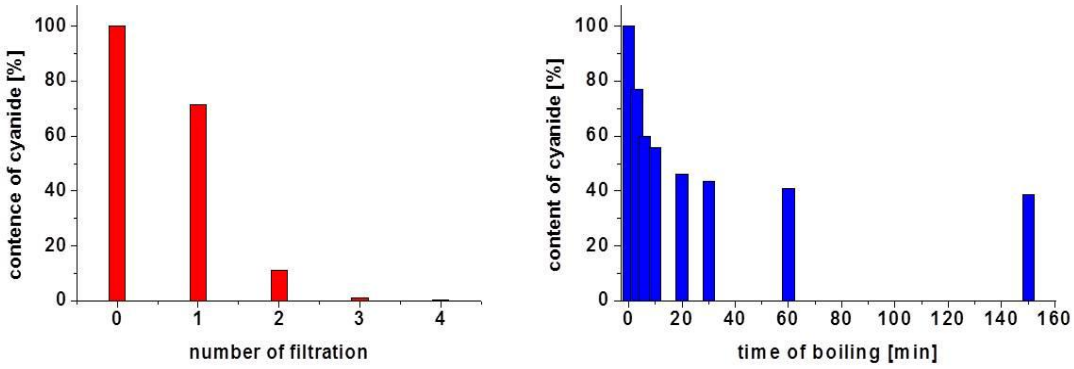

Figure 36. Percentaged decrease of cyanide (*left*) during washing and filtration and (right) boiling of a ground cassava sample (1 g) over a period 150 minutes.[73]

After four repetitions no more cyanide was detected. These results agree with the results of time consuming and complex studies of process control by Nambisan[200] and Cooke.[201]

2.6.4 Wastewater

The cyanide concentration of different wastewater samples and of a silver-bath solution from the electroplating company Elektrolyse AG Sins were analysed with ACCbs using a calibration curve.

The results in Table 15 show a high concentration of 650 g/L of cyanide in the silver-bath solution. The company stores the wastewater for weeks in 20 000 L tanks.[202] During this time the cyanide partly decomposes. After storage, the cyanide content was already very low at 5.2 mg/L. After treating the wastewater with UV oxidation and with subsequent stripping, no more cyanide could be detected. The efficiency of the treated water is controlled with Merck cyanide test tubes.

Sample	Content of cyanide (mM)
Waste water	0.2 mM (5.2 mg/L)
Waste water after UV oxidation	< 1.5 µM (0.039 mg/L)
Waste water after UV oxidation and stripping	< 1.5 µM (0.039 mg/L)
Silver bath solution	25 M (650 g/L)

Table 15. Cyanide concentration of different wastewater samples and a silver-bath solution from the electroplating company Elektrolyse AG Sins; average values derived from 3 measurements each.

2.6.5 Cyanide detection in complex samples using colorimetric solid phase extraction

The principle of serially connected cartridges containing spatially separated extraction and detection zones (described in 2.4.2) was applied for cyanide detection in complex samples. In a first example, endogenous cyanide was identified in raw extracts of cassava leaves which are consumed as vitamin- rich carbohydrate source in tropical countries. A sample solution of ground leaves of cassava was prepared as described in the experimental section and passed through the CSPE kit. In the extraction cartridge, green components of the sample solution were absorbed on the hydrophobic silica surface, while cyanide was identified in the consecutive detection cartridge by a colour change of immobilised $ACCbs_{C18}$ from orange to violet ($DCCbs_{C18}$).[187] The reflection spectrum (Figure 37, red line) shows the characteristic absorbance maxima of $DCCbs_{C18}$ (Figure 37, black line).

The second example uses cigarette smoke which contains a mixture of hundreds of different compounds. It is demonstrated how cyanide is identified in the tobacco smoke.[187] Similar to the procedure in aqueous solution, the smoke of the cigarette first passed through an extraction cartridge to absorb tear components. Then it passed through the detection zone containing $ACCbi_{C18.}$

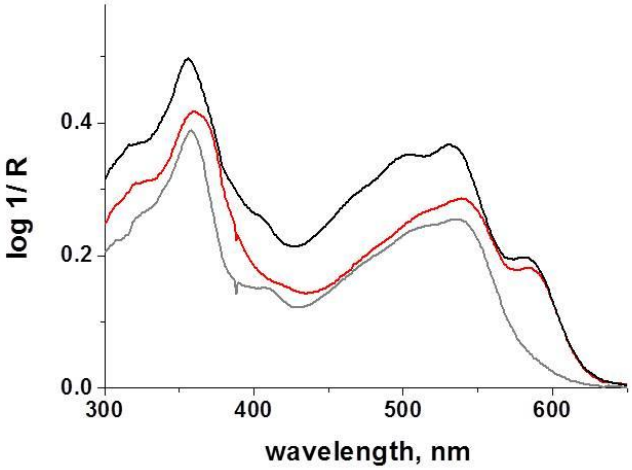

Figure 37. DRUV-vis spectra of $ACCbs_{C18}$ before (grey) and $DCCbs_{C18}$ (red) after passing an aqueous solution of ground raw cassava leaves through the detection kit; DRUV-vis spectrum of a mixture of $ACCbs_{C18}$ and $DCCbs_{C18}$ with comparable concentration of $DCCbs_{C18}$ as reference (black).[187]

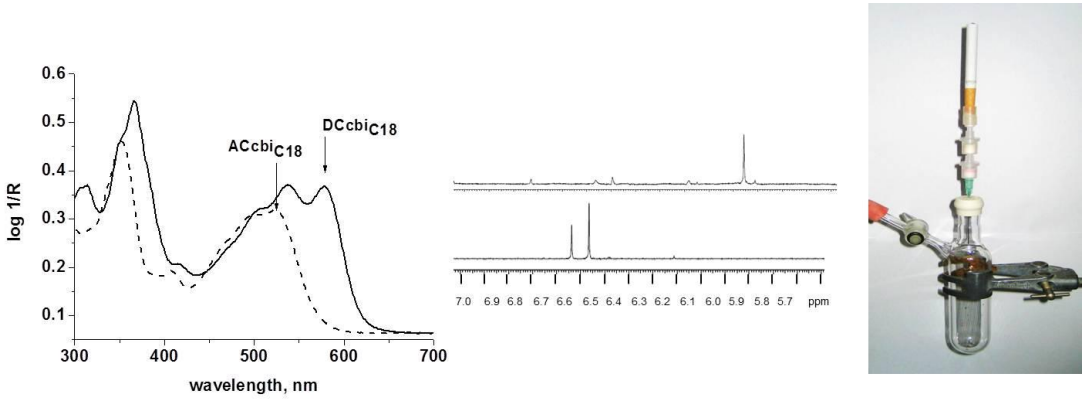

Figure 38. (*from left to right*) DRUV-vis spectrum of $ACCbi_{C18}$ (*dashed line*, α-band = 525 nm) and $DCcbi_{C18}$ upon passing tobacco smoke cigarette through the $ACCbi_{C18}$ containing C18ec-cartridge (*solid line*, α-band = 578 nm). ^{1}H NMR signals of the H10 proton of $ACCbi_{C18}$ before (bottom) and of $DCcbi_{C18}$ after reaction with tobacco smoke (top). Experimental setup for the detection of cyanide in tobacco smoke.[187]

The formation of $DCcbi_{C18}$ from tobacco smoke was identified by the typical α-band of the DRUV-vis spectrum ($\Delta\lambda max$ = 578 nm; see Figure 38).[187] The ^{1}H NMR spectrum was measured after elution of the violet coloured product from the silica C18 material.

A characteristic downfield shift (Δδ = 0.54 ppm, 0.62 ppm; Figure 38) is observed for the signals of the H10 proton compared to ACCbi. The two signals for the H10 proton of ACCbi correspond to the α, β- aquacyano isomers of ACCbi.

2.6.6 Rapid colorimetric cyanide detection in blood

The discussion in this section describes the development of the first method for the visual detection of cyanide in blood. It is the very first one that offers the possibility to determine the cyanide content of a blood sample within a few minutes entirely without laboratory equipment.

Analysing the cyanide content in blood is challenging because blood is composed of cellular constituents such as red blood cells which contain strongly coloured haemoglobin, proteins, salts and water. As a result, current methods of determination of blood cyanide are based on microdiffusion or microdestillation of HCN from the blood sample and its subsequent identification by various methods.[203]

Experiments using solid phase extraction with silica C18ec to remove coloured components of the blood according to the procedure described in chapter 2.5.6 failed. Fresh blood was completely eluted from the silica C18ec columns. Looking for a new approach, aquacyano corrinoids were considered most promising for the analysis of blood cyanide because of their selective and strong binding to cyanide. The binding affinities of cyanide to ACCbi and ACCbs in water (pH 7.5; $1.8 \cdot 10^6$ M^{-1} and $2.7 \cdot 10^6$ M^{-1}, see chapter 2.3.2)[169, 174] are slightly higher compared to its binding to methhaemoglobin as the favoured binding partner for cyanide in blood ($4.5 \cdot 10^5$ M^{-1}).[204] As a reminder, hydroxocobalamin is administered into the blood stream as an antidote against toxic cyanide.[58, 63, 205, 206]

To take advantage of these features we developed a new strategy for the cyanide detection in blood. A schematic overview of the procedure is presented in Scheme 19. ACCbs was added to the blood sample (step A) to coordinate cyanide forming DCCbs under homogeneous conditions. Subsequently it is extracted on the top of the white silica C18ec as $DCCbs_{C18}$. Washing with water is necessary to remove red components of the blood from the column while the violet colour of $DCCbs_{C18}$ (step B) appears (λ_{max} = 357, 533, 583 nm, see in chapter 4,Table 18). Detailed

information is given in the Experimental part. First, the selective binding of cyanide to ACCbs in blood was verified. As seen in Figure 39 (left), the diffuse reflectance spectra of $ACCbs_{C18}$ extracted from water or blood agree in their reflectance maxima at 356, 501 and 529 nm and confirm the formation of $DCCbs_{C18}$.[203]

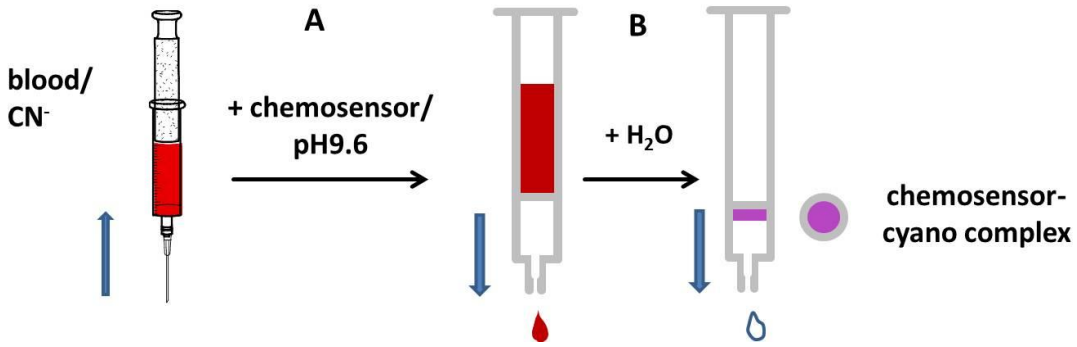

Scheme 19. Schematic overview of the two-step method for the visual detection of cyanide in blood; (*A*) mixing the blood (0.5 mL) with a buffered indicator (pH 9.6) and passing through a C18ec column (1mL), (*B*) washing the column with water (2 mL).[203]

Quantifications of the eluted ACCbs from blood by UV-vis spectroscopy showed only a slow recovery rate of the complex in contrast to comparable experiments in water. It is assumed that the loss of ACCbs is caused by binding of Co(III) to active sites of proteins.[207, 208] Well-known in biological systems is the coordination of corrinoids via thiolate to glutathione that exists in whole blood in concentrations which are 10^3 times higher compared to the concentration of ACCbs.[209] In contrast, binding of a second axial cyano-ligand liberate DCCbs from the protein hence the adsorption on silica C18 during CSPE is possible.

Subsequently the binding of ACCbs to cyanide either enclosed in the plasma or in the cells was tested. Cyanide spiked blood was centrifuged for 10 minutes and both constituents were separately analysed. As depicted in Figure 39(right), the content of $DCCbs_{C18}$ from plasma constituted only about 50% of the content of $DCCbs_{C18}$ from cells. But it reflects that ACCbs binds cyanide from plasma and blood cells as well. Further studies are necessary to understand the different cyanide content in the blood cells samples compared to the plasma. For the detection of total blood content in this work all further experiments were performed from the whole blood.

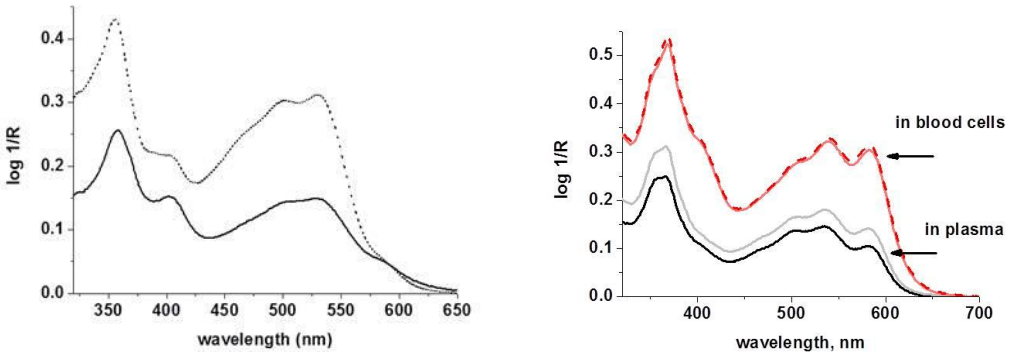

Figure 39. (*left*) DRUV-vis spectra of $ACCbs_{C18}$ extracted from either water (*dashed line*) or from blood (*solid line*). (*right*) DRUV-vis spectra of $DCCbs_{C18}$ extracted from blood serum (*black line* $[CN^-]$ = 30 µM and *grey line*, $[CN^-]$ = 40 µM), or from blood cells (*red lines*, $[CN^-]$ = 40 µM). For all extractions: [CHES] = 0.5 M, pH 9.6.[203]

Earlier studies showed that different results of blood cyanide content depend on the time interval between taking a blood sample and analysis (storage time).[49, 210] Furthermore, the cyanide content depends on the time between spiking the sample with cyanide and analysis (retention time). In order to prove this interdependence and to consider it in quantifications, time-dependent investigations were performed.

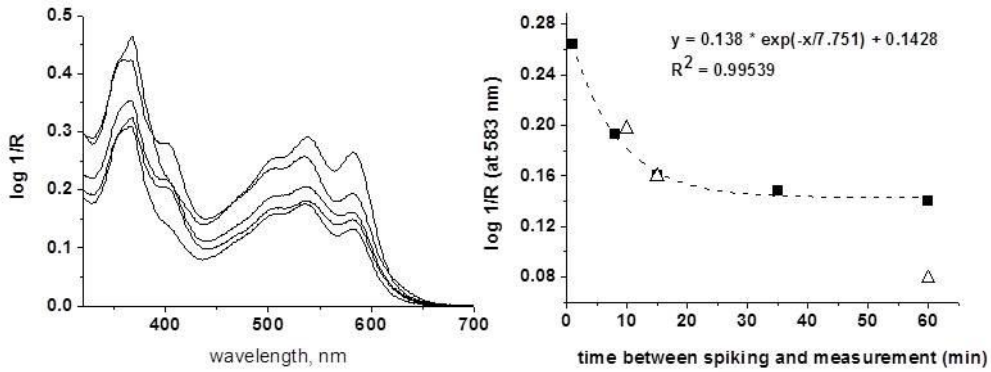

Figure 40. (*left*) DRUV-vis spectra of $DCCbs_{C18}$ recorded at different retention times for cyanide in blood ($[CN^-]$ = 30 µM; [ACCbs] = 60 µM). (*right*) Corresponding shifts of the reflection maxima of the α-band (583 nm) in dependence of the retention time (experiments performed 3 h upon taking a blood sample: black squares). Analogue data for measurements performed upon 24 h (triangles).

Blood samples, each spiked with cyanide (30 µM), were pressed through the silica C18ec columns upon increasing time intervals. The recorded DRUV-vis spectra in Figure 40 illustrate how the detected amounts of $DCCbs_{C18}$ decrease with time. The associated decreasing shifts of the maxima of the α-band (583 nm) are a function of the retention time and could be fitted with an exponential decay $y = y_0 + A \cdot \exp(-x/t)$. In measurements, performed with blood that was stored for one day at 4°C, the content of $DCCbs_{C18}$ after a retention time of 60 minutes is only around 50% of the corresponding value from the day before (see Figure 40 right, triangles). Therefore, all subsequent measurements were performed with fresh blood.

Quantifications of blood cyanide content were performed with a series of blood samples spiked with increasing amounts of cyanide and a retention time of 15 minutes. The DRUV-vis spectra in Figure 41 (left) show an increase in the absorbance at 445 and 583 nm at increasing blood cyanide concentrations. This suggests that progressively more reagent cyano-metal complex DCCbs is extracted from the sample. We assume that mainly DCCbs is adsorbed as $DCCbs_{C18}$ on silica C18ec while coordinative binding from proteins to ACCbs facilitates its remaining in the blood.

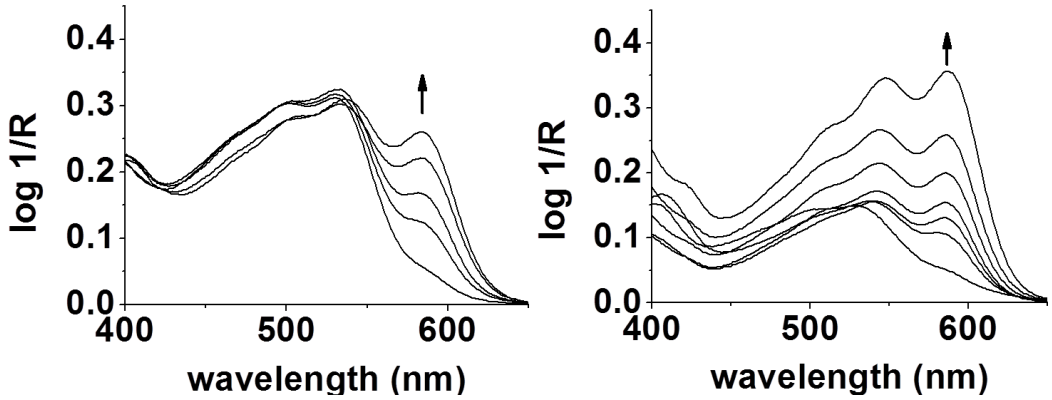

Figure 41. (*left*) DRUV-vis spectra of increasing concentrations of $DCCbs_{C18}$ (0-7 µM) upon CSPE with aqueous solutions of increasing concentration of cynide (20mM CHES, pH 9.5).[187] (*right*) DRUV-vis spectra of $DCCbs_{C18}$ upon CSPE with blood samples spiked with increasing concentrations of cyanide ($[CN^-]_{blood}$ = 10 - 100 µM), (0.5 mL blood, 15 min after spiking).[203]

We remind that the reflectance spectra for the extraction of DCCbs from water instead of blood (Figure 41, right) show a red shift of the α- and β-bands ($\Delta\lambda_\alpha$ = 32 nm; $\Delta\lambda_\beta$ = 52 nm). In this case - as expected for titration experiments and as observed earlier in solution studies - both species, ACCbs and the DCCbs are adsorbed on the solid phase.

Calibration curves were obatined by plotting either the diffuse reflectance at 583 nm (see Figure 42, right) or the b*-values (see Figure 42, left) of the immobilised chemosensor-cyanide complexes versus the concentration of cyanide in blood (Figure 42, red squares).[203] The negative b*-values of the CIELab system are associated with growing shade of blue and are linearly correlated with the concentration of $DCCbs_{C18}$.[211] B*-values of comparative measurements performed upon CSPE with aqueous cyanide solutions agree with the b*-values from blood samples. These results demonstrate that an excellent quantification of the blood cyanide content is possible either by means of a comparing colour chart, with a hand-held spectrophotometer or with reflectance spectra.

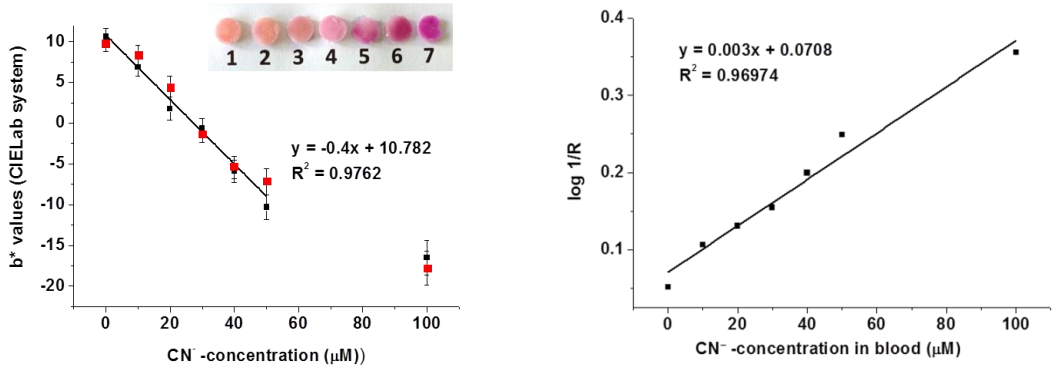

Figure 42. (left): Plot of b*-values (CIELab-system; n = 3) of the surfaces of silica C18*ec* after blood cyanide detection vs. concentrations of cyanide ($[CN^-]$ = 0 -100 µM) in blood (*red squares*, V = 0.5 mL, [ACCbs] = 42 nmol) and in water (*black squares*, V = 0.5 mL, 0.38 % Vol. of sodium citrate, [ACCbs] = 42 nmol). *Inset:* Photographs of the surfaces of silica C18*ec* after blood cyanide detection. (*right*): Plot of the reflection maxima at 583 nm of $DCCbs_{C18}$ versus concentrations of cyanide in spiked blood.[203]

The CSPE method for the detection of blood cyanide was verified by a standard method using microdiffusion and potentiometric cyanide detection. Detailed

information is provided in the chapter 4. As presented in Figure 43 (right), the results of the two methods correlate linearly. An additional test was performed by eluting $DCCbs_{C18}$ with methanol from the solid phase as described in the Experimental part (*method II*). The UV-vis absorbance maxima of the eluted DCCbs in methanol (Figure 43, right, black squares) correlate very well with the reflection maxima at 583 nm of $DCCbs_{C18}$ (Figure 43 right, triangles). Additional UV-vis measurements with DCCbs in methanol (with 50% [CN^-] in methanol = [CN^-] in blood) agree with the results from the CSPE as well.[203]

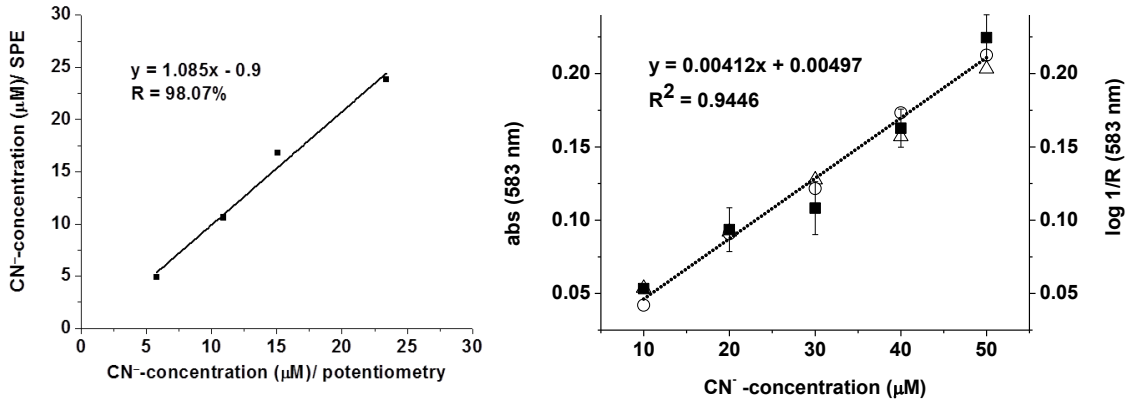

Figure 43. (*left*) Plot of concentrations of cyanide determined with the CSPE-method (DRUV-vis spectroscopy) versus potentiometric measurements upon microdistillation. (*right*): Correlation of the absorbance maxima at 583 nm of DCCbs (eluted from the column prior to its detection, black squares), of DCCbs in methanol (50% of the starting concentration that was used in blood; circles) or using the CSPE-method (triangles) versus concentrations of cyanide.[203]

In summary, the first method for the rapid detection of cyanide in blood using colorimetric solid phase extraction has been developed. The formerly necessary time-consuming step of microdistillation is avoided via the selective coordination of a corrinoid to cyanide directly in the blood and the subsequent adsorption of a newly formed complex on hydrophobic silica. This method is of high interest for applications in emergency situations because it allows for the first time to detect blood cyanide within a mere few minutes and without any laboratory equipment. Kinetic studies of the exchange of cyanide between cyanomethaemoglobin and the corrinoid are necessary to get a better insight into the reaction mechanism. Investigations of

interactions between corrinoid and other blood components are required to optimise the procedure.

2.6.7 Colorimetric cyanide detection in food using metal indicator systems

The zincon/Zn^{2+} system (see chapter 2.5) was successfully applied for the detection of endogenous cyanide on the surface of a freshly cut cassava slice.[192] The liberation of glycosidically bound cyanide with endogenous linamarin was already probed with ACCa as described in chapters 2.6.1 and 4. The enzymatically liberated cyanide on the surface of the cassava slice reacts with the zincon/Zn^{2+} system under formation of $Zn(CN)_2$ and the free indicator zincon, indicated by the orange color at the left side of the cassava (see Figure 44, A). The reaction is nearly completed upon 30 min.[192]

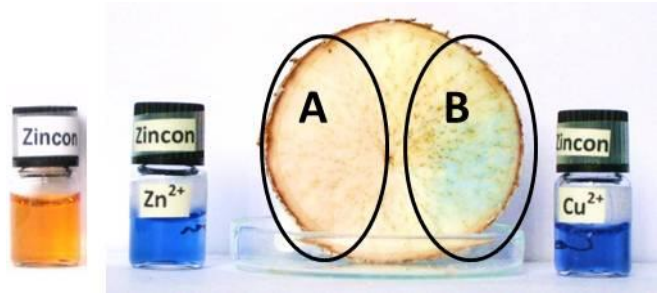

Figure 44. Application of the zincon/Zn^{2+}-sensor for the detection of endogenous biological cyanide on the surface of a freshly cut slice of cassava. The blue colored mixture of the sensor zincon/Zn^{2+} (40 µM/20 µM) in water ([CHES] = 20 mM; pH 9.0) *(second right vial)*, dropped on the surface of a freshly cut slice of cassava (A). The same procedure with the zincon/Cu^{2+} -complex did not show any color change (B). The solutions of the Cu^{2+}-zincon complex *(right vial)* as well as metal-free zincon *(left vial)* are shown for comparison.

Application of the zincon/Cu^{2+} system, described in literature, did not work under these reaction conditions (see Figure 44, B).[191] Tests in solution confirmed the result. Minimum concentrations of 0.6 mM were necessary to obtain a colour change to slightly yellow after 2 h.

Further successful applications in biological matrixes are reported in the publication in Appendix IV.[192] High levels of endogenous cyanide were determined in a

preserving solution of commercially available pickled bamboo shoots with the murexide/Ni^{2+} sensor whereas the zincon/Zn^{2+} system was used to identify cyanide in a crude aqueous suspension of crushed flax seeds.

3 Conclusions and outlook

Aquacyanocorrinoids belong to the most promising chemosensors for the colorimetric detection of cyanide with the naked eye. Quantitative determination is possible by UV-vis or DRUV-vis spectroscopy. The side chains of the corrin macrocycle influence the physico-chemical properties of these chemosensors and allow the selection of the most appropriate system for a particular problem and application.

Stopped-flow kinetic measurements of aquacyano diastereomers and isolated isomers provided insight into the mechanism of cyanide binding to these species. An additional equilibrium with an aquahydroxo-complex that has been proposed in the literature could not yet be verified.

The immobilisation of cobalamins on hydrophobic surfaces extended the coordination chemistry at the α-face of natural cobalamins. The altered intramolecular binding properties of the Dmbz base resemble structural features of cobalamins in proteins. This immobilisation strategy allows the design of biomimetic complexes and offers the possibility of new reaction pathways. Primary applications of this concept in optical cyanide detection using colorimetric solid phase extraction substantially increased the sensitivity.

The immobilisation approach combined with colorimetric solid phase extraction was applied to aquacyanocorrinoids which had already been proven viable for cyanide detection in solution. The studies resulted in detection limits of cyanide concentrations below the WHO’s guidelines level for drinking water of 0.05 mg/L. Proof-of-principle applications have been demonstrated and provide the basis for further application-oriented research. We envisage the design of a short test for the semi-quantitative detection of cyanide. This test provides an effective, economic and ecologic solution for cyanide detection in food and drinking water in tropical countries. Advantages are a fast visual response within a few minutes, the applicability by non-experts, the low manufacturing costs, the use of nontoxic materials and the re-usability upon washing with water.

An extension of the method for the detection of multiple anions was representatively demonstrated for thiocyanate and cyanide. The development of a detection device is desirable for applications in diagnostics tests for increased thiocyanate levels in urine which may be indicative of chronic cyanide poisoning. Such a test is particularly needed for simple surveys in tropical countries.

The results obtained in the studies (i) with aquacyanocorrinoids, (ii) on the immobilisation strategy and (iii) the use of CSPE all contributed to the development of a procedure for the detection of blood cyanide. This diagnostic test is certainly the most promising result of this thesis. Quantitative determinations of blood cyanide concentrations in spiked blood were demonstrated. This method is potentially applicable in emergency situations in order to immediately decide about the administration of an antidote against cyanide poisoning. The next step toward this goal will be the proof of this diagnostic test in primary healthcare settings. The design of an apparatus to process samples might be advantageous. Ideally, the quantitative determination of blood cyanide content will require a sample of less than 1 mL of a patient’s blood and the result will be provided immediately on a LED display.

A degradation of cyanide in blood, as described in literature, was confirmed with our investigations and should be analysed further. Moreover, kinetic and mechanistic studies are necessary to understand the mode of action of the cyanide transfer from blood, in particular from methaemoglobin to the corrinoid.

The implementation of the two-step screening procedure has yielded several new detection systems for micromolar cyanide and phosphate and millimolar oxalate. This success demonstrates the tremendous potential of multistep optical screening and strongly encourages its future application for the identification of sensors for other compounds of interest.

4 Experimental procedures

4.1 Materials and general information

All reagents were purchased either from Sigma-Aldrich, Switzerland or from Fluka, Switzerland and used without further purification. Unless specified differently, doubly distilled water was used for the experiments. Dicyanocobyrinic acid was synthesized by the hydrolysis of dicyanocobyrinicacidheptamethylester with 2N NaOH.[20, 212] Aquacyanocobinamide (ACCbi), aquocyanocobyrinicacid (ACCa) and aquocyanocobyrinicacidheptamethylester (ACCbs) were synthesized from their corresponding dicyano forms DCCbi, DCCa and DCCbs as pairs of diastereomers from their corresponding dicyano-forms as described in literature.[20, 166, 213, 214]

Aa far as possible, the compounds were characterized by HPLC, UV-vis spectroscopy, ^{1}H-NMR and mass-spectrometry analysis.[20, 212, 213, 215]

Chromabond *C18ec* polypropylene columns (100 mg), Chromafix *C18ec* cartridges (270 mg), Chromabond adapter PP, Polygram polyester sheets Alox N and Octadecyl-modified nano silica layers RP-18W were obtained from Machery-Nagel AG, Switzerland. Syringes (V = 10 mL) and were connected via the adapter to the columns.

Waxed cassava roots (*Manihot esculenta* Crantz) imported from Costa Rica and cigarettes were purchased at local supermarkets in Zurich, Switzerland. The cassava roots were either freshly used or tightly wrapped in plastic wrap and stored at 4 °C until use. Leaves of *Manihot esculenta* Crantz were a generous gift from the botanical garden of the University of Zurich.

Blood of hogs was received freshly from the slaughterhouse of the Veterinary Clinic of the University of Zurich. To avoid blood coagulation, the samples were immediately diluted (V = 9:1) with a solution of Na-citrat (3.8% in water). The blood was stored at 5°C and was used at the latest 3 days upon slaughter.

4.2 Methods and measurements

Spectroscopic measurements[73, 174, 180, 187, 203]

UV-vis spectra were measured at T= 21 ± 1°C with a Cary 50 spectrometer using quartz cells with a path length of 1 cm. The UV-vis data were generally recorded one minute after mixing the solutions. It had been verified previously that the absorbance was constant over at least 5 hours. The pH values were determined with a Metrohm 827 pH meter.

DRUV-vis spectra were recorded on a Varian Cary 500 spectrophotometer equipped with Internal DRA 110 mm (kinetic studies of the liberation of cyanide). All other DRUV-vis spectra were recorded on a Perkin-Elmar Lambda 50 spectrometer equipped with an integrating sphere setup (diameter 110 mm) and pure $MgSO_4$ as reference material.

NMR spectra were recorded on a Bruker *AV-500* spectrometer (Karlsruhe, Germany). The chemical shifts are given in ppm relative to the signal from the deuterated solvent. The data were processed with ACD/SpecManager (*Advanced Chemistry Development*).

Mass spectra were recorded either in the positive or negative mode on an Esquire HCT from Bruker (Bremen, Germany).

LC-MS was performed using a *Waters Acquity Ultra Performance LC* with a Macherey Nagel column C-18ec RP (5 µm particle size, 100 Å pore size, 250 x 3 mm. Flow rate: 0.3 mL min^{-1}); solvent system: 0.1% formic acetic acid in water (solvent A); MeOH (solvent B); gradient: 25% B for 5 min, then 100% B for 25 min and 100% B for 10 min.

HPLC was performed using a Merck Hitachi system equipped with an Interface 7000, a Diode Array Detector L-7455, a pump L-7100 and Macherey Nagel *Nucleosil C-18ec* RP columns (5 µm particle size, 100 Å pore size, 250 x 3 mm. Flow rate: 0.5 mL $\cdot$ min^{-1}). The solvent system and the gradient were the same as for LC-MS. Preparative HPLC purification was performed using a Merck RP 18 LiChroCART®

250-10 column (5 µm particle size, 100 Å pore size, 250 x 10 mm. Flow rate: 14 mL min^{-1}). The solvent system and the gradient were the same as for LC-MS.

Potentiometric measurements were performed with a crystal membrane electrode 6.0502.130 (CN-sensitive electrode) from Metrohm, Schweiz, using an Ag/AgCl reference electrode 6.0726.100 and a Methrom pH 713 Meter (in mV).

A handheld spectrophotometer CM-2900d from Minolta was used to measure the differences of color in the CIELab-system with Specular Component Excluded (SCE).[211] All values are averaged from at least 8 measurements.[211] The differences in color ΔE have been estimated according to:

$\Delta E = [(\Delta L^*)^2 + (\Delta a^*)^2 + (\Delta b^*)^2]^{1/2}$.

The major sphere of ΔE was used for the description of color[211] differences.

Kinetic measurements were carried out on a SX20 (Applied Photophysics) coupled to an online data acquisition system. 1000 UV-vis spectra from 185 to 723 nm were recorded in 1.26 s with a xenon lamp.

4.3 Preparation of solutions and biological samples

Preparation of solutions[174]

The 0.1 M stock solutions of the buffer standards HEPES (pH 7.0 and 7.5), Tris (pH 8.0 and 8.5), CHES (pH 9.0 and 9.5) and Caps (pH 10.0 and 10.5) were prepared and the desired pH values adjusted by adding a solution of 2 N NaOH or 1 N HCl. All sample solutions were used as 20 mM buffer solutions.

The cyanide stock solution (KCN, 6.512 mg, and 0.1 mmol) in H_2O (10 mL, 10 mM) was freshly prepared every day and protected from light.

Preparation of cassava root extract[187]

Sectors of the freshly peeled roots were ground with a zest grater and subsequently homogenized with a pestle and mortar. Before further processing, the cassava extract was stored in a sealed tube for 60 min at room temperature in order to hydrolytically cleave the linamarin with endogenous enzymes. It had been verified

previously that no longer reaction times are necessary. Usually 2 g of finely ground material was diluted with 5 mL of water and centrifuged for 10 min at 6000 U. Aliquots of 10 -100 µL of the supernatant were used for further analysis. All analyses were performed with chemosensor **3** (40 µM) in water at pH 9.5 (CHES, 20 mM). The UV-vis spectra generally were recorded 10 min after the addition of the aliquot of the biological extract.

Preparation of cassava slices[73]

Slices of cassava were freshly prepared with a diameter of 15.0 ± 0.2 mm, a thickness of 2.0 ± 0.2 mm and a mass of 0.40 ± 0.04 g. Special care was taken not to touch the surface area. A DRUV-vis spectrum was recorded as a reference 1 min after slicing. Thereafter, 20 µL of chemosensor **3** (2.8 mM) was distributed uniformly on the surface. The kinetic measurements were started with a delay of 3 min from the time of slicing.

Sample preparation from cassava extracts for NMR spectroscopy

Sample preparation of colored plant material[73]

A cassava leaf extract was prepared by (i) grinding about 2 g of the cassava leaf with mortar and pistil, (ii) dilution with water (5 mL; pH 9.5, [CHES] = 0.1 M) and (iii) centrifugation at 6000 U for 10 min. The green coloured supernatant was used directly for CSPE.

Sample preparation for diffuse reflectance (DRUV-vis) spectroscopy[180]

For DRUV-vis measurements of immobilised reagent and immobilised reagent-analyte complexes, the cartridges were opened under greatest care. The top layer of the *silica C18ec* column (~ 1 mm) containing the immobilised reagent-analyte complex was removed from the cartridges or columns, dried (10 min at 45°C and 30 min in the open) and used for DRUV-vis measurements.

4.4 General procedures

Determination of binding constants[216]

The denoted binding constants are conditional constants, K, for the following reversible equilibrium:

$$[NC - Co^{III} - OH_2]^+ + CN^- \rightleftharpoons [NC - Co^{III} - OH_2] + H_2O$$

Solution composition	[CN] range	(0-45)·x 10^{-6} mol·l^{-1}
	[SCN] range	(0-30) x 10^{-3} mol·l^{-1} for 1, 3
		(0-0.6) mol·l^{-1} for 2
	[NC-Co-OH_2]	40·10^{-6} x mol·l^{-1}
	Ionic strength	0.02 mol·l^{-1}
	pH	7.5 or 9.5
Experimental Method		Spectrophotometric titration
Temperature		21 ±1°C
Total number of data points		Minimum: 144; 2 titrations
Method of calculation		Hyperquad2006
Stability constants		see: Table 1 in Appendix I

Table 16. Summary of experimental parameters for the system: NC-Co-OH_2 (**2**, **3, 4**)/ CN^-, SCN^-.[217]

Stopped-flow kinetic measurements and calculations[73]

All kinetic measurements were carried out under a controlled temperature of ±0.1 °C and pseudo first order conditions with an excess of CN- of at least 10-fold. Kinetic traces were analysed at λ_{max} = 578 nm. The measurements for the mixture of $ACCa_i$ and $ACCa_{ii}$ were performed under consideration of the molar ratio of $ACCa_i$ and $ACCa_{ii}$ of 1:1.2 as well as the extinction coefficients ε_{578} = 570 and 9200 L·mol^{-1}·cm^{-1} for ACCa and DCCa, respectively.

Every experimental series was measured at 6 different temperatures and, according to a pseudo first order reaction, every compound with 4 different excess rates of cyanide (unless stated otherwise). The cyanide solutions were buffered at pH 9.5 with CHES (10 mM).

c_{KCN} (in the measurement chamber) mM	V_{KCN} (10 mM) mL	V_{CHES} (pH 9.5, 0.1 M) mL	V_{H2O} mL	**Excess** $c_{(CN-)/c(sensor)}$
0.5	1	4	5	10 x
1	2	4	4	20 x
1.5	3	4	3	30 x
2.5	5	4	1	50 x

Table 17. Cyanide concentration of the sample solution and the resulting concentration in the measurement chamber of the SX-20.

$ACCbi_{\alpha}$ and $ACCbi_{\beta}$ were dissolved in water just before each measurement or were prepared as stock solutions and stored at 5°C without light. The spectra were recorded for temperatures of 5°, 10°, 15°, 20°, 25° and 30°C for cyanide concentrations of 0.5, 1.5 and 2.5 mM in a dark room.

The analysis was performed with OriginPro 8.5 from OriginLab Corporation. The resulting curves were fitted with the exponential function ExpDec1 ($y = y_0 + Ae^{-x/t}$) or ExpDec2 ($y = y_0 + A_1e^{-x/t1} + A_2e^{-x/t2}$), data selection GlobalFit, a maximum of 400 iterations and a tolerance of 10^{-9}.

Values of $\Delta H^{\neq}$ and $\Delta S^{\neq}$ were calculated from the slopes and intercepts of plots of ln(k/T) versus 1/T.

Determination of cyanide content in wastewater samples

The samples were stored in closed lightproof plastic bottles for 2 weeks before analysis. 40-100 µL of the waste water were added to a solution of chemosensor ACCbs **(**40 µL, 1.4 mM), CHES (200 µL, 20 mM) and filled with water to 1 mL. The UV-vis absorption at 578 nm was determined and the cyanide concentration was

estimated via a correlation curve. The silver bath solution was 10^{13} times diluted for UV-vis measurements.

Determination of cyanide content in ground cassava samples[73]

The quantitative determination of the cyanide content in a ground cassava sample is based on a correlation curve for the absorptions at 365 nm and 578 nm. The data fit a straight line with r^2 = 0.996 for the absorbance at 365 nm and r^2 = 0.998 for the absorbance at 578 nm. The following equation gives a general term to determine the total cyanide concentration:

$$ppm = \frac{[CN^-] \times V_{H_2O} \times 26}{m \times V_{sample}}$$

where [CN^-/ µM] is the concentration of cyanide in the sample, estimated from the correlation curve, V_{H2O} /L is the volume of water, added to the sample, m/kg is the sample mass of ground cassava and V_{sample} is the volume of the sample used for the spectroscopic measurement.

Acid hydrolysis methodology[73]

The acid hydrolysis methodology was applied as described by Haque and Bradbury[104, 199] as an alternative for the enzymatic release of total cyanide from cyanogenic glycosides. Therefore, 2 g of mashed biological material was diluted to 5 mL with phosphoric acid (0.1 M). The mixture was centrifuged for 10 min at 6000 U and 2 mL of the supernatant solution was added to 2 mL of sulfuric acid (4 M). It was heated at 100°C for 90 min in a tightly closed heavy-walled Schlenk flask with a Teflon plug valve. After cooling the reaction mixture to 4°C, the pH was adjusted to 7 with sodium hydroxide (3.6 M). Aliquots between 10 and 100 µL were used for further analysis.

CSPE method[218-220]

General. The colorimetric solid phase extraction (CSPE) device consisted of a 10 mL syringe that was either connected directly or via a Chromabond adapter PP (Macherey-Nagel) to *C18ec* columns or *C18ec* cartridges. The procedure is exemplified for indicator **3**.

1. Conditioning. The *C18ec* column was washed with methanol (0.5 mL) and water (10 mL).
2. Adsorption of indicator. The indicator was adsorbed on the top of the *C18ec* material while an aqueous solution of **3** (0.5 mL; 40 µM) was passed through the filter material. The immobilised indicator $\mathbf{3_{SP}}$ (SP for "solid phase") was visible as a red colored ring (height ~ 1 mm).
3. Analysis. A sample solution (usually 5 mL) was passed through the filter with a rate of approximately 2 mL/min. Detection with $\mathbf{3_{SP}}$ was indicated by a change of color.
4. Regeneration. $\mathbf{3_{SP}}$ was regenerated from $\mathbf{3_{SP}}$**-CN** while passing 1 % of an aqueous acid (3 mL) and water (20 mL) through the filter**.**

pH dependent measurements[180]

A Chromabond *C18ec* column that was connected to a 5 mL syringe via a Chromabond adapter PP (Macherey-Nagel) was loaded with aqueous solutions of the desired Cbl (1 mL, 20 µM). pH dependent measurements were performed by passing solutions with the desired pH value (5 mL) through the column and allow to equilibrate for 2 h -24 h. The remaining solution was removed afterward from the solid-phase and the pH value was rechecked.
The silica *C18ec* material was pressed out of the column with a second syringe connected to the lower side of the column. The colored part of the C18ec material with the immobilised Cbl was used for DRUV-vis measurements. Investigations with unmodified silica were performed in the same way.
The $pK_{base\text{-}off}$ values were obtained from the analysis of a Boltzmann function: $y = A_2 + (A_1 - A_2) / (1 + \exp((x - x_0) / dx))$ fitting the shift of the γ-band for all Cbls but AdoCbl (α/β-band).

Quantification of the cyanide content using CSPE[187]

The percentage of reflectance (R) was measured with respect to silica *C18ec* as standard white. The Kubelka Munk equation gives the relation between the percentage of reflectance (R) and the concentration of the analyte under the assumption of a constant molar absorptivity (ε) and scattering coefficient (s) for a given wavelength.[219]

$$F(R) = (1 - R)^2 / 2R$$
$$F(R) = \varepsilon \cdot C / s.$$

Limit of detection[187, 192]

The limit of detection (LOD) was determined as the mean of the blank measures at 583 nm plus three times the standard deviation of the blank from at least 10 measurements.

Detection of HCN in tobacco smoke[187]

To detect hydrogen cyanide (HCN) in tobacco smoke, a cigarette was connected to two attached *C18ec* cartridges. The first cartridge was used to remove tar and other potential interferents from tobacco smoke, whereas the second column containing $\mathbf{1_{SP}}$ or $\mathbf{2_{SP}}$ was used for HCN detection.

A vacuum (500 mbar) was applied to pull the tobacco smoke through the cartridges. The top layer of cartridge 2 containing the immobilised reagent-analyte complex was then carefully removed, dried (10 min at 45°C and 30 min on air) and used for DRUV-vis measurements.

Blood cyanide detection[203]

General. Methanol (0.5 mL) and subsequent water (10 mL) were pressed through the columns using a syringe in order to condition the *C18ec silica* material before further use.

1. Preparation of the blood sample. Blood (0.5 mL) was spiked with cyanide ([CN^-] = 0- 100 µM). Fifteen minutes later, the blood was adjusted to pH 9.6 with CHES buffer (0.47 mL, 1M) and ACCbs (30 µl; 1.4 mM) was added.

2. Adsorption of the chemosensor.

After one minute, the sample was pressed through the *C18ec* column (1 mL). The column was subsequently washed with water (3 mL) to remove adhering blood from the C18ec material. Thereby a red to violet coloured ring of ACCbs was visible on the top of the C18ec material (Figure 1, right). The colour depends on the concentration of cyanide (Figure 3 inset).

3. Analysis.

Method I. The top layer of the *silica C18ec* material (~ 2 mm) containing immobilised CNCbl was used for spectroscopic measurements.

Method II. Immobilised ACCbs was eluted with MeOH (400 µl) from the C18ec column. The volume was adjusted to 500 µL, transferred to a quartz cuvette and analysed with UV-vis spectroscopy. The concentration of DCCbs was determined with a calibration curve obtained from different concentrations of DCCbs (10- 100 µM) in methanol.

Cyanide detection with potentiometric measurements after microdestillation[203]

The microdiffusion cascade consisted of 4 flasks (10 mL), closed with septa and connected to each other with syringes and PVC-tubes. The first flask was filled with water. The second one contained blood (1.0 mL) spiked with cyanide ([CN^-] = 0 - 50 µM), ascorbic acid (1 mL; 60 mM)[221], water (850 µl), 3 drops of antifoam A concentrate and was subsequently adjusted to pH 3.3 with phosphoric acid (10%; 150 µl). The third and fourth flask contained KOH (0.1 M; 3 mL). The second flask was heated to 80°C for 40 min, while a stream of N_2 (3 bubbles per second) was passed through the solutions. Afterward, an aliquot of flasks three and four (300 µl) was diluted with aqueous KOH (0.1 M, 9.7 mL) to a final volume of 10 mL. The amount of cyanide was determined with a CN-sensitive electrode and the help of a calibration curve.

The calibration curve was obtained by adding various concentrations of cyanide (10-100 µl, 10^{-4} M) to an aqueous KOH solution (0.1 M; V_{final} = 10 mL). The corresponding voltage was measured with a CN-sensitive electrode.

4.5 Experimental procedures[180]

Compound DCCbl (**1-CN**).[180] A Chromabond C18ec column was loaded with vitamin B12 (1 mL, 20 µM). An aqueous solution of KCN (5 mL; 1.04 mg/L; [HEPES] = 20 mM; pH 7.5) was passed through the column (1 mL/s). Compound $DCCbl^-_{SP}$ was indicated by a color change from red to violet. The preparation for DRUV-vis measurements was carried out as described in the section of pH depending investigations. DCCbl was eluted from C18ec material for the ^{1}H NMR measurement with methanol. The methanol was removed and the product lyophilized.
DRUV-Vis: (see Table 19)
^{1}H-NMR (500 MHz, D_2O,): 6.03 (*s*, 1H, C10); 6.30 (*s*, 1H, C1R); 7.23 (*s*, 1H, C7N); 6.46 (*s*, 1H, C4N); 7.04 (*s*, 1H, C2N).

Compound 5. (α-cyano,β-aqua-cobyrinicacid a,b,d,e,f,g-hexamethylester). The procedure described by Pfammatter et al.[179] was modified. Vitamin B12 (**1**, 100.0 mg, 73.8 µmol) was dissolved in a degassed solution of 2M AcOH (10 mL) under inert atmosphere. *N*-Bromosuccinimide (16.1 mg, 90.5 µmol) was added in one portion and the reaction mixture was stirred for three hours in the dark at room temperature (monitored by HPLC). The solvent was evaporated in the dark and the residue resolved in H_2O (3 mL) and dried overnight on the freeze-drier. The crude intermediate product was processed without further purification. The residue was taken up in MeOH (10 mL) under inert atmosphere and a solution of con. H_2SO_4 (0.5 mL) in MeOH (5 mL) was added. The solution was degassed and then slowly heated to gentle reflux for 5 days. H_2O (10 mL) was added slowly under cooling of the solution. The solution was neutralized to pH 7 by the addition of solid $NaHCO_3$ and the solution was extracted with CH_2Cl_2 (3 x 25 mL, 1 x 10 mL). CH_2Cl_2 was evaporated and the residue was dissolved in H_2O (10 mL). KCN (8.8 mg, 135.1 µmol) was added at room temperature and the color changed from red to dark violet. The solution was extracted with CH_2Cl_2 (3x 25 mL), dried with Na_2SO_4 and the solvent evaporated. The residue was dissolved in H_2O (3 mL) and dried overnight on the

freeze-drier. The crude intermediate product was processed without further purification. The residue was dissolved in toluene (10 mL) under inert atmosphere. AcOH (1 mL) was added and the solution was flushed with Ar. Zn (217.3 mg, 3.3 mmol) was added under slight Ar-counterflow and the reaction solution was stirred for 3 hours meanwhile the color changed to brown. The reaction solution was treated with 1M phosphate buffer (pH 7, 25 mL) and filtered. The solution was extracted with CH_2Cl_2 (3 x 30 mL) and the solvent was evaporated. The residue was dissolved in H_2O (3 mL) and dried overnight on the lyophilisator. The crude product (**5**) was purified by preparative HPLC (gradient from 50 % till 100 % MeOH) to give pure *c*-acid cobester (**5**, 14.2 mg, 13.5 µmol, 18.3 %) as a dark orange solid. Additionally two fractions with few impurities were obtained (9.4 mg, 9.0 µmol, 12.2 %) leading to an overall yield of 30.5 %.

HPLC: 24.8 (100%, gradient: see spectroscopic measurements).

UV: λ_{max}= 353, 498, 526 nm.

LC-MS: 1048.5 ($[M]^+$).

^{1}H-NMR (500 MHz, [D_3]MeOD): 1.29 (*s*, 2H, H2O); 1.35 (*s*, 3H, C12B); 1.39 (*s*, 3H, C1A); 1.49 (*s*, 3H, C12A); 1.57 (*s*, 3H, C7A); 1.63 (*s*, 3H, C17B); 1.68 (*s*, 3H, C2A); 1.68 – 2.85 (*m*, 22H, C21, C31, C32, C71, C81, C82, C131, C132, C171, C172, C181) superimposed by 2.40 (*s*, 3H, C51) and 2.41 (*s*, 3H, C151); 3.08 (*dt*, 1H, C18); 3.51 (*t*, 1H, C13); 3.60 – 3.70 (*m*, 1H, C8) superimposed by 3.60, 3.64, 3.69, 3.70, 3.73, 3.78 (*s*, 18H, C24, C35, C85, C135, C175); 4.04 (*d*, 1H, C3); 4.08 (*d*, 1H, C19); 6.40 (*s*, 1H, C10).

Compound 8^+.[180] A Chromafix C18ec cartridge (270 mg) was loaded with vitamin B12 (10^{-4} M, 1 mL, 2% MeOH). Compound $\mathbf{8^+}$ was prepared by pressing 2 mL of methyl iodide through the cartridge. The upper and the lower sides of the cartridge were closed by syringes. After 4 days, excess of methyl iodide was removed from the cartridge and the orange product was subsequently eluted with methanol. The solvents were removed under reduced pressure. The residue was purified by preparative HPLC to afford **8** ($\mathbf{8^+CF_3COO^-}$) (yield of 4 cartridges: 1.4 mg, 0.9 µmol, 38 %).

DRUV-Vis: (see Table 19)

^{1}H-NMR (500 MHz, D_2O): (see Table S2); ^{1}H-NMR: 1.01 (*s*, 1H, C12N); 1.03 (*s*, 2H, C81); 1.04 (*s*, 2H, C181); 1.20 (*s*, 3H, C12A); 1.21 (*s*, 3H, C12B); 1.45 (*s*, 3H, C7A); 1.67 (*s*, 3H, C1A); 1.84 -1.96 (*m*, 3H, C31, C81'); 2.05 – 2.10 (5H, C2A, C32); 3.08 – 3.25 (1H, C18); 3.51 (*t*, 1H, C13); 2.38 - 2.44 (*m*, 1H, C8); 2.22 - 2.31 (18H, C51, C151, C32, C132, C21, C10N, C11N); 2.92 (2H, C18, C172); 2.92 (*t*, 1H, C175'); 3.29 (*d*, 1H, C8); 3.52 (*t*, 1H, C175); 4.07 (*d*, 1H, C19); 4.16 (*s*, 1H, C3); 6.38 (*s*, 1H, C10); 7.45 (*s*, 1H, C1R); 7.51 (*s*, 1H, C7N); 7.52 (*s*, 1H, C4N); 9.18 (*s*, 1H, C2N).
MS (ESI-MS): m/z (%): 1370.1 (100) $[M + H]^+$.
LC-MS: R_t = 20.1 min

Compound 9.[180] A Chromabond C18ec column was loaded with vitamin B12 (1 mL, 40 µM). An aqueous solution of DL-histidine (1.8 mM; 7 mL) was pressed through the cartridge and it was allowed to react for 24 hours at room temperature. The preparation for DRUV-vis measurements was carried out as described in the section of pH depending investigations.
DRUV-Vis: (see Table 19)

Tables

Tables of DRUV-vis maxima

	λ_{max} (in CH_2Cl_2)	**λ_{max} (C18ec column)**
ACCbs	355, 497, 526	358, 501, 531
ThiocyanatoCCbs	362, 522, 553	361, 523, 554
iodoCCbs	373, 555, 590	358, 536, 597
cyanatoCCbs	365, 524, 556	364, 524, 553
DCCbs	372, 551, 590	357, 533, 583

Table 18. Comparison of the absorption maxima of XCCbs in dichloromethane with the maxima of $XCCbs_{C18}$ (X: Cl, SCN, I, OCN, CN).[187]

Cbl	Diffuse reflectance spectroscopy				
	pH	λ_{max} (nm)			
CNCbl (**1_{SP}**)	0.1	355	403	497	527
	7.0	358	403	-	528
DCcbl (**1-CN_{SP}**)	7.0	367	419	543	578
AdoCbl (**6_{SP}**)	7.0	-	-	375	457
AqCbl (**7_{SP}**)	0.2	352	405	496	520
	9.0	355	417	511	533
N-MeCbl (**8^{+}_{SP}**)	7.0	355	403	497	527
9_{SP}	7.0	361	410	520	551

Table 19. Selected diffuse reflectance data for Cbls **1_{SP}**, **1-CN**, **6_{SP}**, **7_{SP}**, **8^{+}**, **9_{SP}**.[180]

Tables of kinetic measurements

T (°C)	$k_i^{II}{}_{ACCa}$ [$M^{-1}s^{-1}$]	$k_{ii}^{II}{}_{ACCa}$ [$M^{-1}s^{-1}$]	k_{ii}^{II}/k_i^{II}
15	7.8 E3	2.22 E3	3.51
20	1.12 E4	3.01 E3	3.72
25	1.56 E4	4.22 E3	3.70
30	2.16 E4	5.84 E3	3.70
35	3.02 E4	7.86 E3	3.84
40	4.33 E4	1.07 E4	4.04
45	6.48 E4	1.40 E4	4.62

Table 20. Second order rate constants k_i^{II} and k_{ii}^{II} of the mixture of the α,β-aquacyano diastereomers of ACCa **2_i and 2_{ii}** at pH 9.5.

T (°C)	k_1^{II} [$M^{-1}s^{-1}$]	k_2^{II} [$M^{-1}s^{-1}$]	$\Delta H^{\ddagger}$[kJ/mol]	$\Delta S^{\ddagger}$ [J/molK]
5.1	1.32 E4 (7)	1.5 E3 (2)	52 (7)	1 (24)
17.4	2.89 E4 (8)	2.9 E3 (4)		
25.2	4.80 E4 (3)	5.1 E3 (5)		

Table 21. Second order rate constants k^{II} of ACCbs at pH 9.6 and activation parameters for the substitution of coordinated water with cyanide (literature values from Chemaly et al.).[169]

T (°C)	$k_{\alpha}^{II}{}_{c\text{-}acid}$ [$M^{-1}s^{-1}$]	$k^{II}{}_{ACCbi\alpha}$ [$M^{-1}s^{-1}$]	$k^{II}{}_{ACCbi\alpha}$ / $k_{\alpha}^{II}{}_{c\text{-}acid}$
5	1.05 E4	2.51 E4	2.4
10	1.52 E4	3.57 E4	2.2
15	2.30 E4	5.61 E4	2.4
20	3.33 E4	8.08 E4	2.4
25	4.55 E4	1.15 E5	2.5
30	5.95 E4	1.49 E5	2.5

Table 22. Comparison between second order rate constants $k_{\alpha}^{II}{}_{c\text{-}acid}$ and $k^{II}{}_{ACCbi\alpha}$ at pH 9.5.

Tables of metal-indicators for the screening procedure[192]

metal indicators	metal ions				
	Fe^{2+}	Fe^{3+}	Co^{2+}	Ni^{2+}	Zn^{2+}
Murexide			□ ◉	□ ◉	
Eriochrom Black T			□ ◉	□ ◉	
Pyrocatechol	□	□	◉	◉	
Pyrogallol	□ ■	□ ■	■		
Xylidyl Blue	□	□	■	■	■
Xylenol orange	□	□	□ ■	□ ■	□ ■
Hydroxo-nitrosonaphtalin	□ ■	□	□ ■		
Tiron	□ ■	□ ■			
Zincon	□ ■	□	□ ◉	□ ■	□ ◉
Alizarin S			■	◉	

Table 23. Master-detail-screen of the 50 selected combinations of metal indicators (50 µM) and metal ions (50 µM) applied in the 2nd round of the screening procedure for metal-indicator systems. (colour change at pH7 = □ **,** at pH9 = ■). Combinations that give a color change after addition of cyanide (3 mM) in water (pH 9.0) are circled**).**

metal indicators	**metal ions**			
	Mg^{2+}	Ca^{2+}	Zr^{4+}	Ce^{4+}
Murexide		◓		
Eriochrom Black T	■ ◓	◓	▲	
Calcon		◓	▲	
Calcon/MeOH	▲	◓		

Table 24. Master-detail-screen of ten selected combinations of metal indicators (40 µM) and four metal ions (50 µM) applied in the 2nd round of the screening procedure B of the screening procedure for metal-indicator systems. (colour change at pH9 = ■ **,** at pH12.1 = ▲). The combinations that showed a color change after addition of anions (1 mM) are circled

4.6 Additional Figures

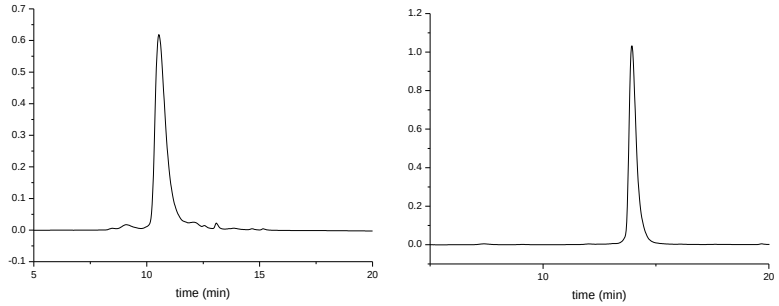

Figure 45. The HPLC spectra of the $ACCbi_{\beta}$ (left) recorded at 13.9 min. $ACCbi_{\alpha}$ (right) recorded at 10.5 min.

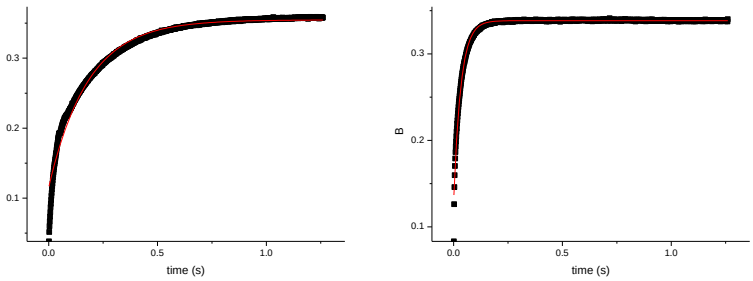

Figure 46. Monoexponential fit of the change of the relative absorbance vs. time at 582 nm of $ACCbs\text{-}c\text{-}acid_{\alpha}$ at 5°C (left) and 30°C (right) with a cyanide concentration of 0.5 mM (pH 9.5).

Figure 47. Mixtures of murexide (36 µM) and Ni^{2+} (20 µM) in water ([CHES] = 20 mM; pH 9.0 ± 0.1). *Top (from left to right):* in the presence of either no anion, F^-, Cl^-, Br^-, I^-, SCN^-, NO_3^-, CN^- (80 µM) CO_3^{2-}, $C_2O_4^{2-}$ (0.3 mM), SO_4^{2-}, $H_2PO_4^-$ (2mM), ClO_4^-, AcO^-, OCN^-, or all 14 anions (If not indicated otherwise, the concentration of the anions are 3 mM). *Bottom:* after the addition of CN^- (60 µM) to the solutions depicted above. The first vial shows the mixture of the murexide/Ni^{2+} sensor as a reference. The corresponding photographs for the murexide/Co^{2+} system are shown in the supporting information of the publication.

Figure 48. Zincon (40 µM) and mixtures of zincon/Zn^{2+} (40 µM/ 20 µM) in water ([CHES] = 20 mM; pH 9.0 ± 0.1). *Top (from left to right):* zincon, zincon/Zn^{2+}, in the presence of either no anion, F^-, Cl^-, Br^-, I^-, SCN^-, NO_3^-, CO_3^{2-}, $C_2O_4^{2-}$, SO_4^{2-}, $H_2PO_4^-$, ClO_4^-, AcO^-, OCN^- (4 mM) or all 14 anions (4 mM each). *Bottom: (from left to right)* in the presence of either no anion and after the addition of CN^- (250 µM) to the solutions depicted above.

5 Literature

[1] U. S. EPA, Office of Health and Environmental Assessment,Cincinnati, OH, Springfield, VA, **1992**.
[2] U. S. EPA*, Vol. Federal Register 56234*, **1991**, pp. 63798.
[3] U. S. EPA*, Vol. EPA 100-B-00-002*, Office of Science Policy, Office of Research and Development, Washington DC, **2000**.
[4] U. S. EPA*, Vol. EPA/100/B-06/002* (Ed.: O. o. R. a. D. Office of Science Policy), Washington, DC, **2006**.
[5] U. S. EPA*, Vol. EPA/ 815/R-03/006*, Office of Water, U.S. Environmental Protection Agency, Springfield, VA, **2003**, pp. PB2003.
[6] Cassava Cyanide Diseases Network (CCDN), http://biology.anu.edu.au/hosted_sites/CCDN/, **2012**.
[7] S. I. Baskin, J. B. Kelly, B. I. Maliner, G. A. Rockwood, C. K. Zoltani, in *Medical Aspects of Chemical and Biological Warfare. Textbook of military medicine.*, Office of the Surgeon General, Department of the Army, Washington, DC, **1997**, pp. 271.
[8] A. H. Sykes, in *Cyanide in Biology* (Eds.: B. Vennesland, E. E. Conn, C. J. Knowles, J. Westley, F. Wissing), Academic Press, New York, NY, **1981**, pp. 1.
[9] D. D. Perrin, *Ionisation Constants of Inorganic Acids and Bases in Aqueous Solution*, 2nd ed., Pergamon Press, Oxford, **1982**.
[10] K. R. Dunbar, R. A. Heintz, *Prog. Inorg. Chem.* **1997**, *45*, 283.
[11] C. Janiak, H.-J. Meyer, D. Gudat, R. Alsfasser, in *Riedel, Moderne Anorganische Chemie* (Ed.: H.-J. Meyer), Walter de Gruyter GmbH & Co. KG, Berlin/ Boston, **2012**.
[12] T. J. Swift, R. E. Connick, *J. Chem. Phys.* **1962**, *37*, 307.
[13] L. Knapton, H. M. Marques, *Dalton Trans.* **2005**, 889.
[14] K. L. Brown, S. Cheng, X. Zou, J. D. Zubkowski, E. J. Valente, L. Knapton, H. M. Marques, *Inorg. Chem.* **1997**, *36*, 3666.
[15] C. B. Perry, M. A. Fernandes, K. L. Brown, X. Zou, E. J. Valente, H. M. Marques, *Eur. J. Inorg. Chem.* **2003**, 2095.
[16] S. M. Chemaly, K. L. Brown, M. A. Fernandes, O. Q. Munro, C. Grimmer, H. M. Marques, *Inorg. Chem.* **2011**, *50*, 8700.
[17] R. A. Firth, H. A. O. Hill, J. M. Pratt, R. G. Thorp, R. J. P. Williams, *J. Chem. Soc. A* **1968**, 2428.
[18] M. A. Watzky, J. F. Endicott, X. Song, Y. Lei, A. Macatangay, *Inorg. Chem.* **1996**, *35*, 3463.
[19] D. Dodd, M. D. Johnson, *J. Chem. Soc. Dalton Trans.* **1973**, 1218.
[20] L. Werthemann, ETH Zürich **1968**.
[21] R. S. Ghosh, D. A. Dzombak, S. M. Drop, A. Zhen, in *Cyanide in Water and Soil: Chemistry, Risk and Management*, CRC Press, Boca Raton, FL, **2006**, pp. 132.
[22] T. C. Young, X. Zhao, T. L. Theis, in *Cyanide in Water and Soil: Chemistry, Risk and Management* (Ed.: D. A. Dzombak), CRC Press, Boca Raton, FL, **2006**.

[23] D. A. Dzombak, R. S. Ghosh, G. M. Wong-Chong, *Cyanide in Water and Soil: Chemistry, Risk and Management*, CRC Press, Boca Raton, FL, **2006**.
[24] S. L. Miller, L. E. Orgel, *The origins of Life on the Earth*, Prentice-Hall, Englewood Cliffs, NJ, **1974**.
[25] J. Oro, A. P. Kimball, *Arch. Biochem. Biophys.* **1961**, *94*, 217.
[26] M. Lechtenberg, in *eLS*, John Wiley & Sons, Ltd, **2011**.
[27] A. Volbeda, E. Garcin, C. Piras, A. L. deLacey, V. M. Fernandez, E. C. Hatchikian, M. Frey, J. C. FontecillaCamps, *J. Am. Chem. Soc.* **1996**, *118*, 12989.
[28] A. J. Pierik, W. Roseboom, R. P. Happe, K. A. Bagley, S. P. J. Albracht, *J. Biol. Chem.* **1999**, *274*, 3331.
[29] Y. Montet, E. Garcin, V. A., C. Hatchikians, M. Frey, J. C. Fontecilla-Camps, *Pure Appl. Chem.* **1998**, *70*, 25.
[30] M. Lechtenberg, in *Encyclpedia of Life Sciences*, John Wiley & Sons, Ltd, Chichester, **2011**.
[31] S. Ebbs, *Curr. Opin. Biotechnol.* **2004**, *15*, 231.
[32] L. R. Ketterer, PhD thesis, Philipps-Universität Marburg **2010**.
[33] G. R. Flematti, D. J. Merrit, M. J. Piggott, R. D. Trengove, S. M. Smith, K. W. Dixon, E. L. Ghisalberti, *Nat.Commun.* **2011**, *2*, 1356.
[34] B. Ballantyne, in *Developments in the science and practice of toxicology* (Eds.: A. Hayes, R. Schnell, T. Miya), Elsevier Science Publishers, New York, NY, **1983**, pp. 583.
[35] EPA, United States Environmental Protection Agency, Cincinnati, OH, **1983**.
[36] *Official Journal EU, Comm. Dir. 1998/83/EC* **1998**, L30.
[37] ANZECC, *Australien Water Quality Guidelines for fresh and Marine Water*, Australien and New Zealand Environmental and Conservation Council, **2000**.
[38] WHO, *Guidelines for Drinking-Water Quality*, 3rd ed., World Health Organization, Geneva, **2008**.
[39] G. Pavlakovic, A. Rathinavelu, G. E. Isom, *Neurochem. Res.* **1994**, *19*, 1289.
[40] D. A. Dzombak, R. S. Ghosh, G. M. Wong-Chong, in *Cyanide in Water and Soil: Chemistry, Risk and Management*, CRC Press, Boca Raton, FL, **2006**, pp. 238.
[41] R. Spörri, *Rettungsdienst* **2004**, *4*, 46.
[42] M. Daunderer, in *Klinische Toxicologie, Vol. 143*, ecomed, Landsberg/ Lech, **1995-2006**, pp. 1.
[43] ATSDR, (Eds.: P. H. Department of Health and Human Services, Service), Agency for Toxic Substances and Disease Registry Atlanta, GA , US, **1989**.
[44] ATSDR, (Eds.: P. US Department of Health and Human Services, Health Service), Agency for Toxic Substances and Disease Registry., Atlanta, GA, **1991**.
[45] ATSDR, (Ed.: P. H. S. US Department of Health and Human Services), Agency for Toxic Substances and Disease Registry, Atlanta, GA, **1997**.
[46] B. Ballantyne, in *Clinical and Experimental Toxicology of Cyanides* (Eds.: B. Ballantyne, T. C. Marrs), Wright Publishers, Bristol, Engl., **1987**.
[47] D. Gee, in *Clinical and Experimental Toxicology of Cyanide* (Eds.: B. Ballantyne, T. C. Marrs), IOP Publishers, Bristol, England, **1987**, p. 209.

[48] WHO, in *Concise international chemical assessment document 61*, World Health Organization, Geneva, **2004**, pp. 4.
[49] A. E. Lindsay, A. R. Greenbaum, D. O'Hare, *Anal. Chim. Acta* **2004**, *511*, 185.
[50] G. Shepherd, L. I. Velez, *Ann. Pharmacother.* **2008**, *42*, 661.
[51] T. F. Cummings, *Occup. Med.-Oxford* **2004**, *54*, 82.
[52] J. E. Huheey, E. A. Keiter, R. L. Keiter, *Anorganische Chemie*, Walter de Gruyter, Berlin, **1995**.
[53] M. Jokusch, in *Biologie* (Eds.: N. A. Campell, J. B. Reece), Pearson Studium, München, **2006**, pp. 196.
[54] K. Yamamoto, Y. Yamamoto, H. Hattori, *Tohoku J. Exp. Med.* **1982**, *137*, 73.
[55] M. Ansell, F. Lewis, *J. Forensic Med.* **1970**, *17*, 148.
[56] C. A. DesLauriers, A. M. Burda, M. Wahl, *Am. J. Ther.* **2006**, *13*, 161.
[57] A. H. Hall, R. Dart, G. Bogdan, *Ann. Emerg. Med.* **2007**, *49*, 806.
[58] J. Hamel, *Crit. Care Nurse* **2011**, *31(1)*, 72.
[59] C. Spagnuolo, P. Rinelli, M. Coletta, E. Chiancone, F. Ascoli, *Biochim. Biophys. Acta* **1987**, *911*, 59.
[60] A. H. Hall, K. W. Kuhlig, B. H. Rumack, *J. Toxicol. Clin. Experim.* **1989**, *9*, 3.
[61] J. L. Fortin, C. Peureux, C. Lambert, T. Desmettre, G. Capellier, *Clin. Toxicol.* **2012**, *50*, 301.
[62] S. W. Borron, F. J. Baud, P. Barriot, M. Imbert, C. Bismuth, *Ann. Emerg. Med.* **2007**, *49*, 794.
[63] J. L. Fortin, J. P. Giocani, M. Ruttimann, J. J. Kowalski, *Clin. Toxicol.* **2006**, *44*, 37.
[64] R. Alcorta, *JEMS Commun.* **2004**, *29*, 6.
[65] P. Lawson-Smith, E. C. Jansen, O. Hyldegaard, *Scand. J. Trauma Resusc. Emerg. Med.* **2011**, *19*.
[66] R. K. Müller, in *Handbuch Gerichtliche Medizin* (Eds.: B. Madea, B. Brinkmann), Springer-Verlag, Berlin Heidelberg, **2003**, pp. 156.
[67] S. Smith, *Med. Leg. J.* **1952**, *20*, 153.
[68] B. Weider, in *Georgian J. Napoleonic. Hist.* , **2000**, pp. 138.
[69] J. Vetter, *Toxicon* **2000**, *38*, 11.
[70] W. Hosel, in *Cyanide in Biology* (Eds.: B. Vennesland, E. E. Conn, C. J. Knowles, J. Westley, F. Wissing), Academic press, London, **1981**, pp. 217.
[71] J. M. McMahon, W. L. B. White, R. T. Sayre, *J. Exp. Bot.* **1995**, *46*, 731.
[72] E. E. Conn, in *Cyanide in Biology* (Eds.: V. Vennesland, E. E. Conn, C. J. Knowles, J. Westley, F. Wissing), Academic Press, New York,USA, **1981**, pp. 1.
[73] C. Männel-Croise, B. Probst, F. Zelder, *Anal. Chem.* **2009**, *81*, 9493.
[74] K. Friedrich, K. Wallenfels, *The Chemistry of the Cyano Group*, John Wiley & Sons, London, **1970**.
[75] L. Brimer, A. R. Cicalini, F. Frederici, R. M. Nout, M. Petruccioli, V. Pulci, *Riv. Biol.* **1996**, *89*, 493.
[76] FAO/IFAD, Food and Agriculture Organization of the United Nations and International Fund for Agricultural Development, Rome, **2000**.
[77] V. Lebot, *Tropical Root and Tuber Crops: Cassava, Sweet Potato, Yams and Aroids.*, CABI, Wallingford, UK, **2009**.
[78] in *Production Year book 2010*, Food and Agricultural Organization of the United Nations, **2010**.

[79] G. Padmaja, *Crit. Rev. Food Sci.* **1995**, *35*, 299.
[80] A. U. Achidi, O. A. Ajayi, M. Bokanga, B. Maziya-Dixon, *Ecol. Food Nutr.* **2005**, *44*, 423.
[81] C. Heuberger, (Zürich), **2005**.
[82] S. Essers, M. Bosveld, R. M. Vandergrift, A. G. J. Voragen, *J. Sci. Food Agric.* **1993**, *63*, 287.
[83] A. Cumbana, E. Mirione, J. Cliff, J. H. Bradbury, *Food Chem.* **2007**, *101*, 894.
[84] A. P. Cardoso, E. Mirione, M. Ernesto, F. Massaza, J. Cliff, M. R. Haque, J. H. Bradbury, *J. Food Comp. Anal.* **2005**, *18*, 451.
[85] M. Ernesto, A. P. Cardoso, D. Nicala, E. Mirione, F. Massaza, J. Cliff, M. R. Haque, J. H. Bradbury, *Acta Trop.* **2002**, *82*, 357.
[86] FAO/WHO, in *Food Standarts Programme. Codex Alimentarius XII, Supplement 4*, FAO, Rome, Italy, **1991**.
[87] S. C. Kobawila, D. Louembe, S. Keleke, J. Hounhouigan, C. Gamba, *Afr. J. Biotechnol.* **2005**, *4*, 689.
[88] A. E. Burns, J. H. Bradbury, T. R. Cavagnaro, R. M. Gleadow, *J. Food Comp. Anal.* **2012**, *25*, 79.
[89] M. N. Adindu, F. F. Olayemi, O. U. Nze-Dike, *J. Food Comp. Anal.* **2003**, *16*, 21.
[90] T. Tylleskar, M. Banea, N. Bikangi, R. D. Cooke, N. H. Poulter, H. Rosling, *Lancet* **1992**, *339*, 208.
[91] S. Peterson, H. Rosling, T. Tylleskar, M. Gebremedhin, A. Taube, *Lancet* **1995**, *345*, 513.
[92] W. P. Howlett, in *ISHS Acta Harticulturae 375*, **1994**, pp. 323.
[93] J. C. Mwanza, D. Tshala-Katumbay, T. Tylleskar, *Environ. Toxicol. Pharmacol.* **2005**, *19*, 491.
[94] O. S. A. Oluwole, A. O. Onabolu, *Acta Neurol. Scand.* **2004**, *110*, 94.
[95] O. S. A. Oluwole, A. O. Onabolu, I. A. Cotgreave, H. Rosling, A. Persson, H. Link, *J. Neurol. Neurosur. PS* **2003**, *74*, 1417.
[96] O. S. A. Oluwole, A. O. Onabolu, K. Mtunda, N. Mlingi, *J. Food Comp. Anal.* **2007**, *20*, 559.
[97] D. Nhassico, H. Muquingue, J. Cliff, A. Cumbana, J. H. Bradbury, *J. Sci. Food Agric.* **2008**, *88*, 2043.
[98] D. McKey, T. R. Cavgnaro, J. Cliff, R. M. Gleadow, *Chemoecology* **2010**, *20*, 109.
[99] J. Cliff, H. Muquingue, D. Nhassico, H. Nzwalo, J. H. Bradbury, *Food Chem. Toxicol.* **2011**, *49*, 631.
[100] D. Mabey, R. W. Peeling, A. Ustianowski, M. D. Perkins, *Nature Rev.* **2004**, *2*, 231.
[101] M. G. Bradbury, S. V. Egan, J. H. Bradbury, *J. Sci. Food Agric.* **1999**, *79*, 593.
[102] J. H. Bradbury, *Food Chem.* **2009**, *113*, 1329.
[103] S. V. Egan, H. H. Yeoh, J. H. Bradbury, *J. Sci. Food Agric.* **1998**, *76*, 39.
[104] M. R. Haque, J. H. Bradbury, *Food Chem.* **2002**, *77*, 107.
[105] A. P. Cardoso, M. Ernesto, D. Nicala, E. Mirione, L. Chavane, H. N'Zwalo, S. Chikumba, J. Cliff, A. P. Mabota, M. R. Haque, J. H. Bradbury, *Int. J. of Food Sci. Nut.* **2004**, *55*, 183.
[106] R. Schnepp, *J. Emerg. Nurs.* **2006**, *32*, S3.

[107] C. Young, L. Tidwell, C. Anderson, *Cyanide: Social, Industrial, and Economic Aspects*, Minerals, Metals, and Material Society, Warrendale, **2001**.
[108] R. S. Ghosh, D. V. Nakles, I. P. Murarka, E. F. Neuhauser, *Environ. Eng. Sci.* **2004**, *21*, 752.
[109] M. J. Logsdon, K. Hagelstein, T. I. Mudder, *The management of cyanide in gold extraction* International Center for Metal and the Environment, Ottava, Canada, **1999**.
[110] F. Brazdil, in *Kirk-Othmer Encyclopedia of chemical Technology, Vol. 1*, John Wiley & Sons, New York, **1993**.
[111] US Department of Health and Human Services, The Agency for Toxic Substances and Disease Registry, Atlanta, GA, p. 4.
[112] K. Bödigheimer, F. Nowak, W. Schoenborn, *DMW* **1979**, *104*, 939.
[113] in *Information Bulletin of the World Fire Statistics, Vol. 27*, **2011**.
[114] K. Stamyr, G. Thelander, L. Ernstgard, J. Ahlner, G. Johanson, *Inhal. Toxicol.* **2012**, *24 (3)*, 194.
[115] F. M. Esposito, Y. Alarie, *J. Fire Sci.* **1988**, *6*, 195.
[116] F. J. Baud, P. Barriot, V. Toffis, B. Riou, E. Vicaut, Y. Lecarpentier, R. Bourdon, A. Astier, C. Bismuth, *New Eng. J. Med.* **1991**, *325*, 1761.
[117] A. A. Stec, T. R. Hull, J. A. Purser, D. A. Purser, *Fire Safety J.* **2009**, *44*, 62.
[118] J. M. Carman, D. A. Purser, T. R. Hull, D. Price, G. J. Milnes, *Polym. Int.* **2000**, *49*, 1256.
[119] F. Moriya, Y. Hashimoto, *J. Forensic Sci.* **2001**, *46*, 1421.
[120] J. E. Bright, R. H. Inns, N. J. Tuckwell, T. C. Marrs, *Hum. Exp. Toxicol.* **1990**, *9*, 125.
[121] Y. Alarie, *Crit. Rev. Toxicol.* **2002**, *32*, 259.
[122] B. Levine, G. W. Kunsman, in *Principles of Forensic Toxicology*, 3. ed. (Ed.: B. Levine), AACC Press, Washington, **2010**.
[123] A. M. Prentiss, *Chemicals in War: A Treatise on Chemical War*, McGraw-Hill, New York, NY, **1937**.
[124] J. P. Robinson, in *The Rise of CB Weapons: A Study of the Historical, Technical, Military, Legal and Political Aspects of CBW, and Possible Disarmament* (Ed.: J. P. Robinson), Humanities Press, New York, NY, **1971**, pp. 155.
[125] S. I. Baskin, in *Encyclopedia of the Holocaust* (Ed.: W. La Cleuer), Yale University Press, New Haven, Conn, **2001**.
[126] M. Eckstein, *JEMS Commun.* **2004**, 22.
[127] A. Khan, A. Levitt, M. Sage, in *MMWR Morb., Vol. 49 (RR04)*, Centers for Disease Control. , **2000**, pp. 1.
[128] T. P. Noeller, *Clev. Clinic J. Med..* **2001**, *68*, 1001.
[129] R. L. Thompson, W. W. Manders, R. W. Cowan, *J. Forensic Sci.* **1987**, *32 (2)*, 433.
[130] H. B. Singh, N. Wasi, M. C. Mehra, *Int. J. Environ. Anal. Chem.* **1986**, *26*, 115.
[131] U. S. EPA, United States Environmental Protection Agency, EPA, Method 9010-9014, **1996**.
[132] WHO, United States Environmental Protection Agency, EPA, Method 9213, **1996**.
[133] in *DIN 38405-13/14, Vol. 04*, Deutsches Institut für Normung e. V., Beuth Verlag, Berlin, **2011**.

[134] J. v. Liebig, *Liebigs Ann.* **1851**, *77*, 102.
[135] G. Jander, E. Blasius, J. Strähle, *Einführung in das anorganisch-chemische Praktikum: (einschließlich der quantitativen Analyse)*, S. Hirzel Verlag, Leipzig, **2005**.
[136] United States Environmental Protection Agency, EPA, Method OIA-1677, **2004**.
[137] *Dräger-Röhrchen & CMS-Handbuch*, Dräger Safety AG & Co KGaA, Lübeck, **2008**.
[138] J. A. Ma, P. K. Dasgupta, *Anal. Chim. Acta* **2010**, *673*, 117.
[139] S. L. Fox, K. A. Daum, C. J. Miller, M. M. Cortez, U.S. Department of Homeland Security, Idaho 83415, **2007**.
[140] F. H. Zelder, C. Mannel-Croise, *Chimia* **2009**, *63*, 58.
[141] Z. Xu, X. Chen, H. N. Kim, J. Yoon, *Chem. Soc. Rev.* **2010**, *39*, 127.
[142] D.-G. Cho, J. H. Kim, J. L. Sessler, *J. Am. Chem. Soc.* **2008**, *130*, 12163.
[143] F. Garcia, J. M. Garcia, B. Garcia-Acosta, R. Martinez-Manez, F. Sancenon, J. Soto, *Chem. Commun.* **2005**, 2790.
[144] J. V. Ros-Lis, R. Martinez-Manez, J. Soto, *Chem. Commun.* **2002**, 2248.
[145] Y. M. Chung, B. Raman, D. S. Kim, K. H. Ahn, *Chem. Commun.* **2006**, 186.
[146] H. T. Niu, X. L. Jiang, J. Q. He, J. P. Cheng, *Tetrahedron Lett.* **2008**, *49*, 6521.
[147] H. T. Niu, D. D. Su, X. L. Jiang, W. Z. Yang, Z. M. Yin, J. Q. He, J. P. Cheng, *Org. Biomol. Chem.* **2008**, *6*, 3038.
[148] J. L. Sessler, D. G. Cho, *Org. Lett.* **2008**, *10*, 73.
[149] N. Gimeno, X. Li, J. R. Durrant, R. Vilar, *Chem.-Eur. J.* **2008**, *14*, 3006.
[150] P. D. Beer, P. A. Gale, *Angew. Chem. Int. Ed.* **2001**, *40*, 486.
[151] R. Badugu, J. R. Lakowicz, C. D. Geddes, *Curr. Anal. Chem.* **2005**, *1*, 157.
[152] A. E. J. Broomsgrove, D. A. Addy, C. Bresner, I. A. Fallis, A. L. Thompson, S. Aldridge, *Chem. Eur. J.* **2008**, *14*, 7525.
[153] V. Ganesh, S. K. Pal, S. Kumar, V. Lakshminarayanan, *Electrochim. Acta* **2007**, *52*, 2987.
[154] Q. Zeng, P. Cai, Z. Li, J. Qina, B. Z. Tang, *Chem. Commun.* **2008**, 1094.
[155] Z. A. Li, X. D. Lou, H. B. Yu, Z. Li, J. G. Qin, *Macromolecules* **2008**, *41*, 7433.
[156] X. D. Lou, L. Y. Zhang, J. G. Qin, Z. Li, *Chem. Commun.* **2008**, 5848.
[157] Y. H. Kim, J. I. Hong, *Chem. Commun.* **2002**, 512.
[158] C. F. Chow, M. H. W. Lam, W. Y. Wong, *Inorg. Chem.* **2004**, *43*, 8387.
[159] J. M. Pratt, in *Chemistry and Biochemistry of B12* (Ed.: R. Banerjee), John Wiley & Sons, New York, **1999**, pp. 113.
[160] K. M. Smith, *General features of the structure and chemistry of porphyrin compounds*, Elsevier, Amsterdam, **1975**.
[161] J. M. Pratt, *Inorganic Chemistry of Vitamin B12*, Academic Press, New York, **1972**.
[162] F. H. Zelder, *Inorg. Chem.* **2008**, *47*, 1264.
[163] K. Poland, E. Topoglidis, J. R. Durrant, E. Palomares, *Inorg. Chem. Commun.* **2006**, *9*, 1239.
[164] M. K. Freeman, L. G. Bachas, *Anal. Chim. Acta* **1990**, *241*, 119.
[165] S. Daunert, L. G. Bachas, *Anal. Chem.* **1989**, *61*, 499.
[166] S. S. M. Hassan, M. S. A. Hamza, A. E. Kelany, *Talanta* **2007**, *71*, 1088.
[167] J. Fuchs, D. Radloff, J. Reichert, H.-J. Ache*, Vol. Ger. Off. DE 19608808*, (Forschungszentrum Karlsruhe G.m.b.H., Germany). Application: DE

DE, **1997**, p. 15 pp.
[168] W. W. Reenstra, W. P. Jencks, *J. Am. Chem. Soc.* **1979**, *101*, 5780.
[169] S. M. Chemaly, M. Florczak, H. Dirr, H. M. Marques, *Inorg. Chem.* **2011**, *50*, 8719.
[170] E. A. Betterton, Ph.D. thesis, The University of Witwatersrand (Johannesburg, South Africa), **1982**.
[171] C. F. Bernasconi, *Relaxation Kinetics*, Academic Press, New York, **1976**.
[172] D. A. Baldwin, E. A. Betterton, J. M. S. Pratt, *Afr. J. Chem.* **1982**, *35*, 173.
[173] H. M. Marques, J. C. Bradleya, K. L. Brown, H. Brooks, *J. Chem. Soc. Dalton Trans.* **1993**, 3475.
[174] C. Männel-Croise, F. Zelder, *Inorg. Chem.* **2009**, *48*, 1272.
[175] S. Daunert, L. G. Bachas, *Anal. Chem.* **1989**, *61*, 499.
[176] C. Kratky, G. Färber, K. Gruber, K. Wilson, Z. Dauter, H.-F. Nolting, R. Konrat, B. Kräutler, *J. Am. Chem. Soc.* **1995**, *117*, 4654.
[177] K. Venkatesan, D. Dale, D. C. Hodgkin, C. E. Nockolds, F. H. Moore, B. H. O'Connor, *Proc. R. Soc. London, Ser. A* **1971**, *323*, 455.
[178] K. Zhou, F. H. Zelder, *Eur. J. Inorg. Chem.* **2011**, *1*, 53.
[179] M. J. Pfammatter, T. Darbre, R. Keese, *Helv. Chim.Acta* **1998**, *81*, 11051116.
[180] C. Männel-Croise´, F. Zelder, *Chem. Commun.* **2011**, *47*, 11249.
[181] K. L. Brown, *Chem. Rev.* **2005**, *105*, 2075.
[182] S. M. Chemaly, *Dalton Trans.* **2008**, 5766.
[183] S. Chowdhury, R. Banerjee, *Biochem.* **1999**, *38*, 15287.
[184] C. L. Drennan, S. Huang, J. T. Drummond, R. G. Matthews, M. L. Ludwig, *Science* **1994**, *266*, 1669.
[185] W. Buckel, B. T. Golding, *Chem. Soc. Rev.* **1996**, *25*, 329.
[186] W. Friedrich, K. Bernhauer, *Chem. Ber.* **1956**, *89*, 2030.
[187] C. Männel-Croisé, F. Zelder, *Appl. Mater. Interfaces* **2012**, *4*, 725.
[188] L. Gall, *Lehrbuch der Lacke und Beschichtungen. Pigmente,Füllstoffe und Farbmetrik*, Hirzel, Stuttgart, Germany, **2003**.
[189] J. H. Bradbury, M. R. Haque, *Clin. Chem.* **1999**, *45*, 1459.
[190] S.-Y. Chung, S.-W. Nam, J. Lim, S. Park, J. Yoon, *Chem. Commun.* **2009**.
[191] X. Lou, L. Zhang, J. Qin, Z. Li, *Chem. Commun.* **2008**, 5848.
[192] C. Männel-Croisé, C. Meister, F. Zelder, *Inorg. Chem.* **2010**, *49*, 10220.
[193] G. Schwarzenbach, H. Flaschka, *Die Komplexometrische Titration*, F. Enke Verlag Stuttgart, **1965**.
[194] G. Schwarzenbach, H. Gysling, *Helv. Chim. Acta* **1949**, *32*, 1314.
[195] Z. D. Hill, P. Maccarthy, *J. Chem. Educ.* **1986**, *63*, 162.
[196] B. L. Moller, D. S. Seigler, in *Plant amino acids biochemistry and biotechnology* (Ed.: B. K. Singh), Marcel Dekker Inc., New York **1999**, pp. 563.
[197] R. D. Cooke, D. G. Coursey, *Cyanide in Biology*, Academic Press, London, **1981**.
[198] W. L. B. White, D. L. Arias-Garzon, J. M. McMahon, R. T. Sayre, *Plant Physiol.* **1998**, *116*, 1219.
[199] J. H. Bradbury, S. V. Egan, M. J. Lynch, *J. Sci. Food Agric.* **1991**, *55*, 277.
[200] B. Nambisan, S. Sundaresan, *J. .Sci. Food Agric.* **1985**, *36*, 1197.
[201] R. D. Cooke, E. N. Maduagwu, *J. Food Tech.* **1978**, *13*, 299.
[202] personal communication.
[203] C. Männel-Croisé, F. Zelder, submitted to Analytical Methods, **2012**.

[204] M. H. Klapper, H. Uchida, **1971**, *246*, 6849.
[205] J. C. Forsyth, P. D. Mueller, C. E. Becker, *J. Toxicol. Clin. Toxicol.* **1993**, *21*, 277.
[206] R. Gracia, G. Shepherd, *Pharmacotherapy.* **2004**, *24*, 1358.
[207] L. Hannibal, A. Axhemi, A. V. Glushchenko, E. S. Moreira, N. E. Brasch, D. W. Jacobsen, *Clin. Chem. Lab. Med.* **2008**, *46*, 1739.
[208] L. Xia, A. G. Cregan, L. A. Berben, N. E. Brasch, *Inorg. Chem.* **2004**, *43*, 6848.
[209] J. C. Harfield, C. Batchelor-McAuley, R. G. Compton, *Analyst* **2012**, *137*, 2285.
[210] P. Lundquist, H. Rosling, B. Sorbo, L. Tibbling, *Clin. Chem.* **1987**, *33*, 1228.
[211] H. G. Völz, *Industrielle Farbprüfung*, Wiley-VCH: Weinheim, **1990**.
[212] R. Stepanek, B. Kräutler, P. Schulthess, B. Lindemann, D. Ammann, W. Simon, *Anal. Chim. Acta* **1986**, *182*, 83.
[213] L. Debussche, D. Thibaut, B. Cameron, J. Crouzet, F. J. B. Blanche, **1990**, *4*, 6239.
[214] M. S. A. Hamza, *J. Inorg. Biochem.* **1998**, *69*
269.
[215] A. I. Scott, A. J. Irwin, L. M. Siegel, J. N. Shoolery, *J. Am. Chem. Soc.* **1978,**, *100*, 7987.
[216] K. A. Conners, *Binding Constants, The Measurement of Moleclar Complex Stabilty*, Wiley-VCH, New York, **1987**.
[217] D. G. Tuck, *Pure Appl. Chem.* **1989**, *61*, 1161.
[218] A. A. L. Hill, R. J.; Fritz, J. S.; Porter, M. D, *Talanta* **2009**, *77*, 1405.
[219] M. P. Arena, M. D. Porter, J. S. Fritz, *Anal. Chem.* **2002**, *74*, 185.
[220] D. B. F. Gazda, J. S.; Porter, M. D, *Anal. Chim. Acta* **2004**, *508*, 53.
[221] Y. Seto, *Arch. Biochem. Biophys.* **1995**, *321*, 245.

At the beginning of the first project, investigating corrinoids as chemosensors for cyanide detection, it was not expected that this work would turn into a four year PhD thesis. As it happened, the results of every subproject gave rise to new hypotheses and questions which were curious to answer. As the work progressed, the prospects for possible practical applications, collaborations and further studies also flourished. However, a thesis needs to come to an end and so I had to stop at this interesting point.

This PhD thesis was developed based on the excellent advices of my excellent supervisor Dr. Felix Zelder. Countless interesting discussions, his enthusiasm for this research and the endurance during the writing of several publications motivated and inspired this work all day long. For all this, I am very grateful!

I would like to thank Prof. Dr. Roger Alberto for his generous support of this work, being always open for questions and for reviewing the publications and this thesis as well.

I would like to acknowledge Prof. Dr. R. K. O. Sigel for being the co-advisor of this theses.

I am indebted to Prof. Dr. Greta Patzke for access to her DRUV-vis machine, Prof. Dr. Gilles Gasser for discussions and reviewing some of our papers, and Prof. Dr. Eva Freisinger for letting to use the shaking apparatus.

A sincere thanks goes to Dr. Kai Zhou for daily chats about our chemistry and about all interesting aspects of the world around us, for service of the mass spectrometry and LCMS at any time, the help for fixing the stopped-flow machine and for always being there as a good friend.

Many thanks, too, to all the current members of our group, Marjorie Sonney, René Oetterli, Balz Aebli and Philipp Pfingsttag for all the help and discussions and, last but not least, for keeping up a great atmosphere in the lab. Sincere thanks René, for your service of the mass spectrometry and LCMS and all the fun and interesting time in the lab.

Many thank goes to Dr. Benjamin Probst for his introduction in the stopped flow

technique and the origin program.

I thank the students Christian Meister and Balz Aebli for their constructive and committed effort in the kinetic projects as well as Christians work on the project of metal indicator systems for cyanide detection. Moreover, I thank the students Alex, Marko, Sarah, Christine and the schoolgirl Romana for letting me share my excitement over corrinoid chemistry with you!

I have greatly appreciated the support by Dr. Ferdinand Wild, Manfred Jörri and Hans-Peter Stalder with computing issues and technical equipment and by Heinz Spring for organizing the blood samples. Sincere thanks are given to all of you!

I would like to thank also all the members from the Alberto group and the Gasser-group for their help in every thinkable situation and in particular Dr. Paul Schmutz, Anna Leonidova, Cristina Mari, Jeanine Hess, Philipp Anstätt and Dr. Malay Patra for all the nice time which you spend with our group.

Thank you, Dr. med. vet. Katrin Stutz your interest and support in the blood project and your assistance during the venture-courses.

A special thanks goes to Liane Schlickenrieder for improving the english.

I am grateful to the Marie-Heim-Vögtlin-Programm of the Swiss National Foundation (Grant PMCD 129054/1) and the University of Zurich for financial support.

Special thank goes to my husband Jean and to my children Almuth and Christoph to give me the time for doing this work and supporting me in every situation! Outstanding thank goes to Jean for your come-back to our world, to Almuth for our joint passion in chemistry and to Christoph for all the wonderful concerts. Sincere thanks to my mother and my brother Stephan for all your support!

Name: Christine Männel-Croisé
Address: Böllistrasse 9, 5702 Niederlenz
Born: April 28, 1961
Nationality: German
Civil status: married
Children: Almuth Croisé (1988)
Christoph Croise (1993)

Education

05/2008 – 04/2012:	PhD study at the Institute of Inorganic Chemistry, University of Zurich under supervision of Dr. F. Zelder in the group of Prof. Dr. R. Alberto
08/ 2008 – today:	MAS SHE-Study in Chemistry at ETH Zurich
02/2008:	Diploma in Chemistry, principal subject: Inorganic Chemistry
2006-2007:	Diploma thesis at the Institute of Inorganic Chemistry/ University of Zurich under supervision of Prof. Dr. R. Alberto with the topic: “A synthetic and spectroscopic approach to ferrocenophane based catalysts”
02/2005	Pre-degree examination in Inorganic, Organic and Physical Chemistry as qualification for the master thesis
2002-2005:	Study in Chemistry at the University of Zurich
1988-2002:	Housewife and mother
1986-1988:	Study in Chemistry at the University of Stuttgart with specialisation in Physical Chemistry
1984-1986:	Internship in medicinal care, Berlin
1980-1984:	Diploma Study in Chemistry at the Humboldt-Universität Berlin
1975-1979:	High school with “Abitur”, Berlin

Grant

2010-2011 „Marie-Heim-Vögtlin Beitrag“ of the Swiss National Foundation (Grant No. PMCDP2_129054/1)

List of publications

1. C. Männel-Croisé, F. H. Zelder, *Inorg. Chem.* **2009**, 48, 1272
2. F. H. Zelder and Männel- Croisé, *Chimia*, **2009**, 63,58
3. C. Männel-Croisé, B. Probst, F. Zelder, *Anal. Chem.* **2009***, 81, 9493-9498*
4. C. Männel.-Croisé, C.Meister, F. Zelder, *Inorg. Chem.* **2010**, 49, 10220-10222
5. C. Männel-Croisé, F. H. Zelder, *Chem. Commun., **2011**, 1-3*
6. C. Männel-Croisé, F. H. Zelder, *Patentanmeldung* EP11/ 161228
7. C. Männel-Croisé, F. H. Zelder, *Appl. Mater. Interfaces,* **2012**, 4, 725-729
8. C. Männel-Croisé, F. H. Zelder, *Anal. Methods,* **2012**

Conference contributions

a) oral presentations

1. SCG Fallmeeting ETH Zürich, September 16, 2010
   "Metal-based chemosensors for biologically important anions"
2. 6. Koordinationschemie-Treffen, Mainz/DE, February 21, 2010
   "Cobalt(III)-basierte Indikatorsysteme für die Cyaniddetektion"
3. 7. Koordinationschemie-Treffen Stuttgart, February 27, 2011
   "Metal-based chemosensors for biologically important anions"
4. 12. XeRR Jahrestagung Centre for Xenobiotic Risk Research, December 8, 2011, *"Rapid visual detection of cyanide"*

b) Poster

1) SCS Fall meeting, ETH Zurich/CH, September 16,2010
   "*Metal-based chemosensors for biologically important anions***"**
2) 5th Annual Dorothy Crowfoot Hodgkin Symposium, University of Zurich, Octobre 11, 2010, **"***Metal-based chemosensors for biologically important anions***"** with price for the best poster
3) 2011 ANAKON, ETH Zurich/CH, March 22-25, 2011
   "*Chemosensors for the visual detection of biologically important anions***"**
4) SCS Fall meeting, EPFL Lausanne /CH, September 16, 2011,
   "Metal-based chemosensors for biologically important anions"
5) BioTech 2011, "Zürcher Hochschule für Angewandte Wissenschaften", September 1-2, 2011, *"Rapid visual detection of cyanide"*
6) 6th Annual Dorothy Crowfoot Hodgkin Symposium, University of Zurich, Octobre 6, 2011 **"***Rapid visual detection of cyanide***"** with price for the best